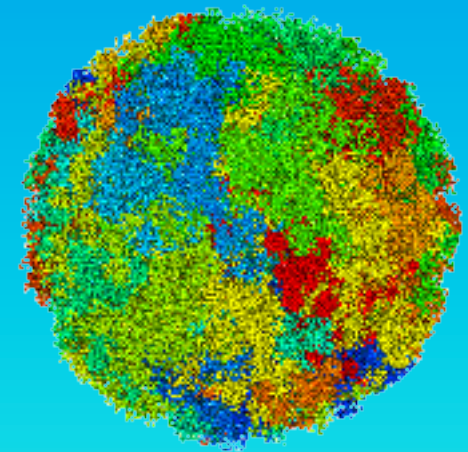
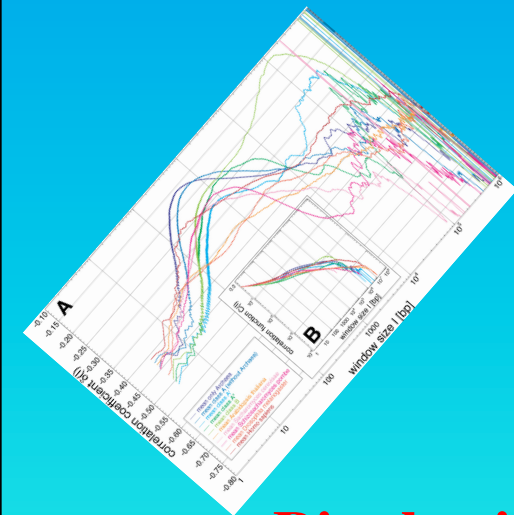


Decoding the 3D Multi-Loop Aggregate/Rosette Chromatin Architecture, Dynamics, and Functional Epigenetics of Genomes

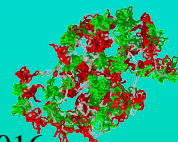
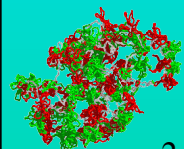


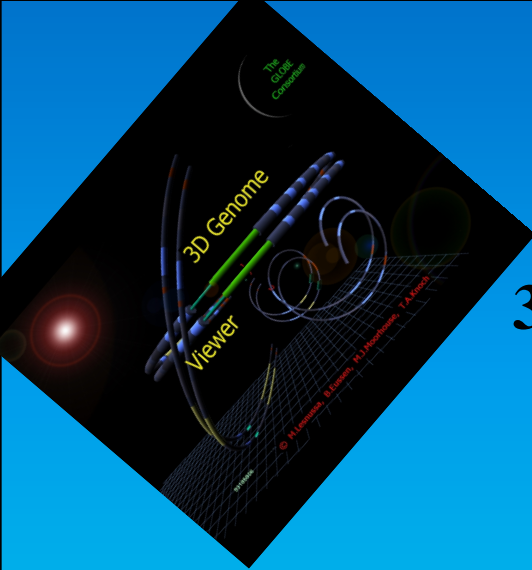
Tobias A. Knoch

Biophysical Genomics & Erasmus Computing Grid

Erasmus Medical Center

TA.Knoch@taknoch.org





Decoding the 3D Multi-Loop Aggregate/ Chromatin Architecture, Function

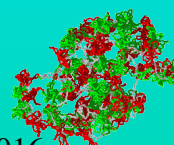
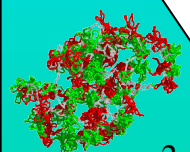
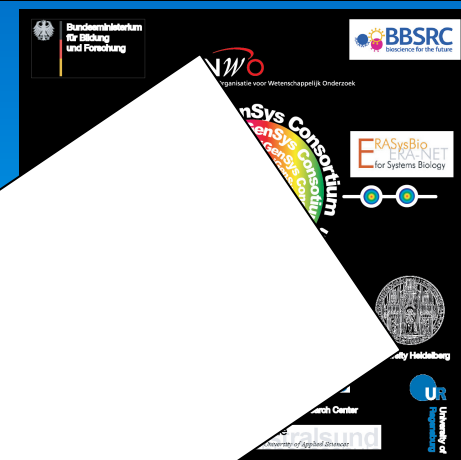
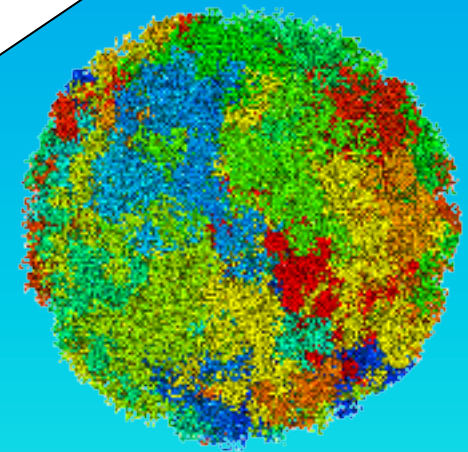
**Results and Perspectives
of a
Finally Solved Challenge!**

Thomas A. Knoch

Genomics & Erasmus Computing Grid

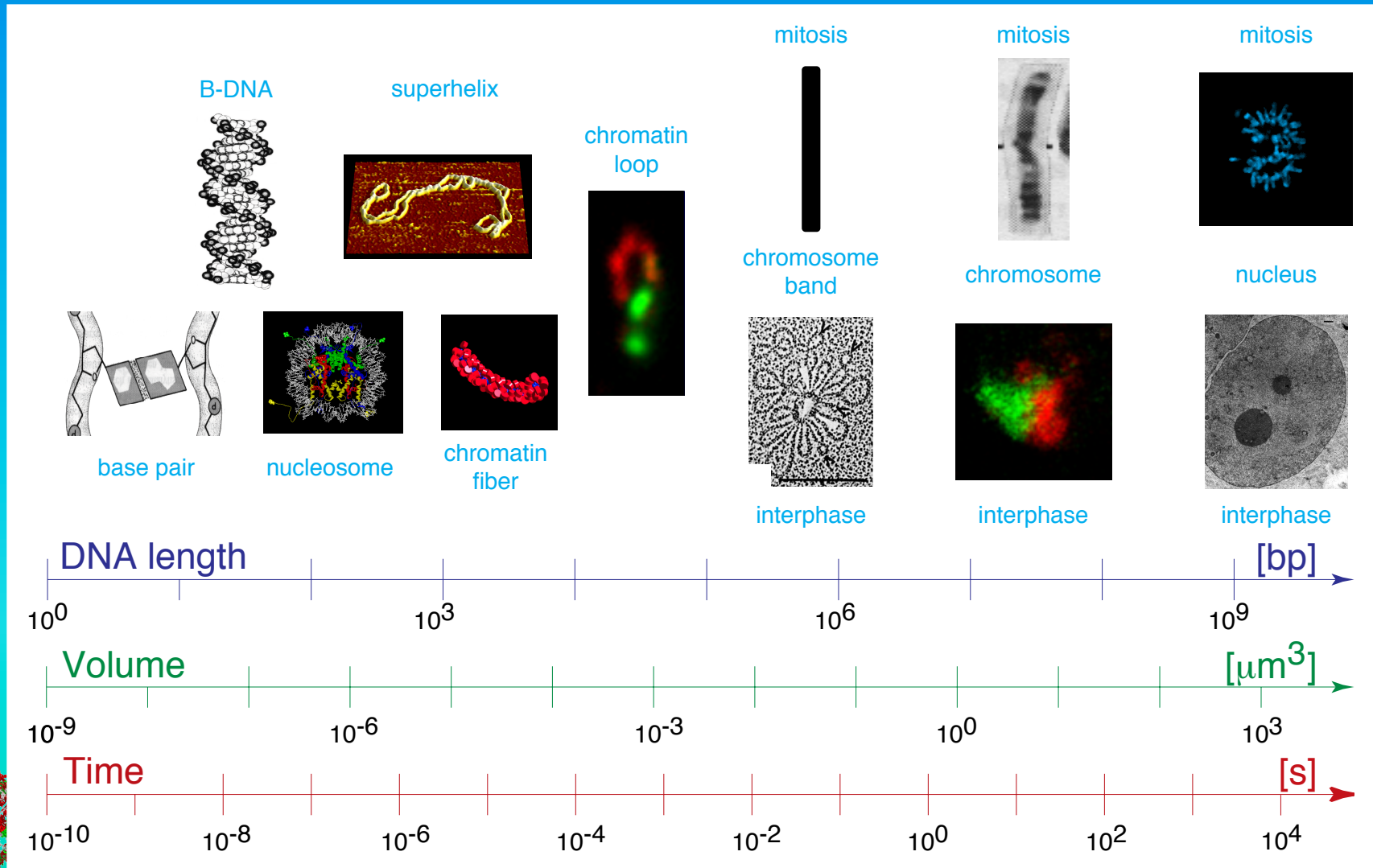
Erasmus Medical Center

TA.Knoch@taknoch.org



Dynamic and Hierarchical Genome Organization

The different organization levels of genomes bridge several orders of magnitude concerning space and time. How all of these organization levels connect to processes like gene regulation, replication, embryogeneses, or cancer development is still unclear?

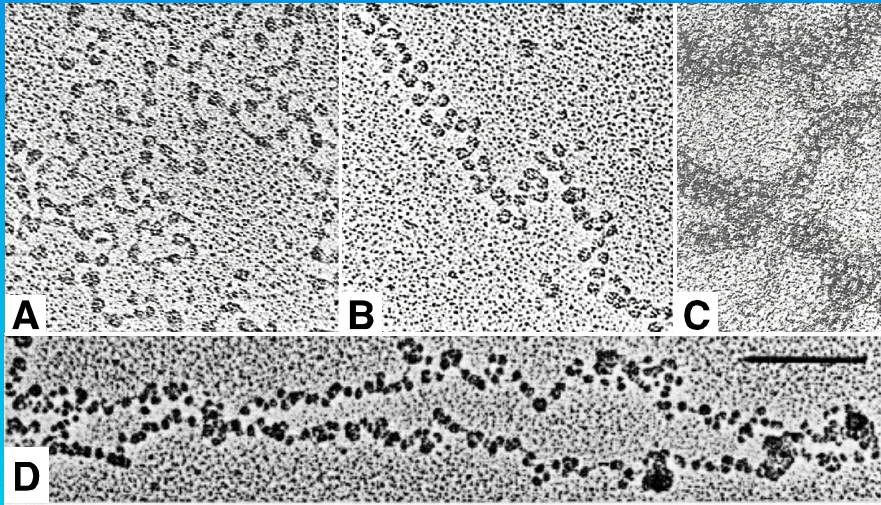


Chromatin Conformation and Higher-Order Topologies

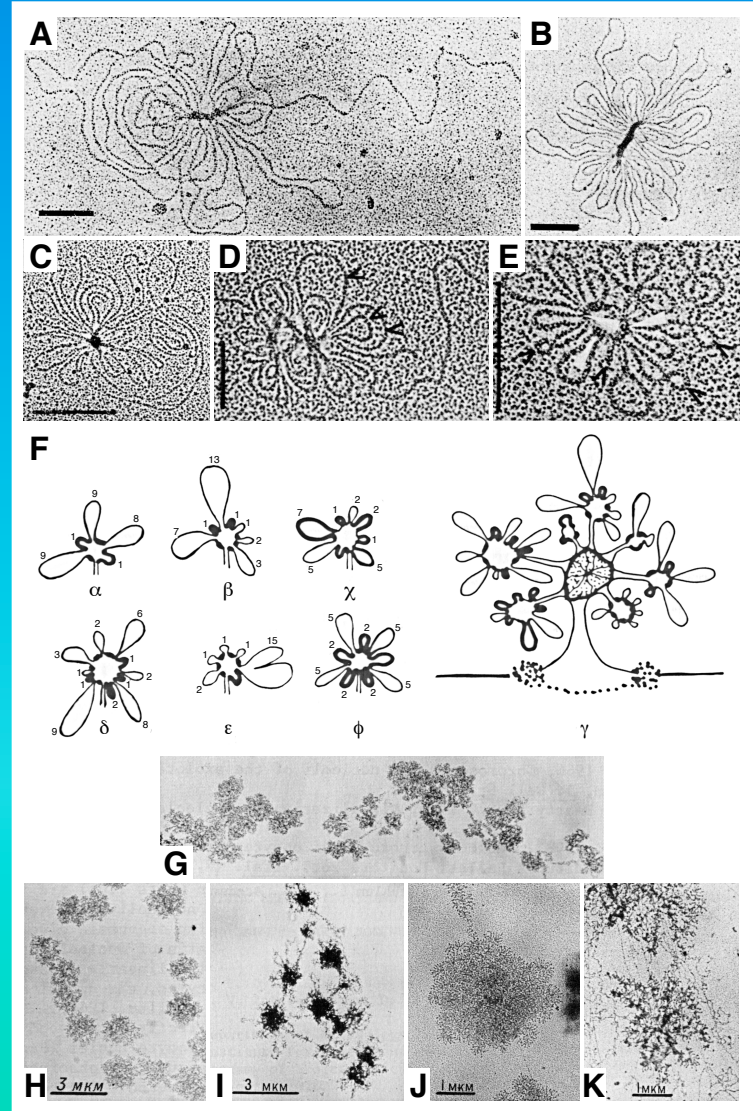
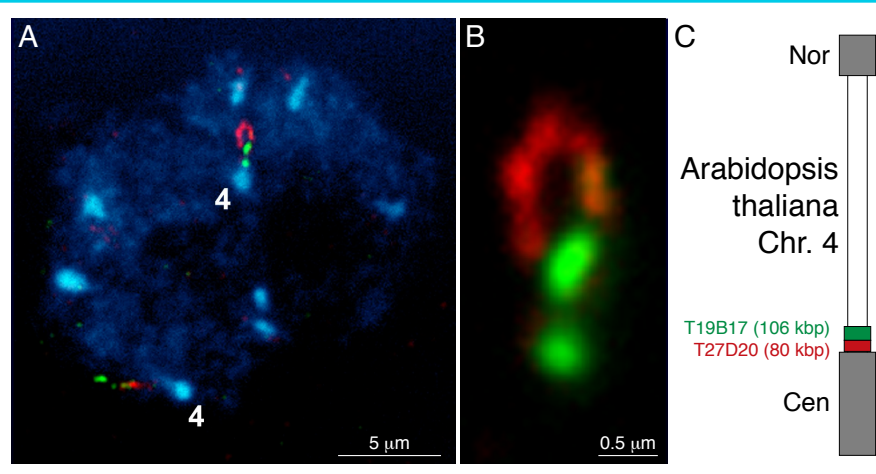
It becomes increasingly clearer, that the chromatin conformation is a random organization of nucleosomes, which depending on external or modification conditions has different condensation degrees, with a prevalence for the 30nm fiber with ~6nucleosomes per 11nm. This seems to make loops which further cluster to form aggregates more or less rosette-like which then constitute the chromosome.



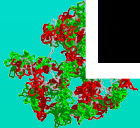
A-C: Voet & Voet; D: Reznik *et al.*



Courtesy P. Fransz, Amsterdam



A: B. Aramova *et al.*; C: Salganik *et al.*; D: G. Frznik *et al.*; G-K: Tsvetkov & Pavlov.

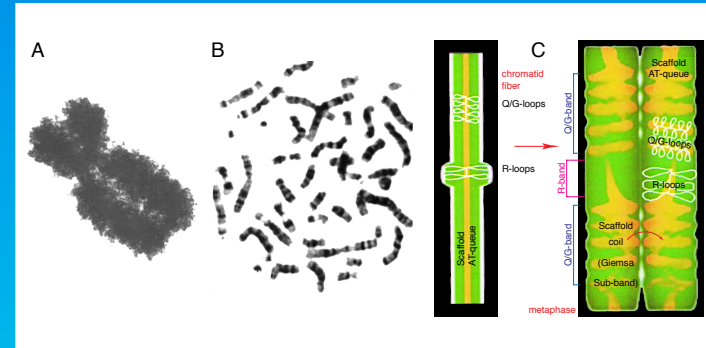
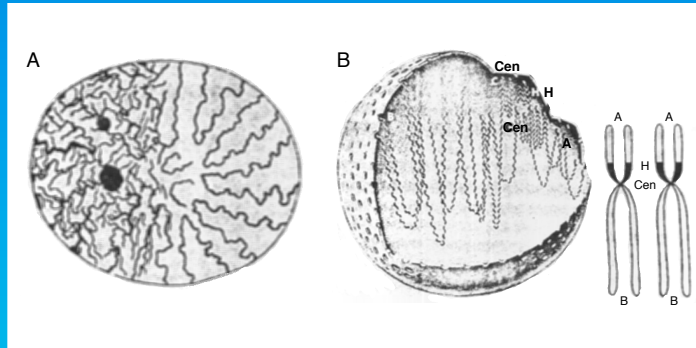


Integral Models of Cell Nuclear Organization I

Already Rabl and Boveri were aware of the obvious fact that the organization of genomes has to be consistent from the sequence level to the morphology of the whole cell nucleus. Although they might be different in detail their common seem is recursive folding and clustering thereof with variation/ modification and dynamics accounting for different nuclear states and function.

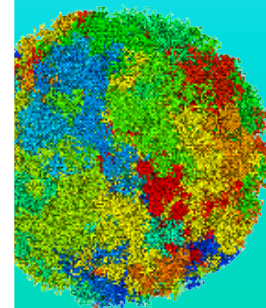
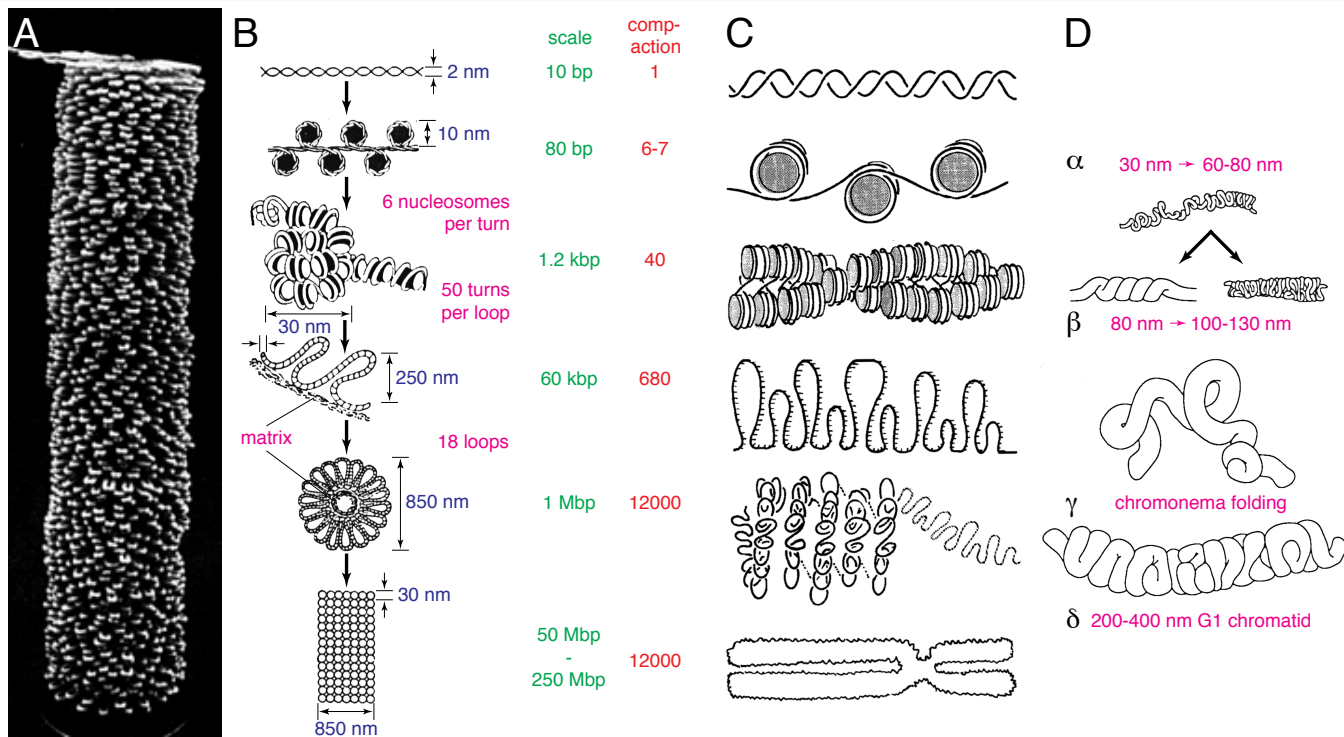


Rabl & Boveri



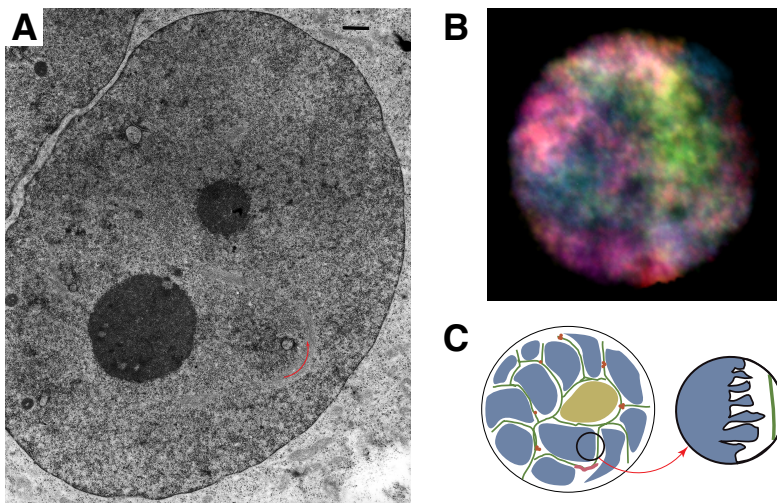
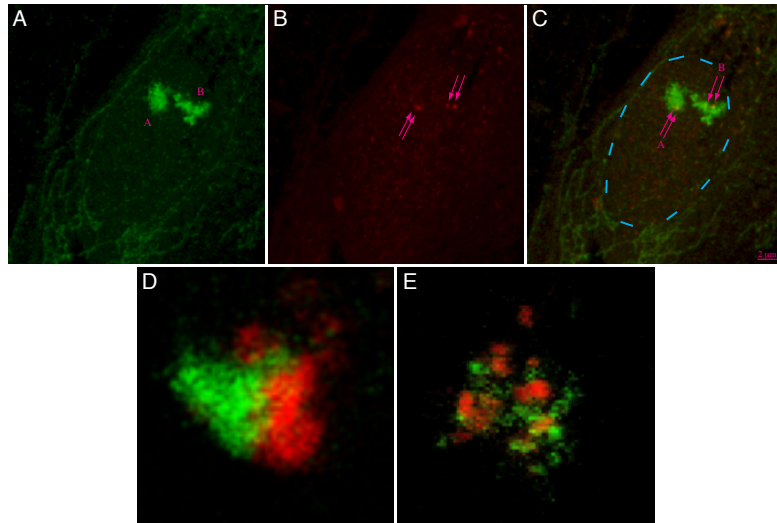
A: Bloom & Fawcett
B: Alberts *et al.*
C: Paulson & Laemmli

A, B: Pienta & Coffey; C: Alberts *et al.*; D: Belmont & Bruce

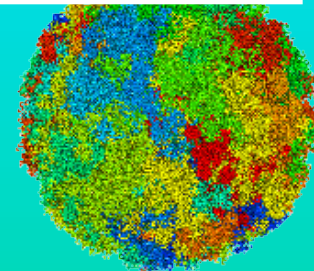
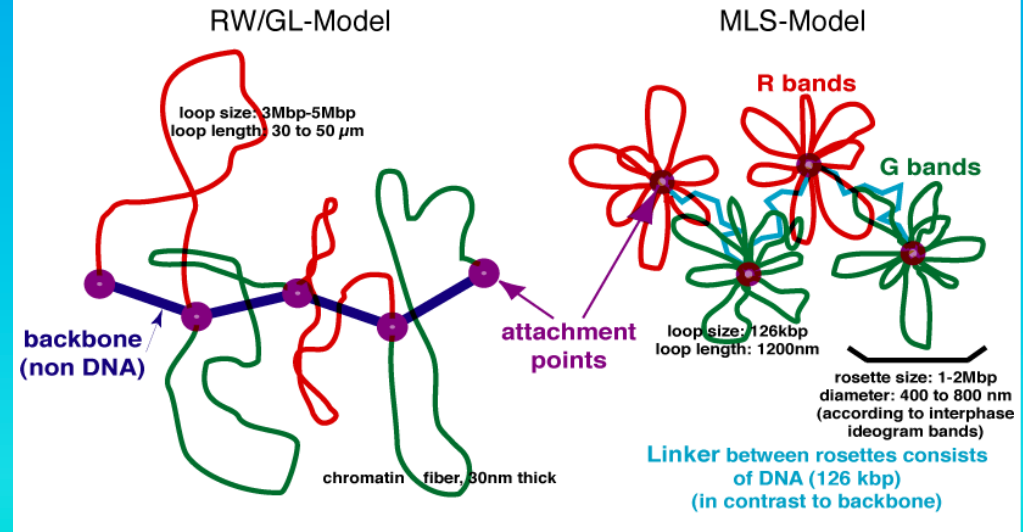


Integral Models of Cell Nuclear Organization

The biggest advantage of integral models is the again obvious and simple fact, that they allow the validation from the consistency of different levels of organization from the other levels. Thus, e.g. the so called Interchromosomal Domain Model can be ruled out by simple voluminous thought...



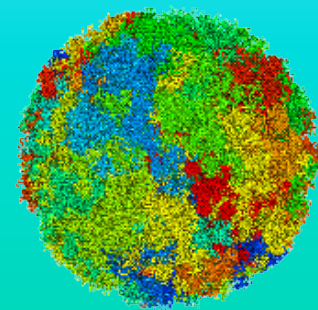
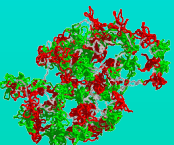
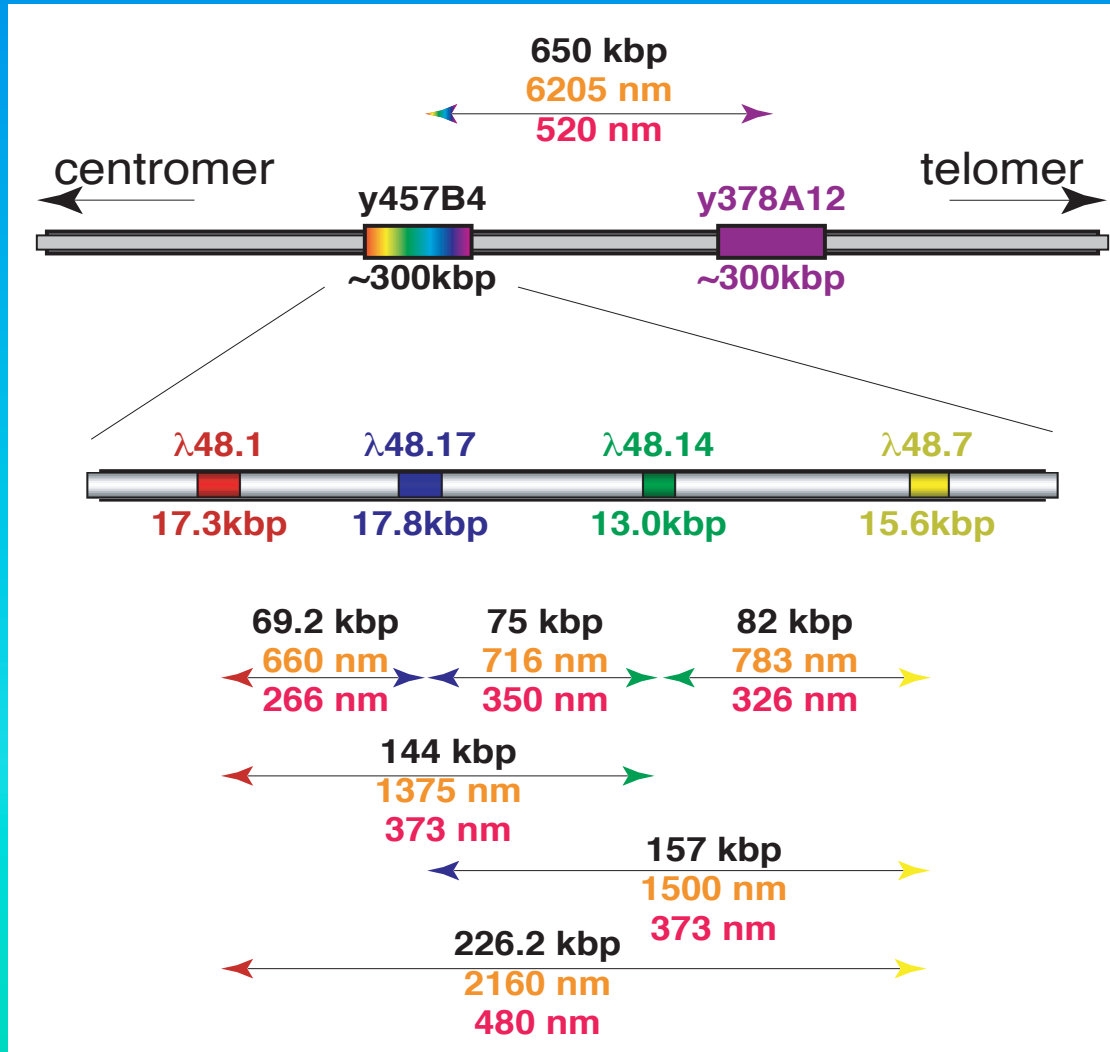
Random-Walk/Giant-Loop Multi-Loop-Subcompartment Model



A: courtesy K. Richter; B: courtesy K. Greulich-Bode

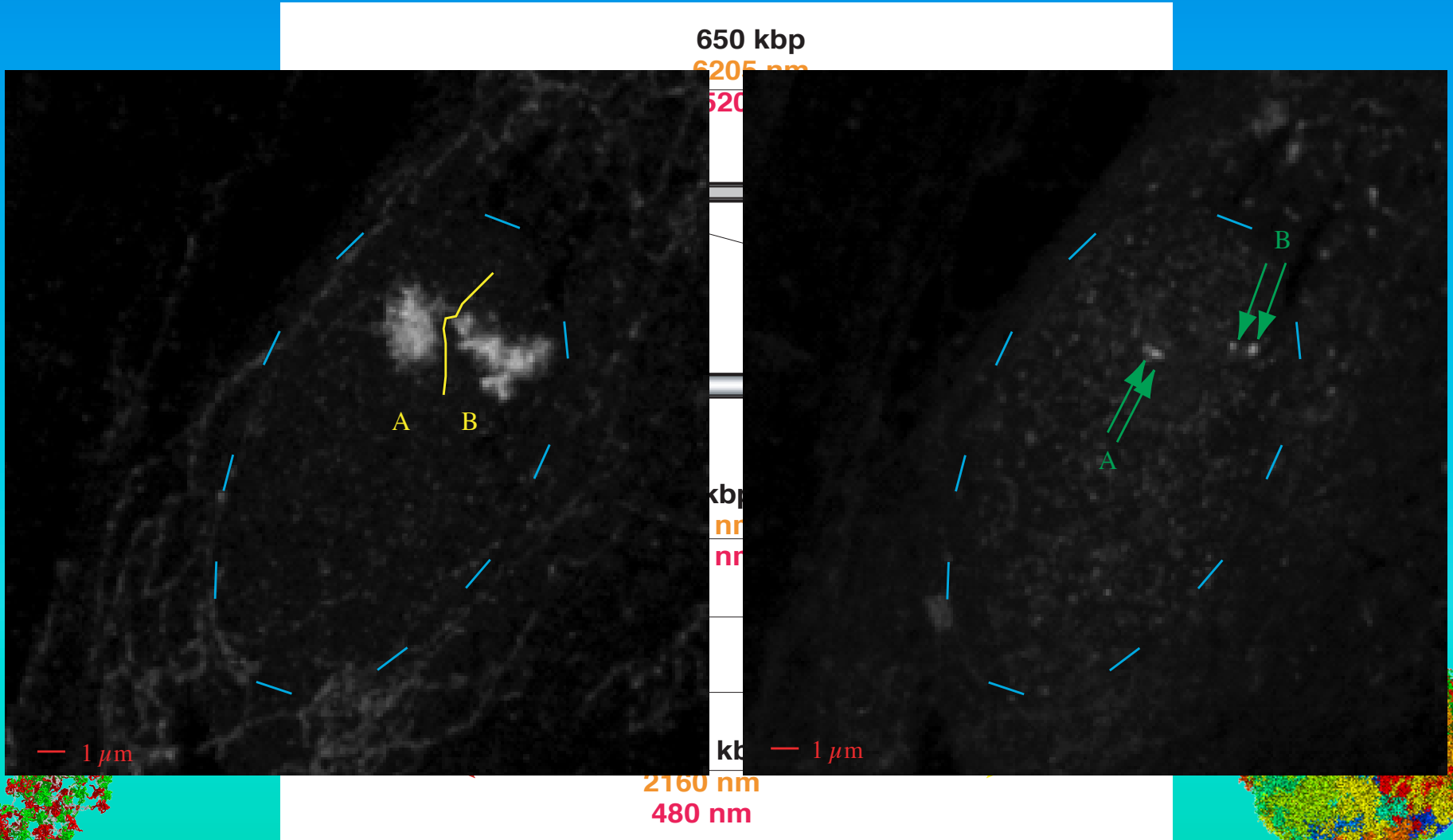
3D Architecture of the Prader-Willi Region

Fluorescence *in situ* hybridization with various protocols of small probes within the Prader-Willi region combined with spectral precision distance confocal laser scanning microscopy and comparison with large-scale computer simulations shows a Multi-Loop Subcompartment organization of the Prader-Willi region.



3D Architecture of the Prader-Willi Region

Fluorescence *in situ* hybridization with various protocols of small probes within the Prader-Willi region combined with spectral precision distance confocal laser scanning microscopy and comparison with large-scale computer simulations shows a Multi-Loop Subcompartment organization of the Prader-Willi region.



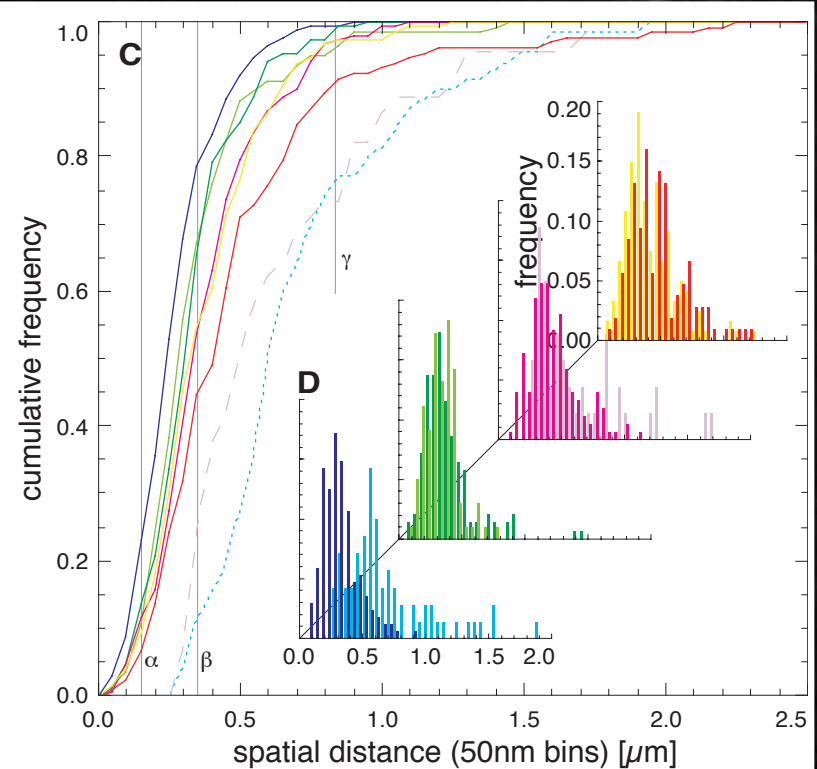
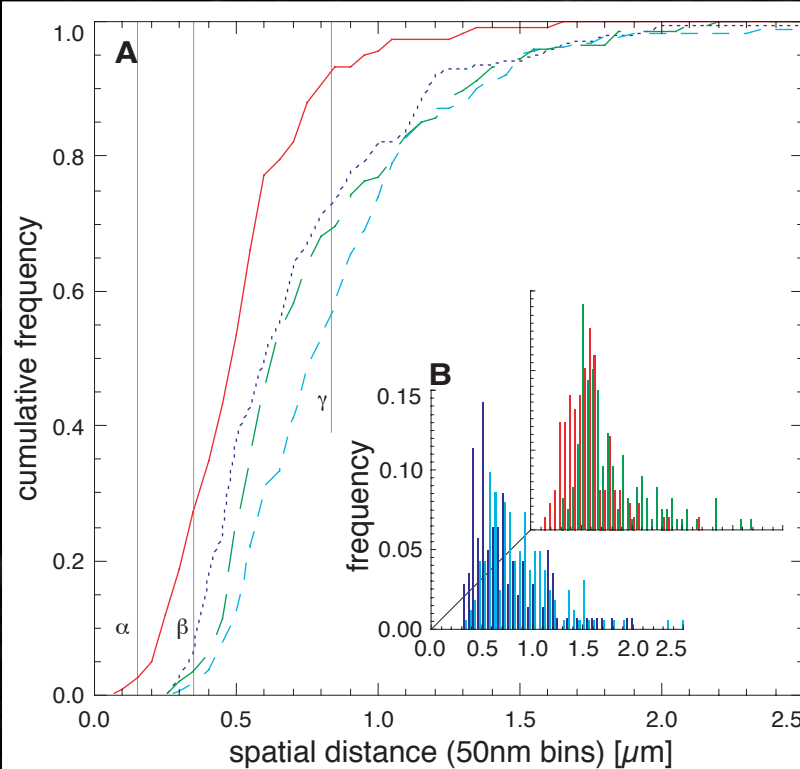
3D Architecture of the Prader-Willi Region

Fluorescence *in situ* hybridization with various protocols of small probes within the Prader-Willi region combined with spectral precision distance confocal laser scanning microscopy and comparison with large-scale computer simulations shows a Multi-Loop Subcompartment organization of the Prader-Willi region.



650 kbp

6205 nm
520



2160 nm
480 nm

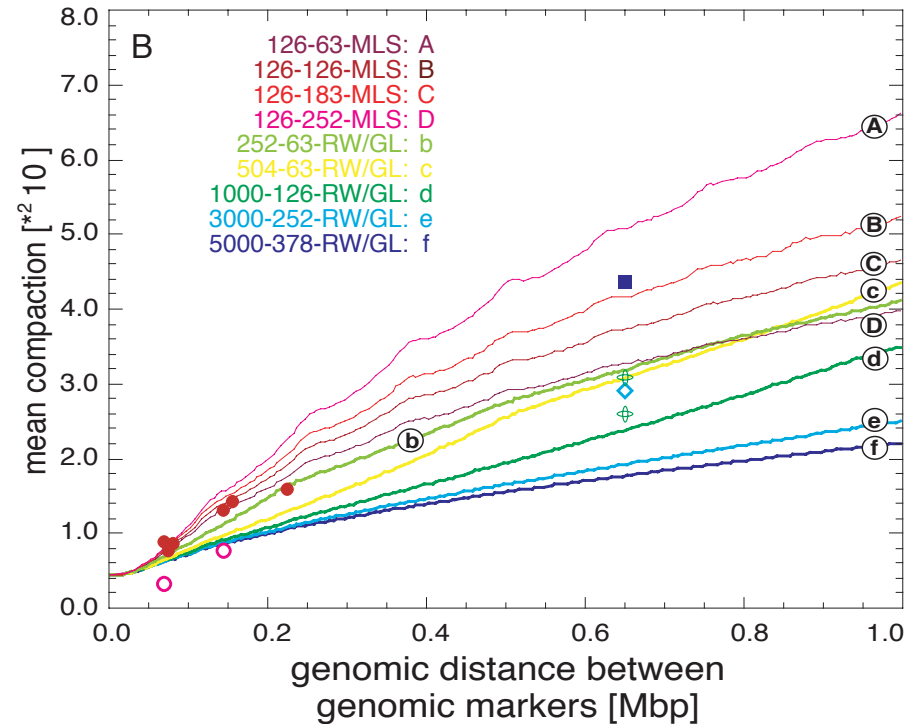
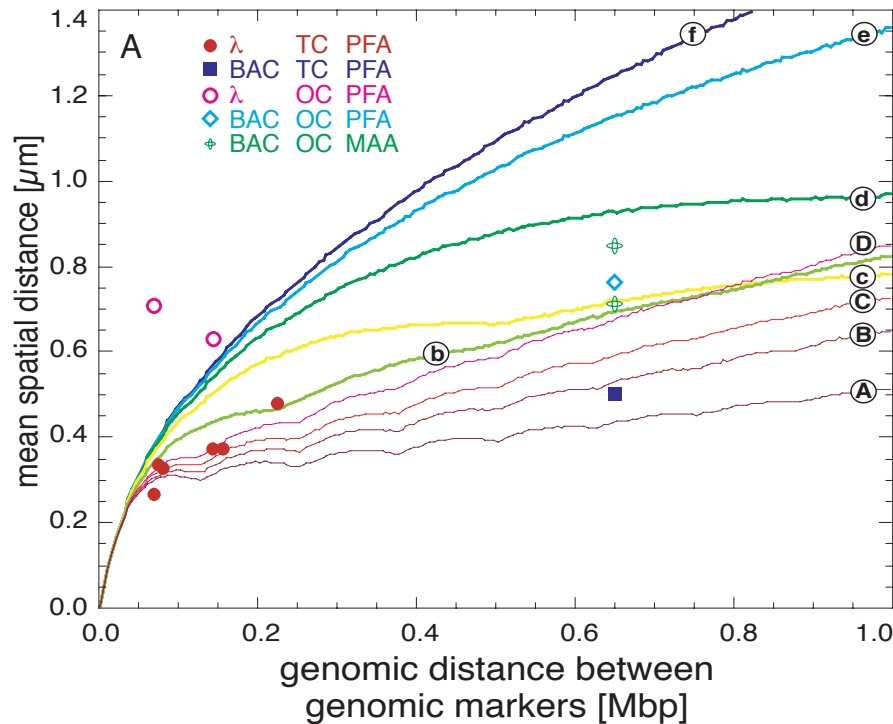
3D Architecture of the Prader-Willi Region

Fluorescence *in situ* hybridization with various protocols of small probes within the Prader-Willi region combined with spectral precision distance confocal laser scanning microscopy and comparison with large-scale computer simulations shows a Multi-Loop Subcompartment organization of the Prader-Willi region.



650 kbp

6205 nm

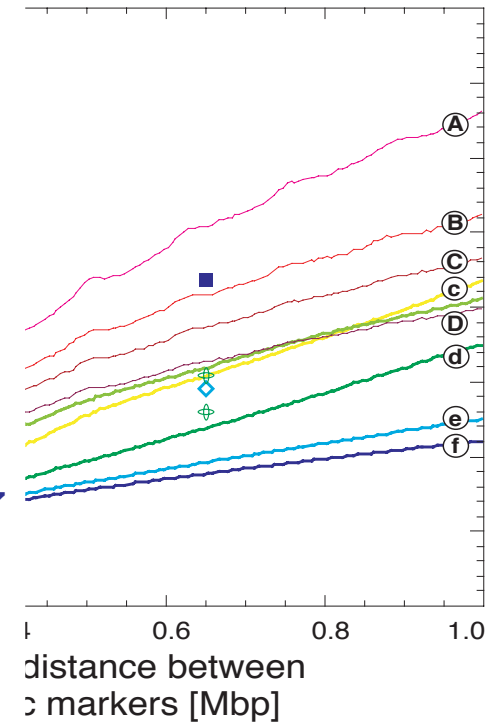
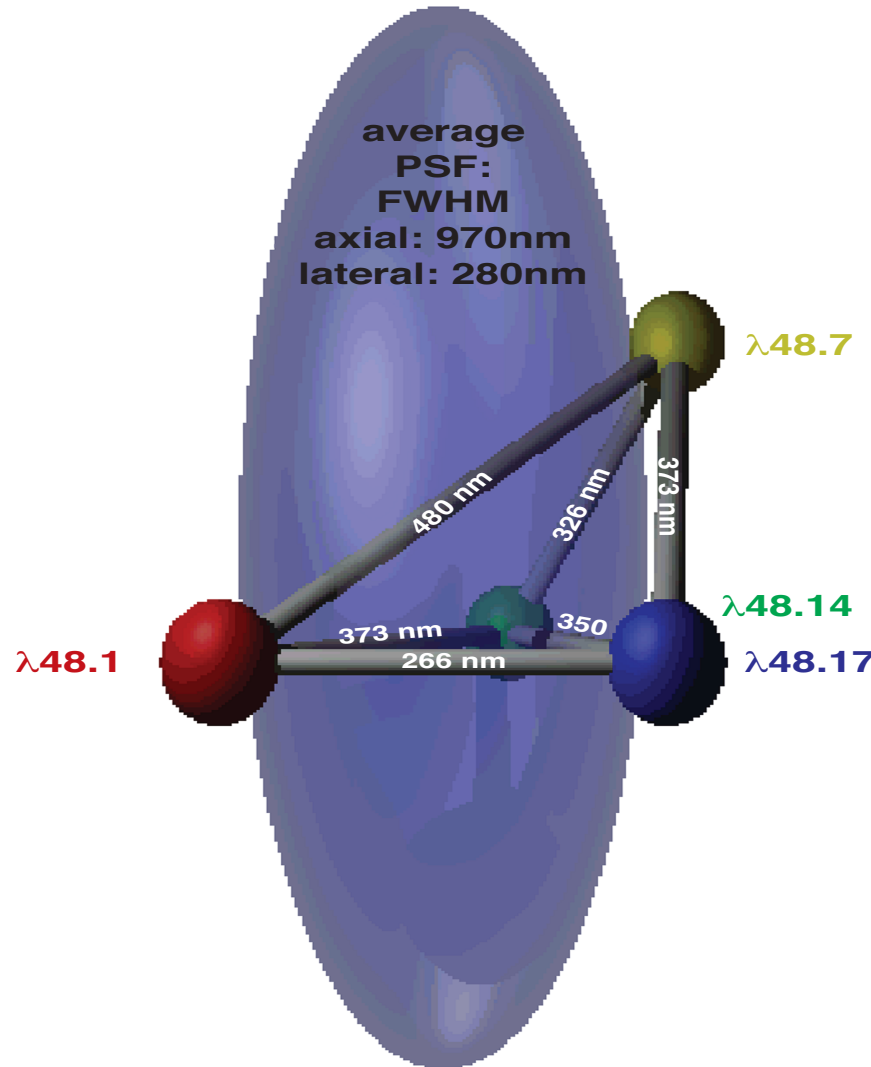
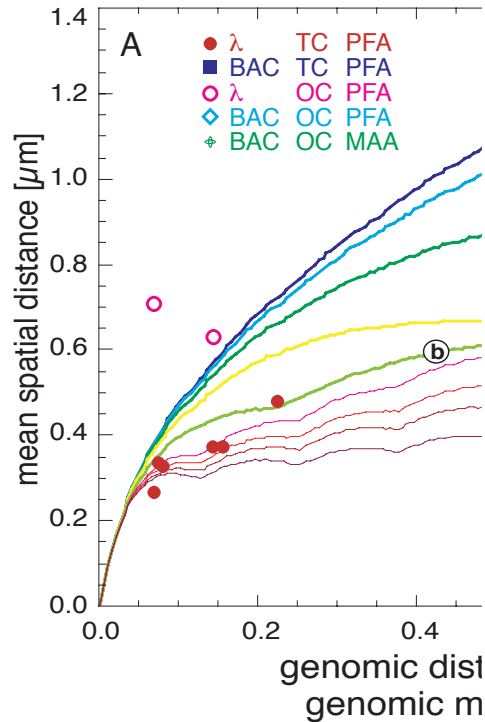


2160 nm

480 nm

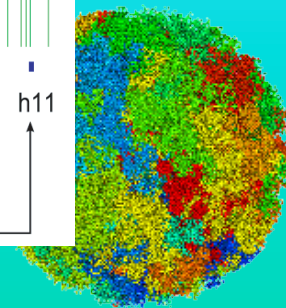
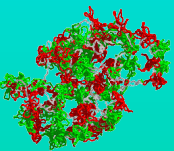
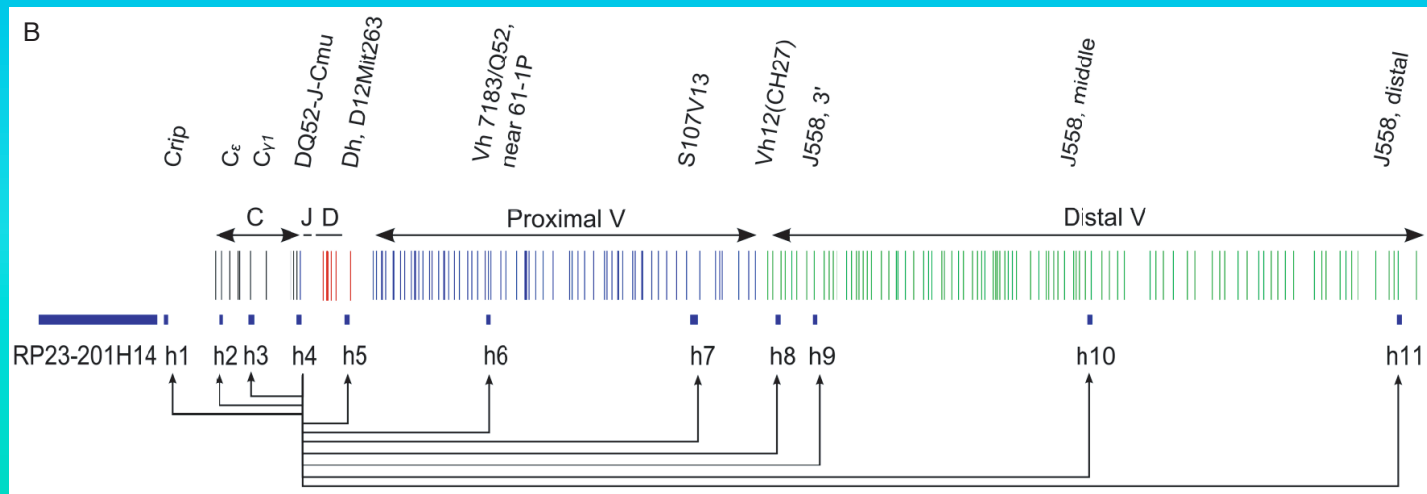
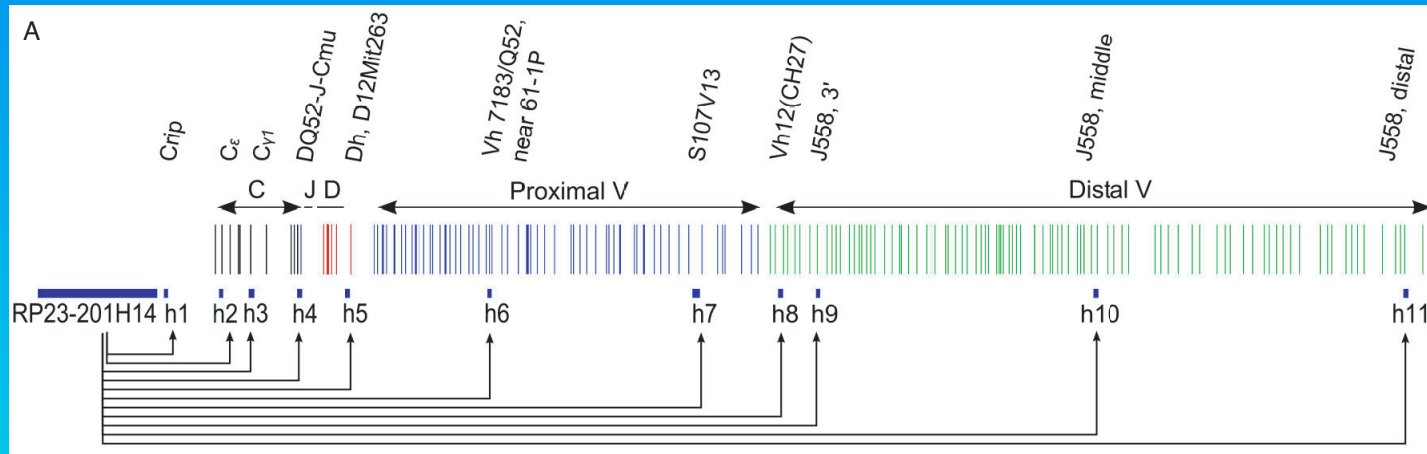
3D Architecture of the Prader-Willi Region

Fluorescence *in situ* hybridization with various protocols of small probes within the Prader-Willi region combined with spectral precision distance confocal laser scanning microscopy and comparison with large-scale computer simulations shows a Multi-Loop Subcompartment organization of the Prader-Willi region.



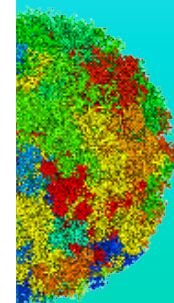
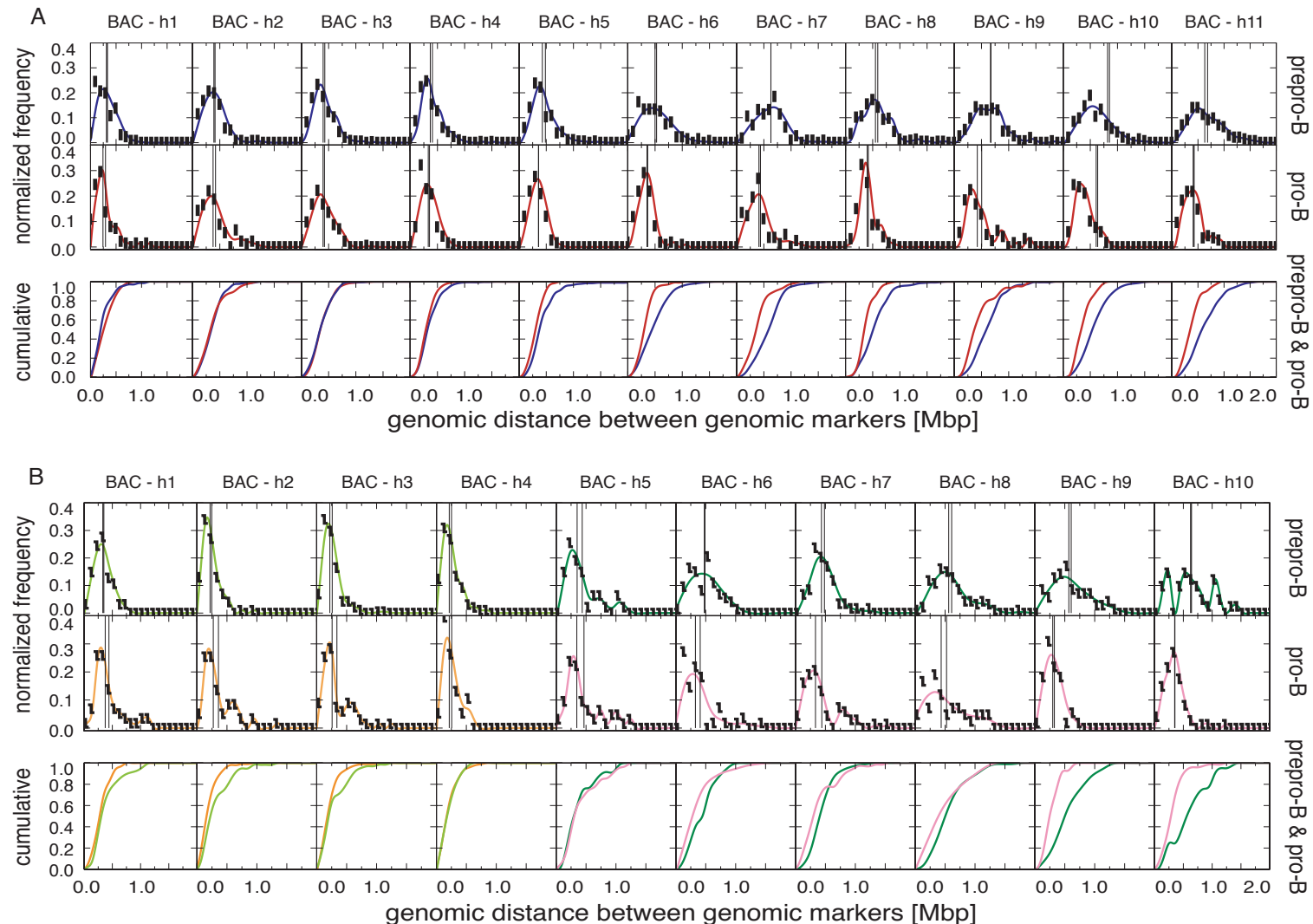
3D Architecture & Function of the IgH Locus

Fluorescence *in situ* hybridization of the IgH locus combined with spectral precision distance epifluorescence microscopy, analytical trilateration and comparison with computer simulations shows again a Multi-Loop Subcompartment organization of the IgH locus with functional relevant distances.



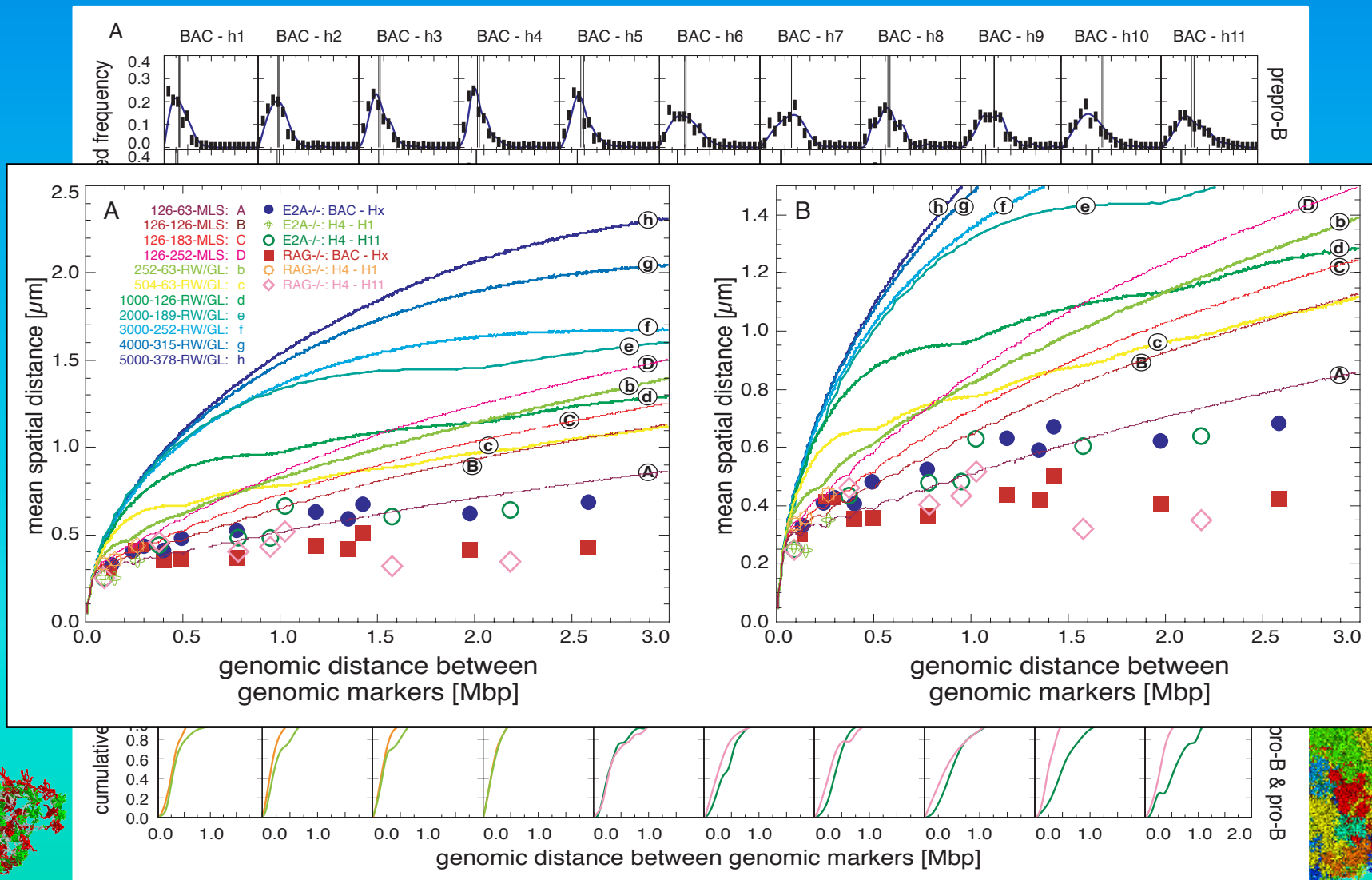
3D Architecture & Function of the IgH Locus

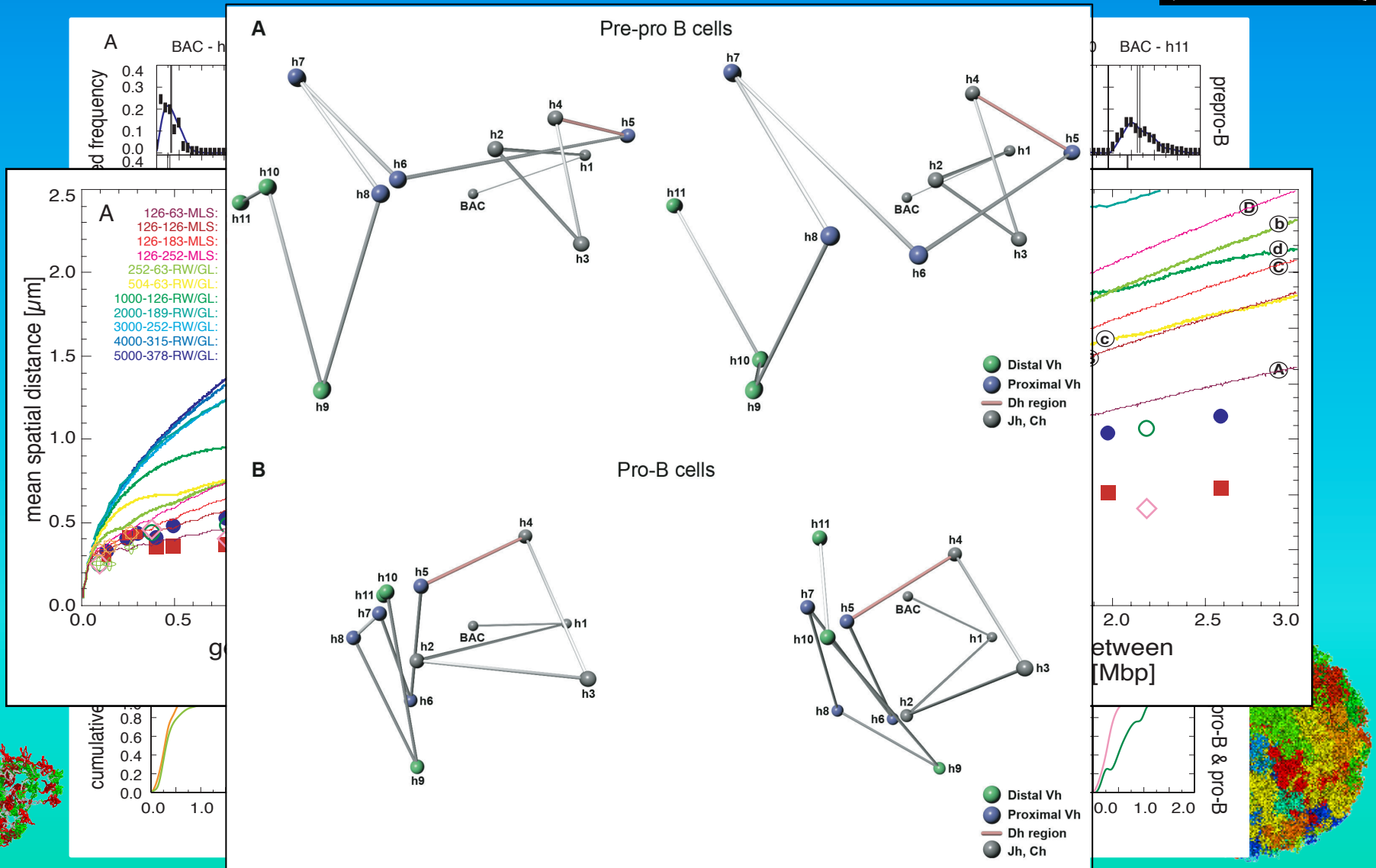

Fluorescence *in situ* hybridization of the IgH locus combined with spectral precision distance epifluorescence microscopy, analytical trilateration and comparison with computer simulations shows again a Multi-Loop Subcompartment organization of the IgH locus with functional relevant distances.



3D Architecture & Function of the IgH Locus

Fluorescence *in situ* hybridization of the IgH locus combined with spectral precision distance epifluorescence microscopy, analytical trilateration and comparison with computer simulations shows again a Multi-Loop Subcompartment organization of the IgH locus with functional relevant distances.





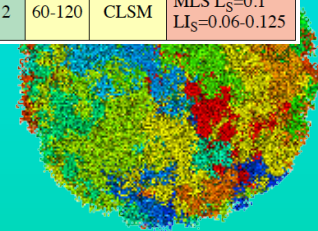
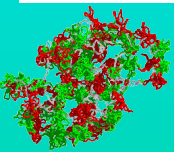
“Synoptic” 3D Architecture of Various Loci

A history “synoptic” comparison of the spatial distance mapping from their original background and aim, FISH methodological protocols, via microscopic imaging and restoration analysis procedures, to their interpretation, reveals that with time Multi-Loop Subcompartment models are favoured.



Study	Location	Preparation of Cells			FISH			Microscopy		Fit to model
		Cell cycle	KCl [nM]	Fixative	Melting	Label	Colours	# of nuclei	Image acquisition	
Fig. 3B, Trask '89	DHFR	UA41 G1-cf	75 dropped	MAA 3:1	FM 50 %	Biotin	1	20-37	photo, wall	RWGL 0.08-J RWGL 1.0
Fig. 3B, Lawrence '90	Dystrophin	WI38F G1	75 dropped	MAA 3:1	FM 50 %	Biotin	1	20-60	photo, wall	RWGL 0.5-1
Fig. 3A, Trask '91	Xq28	F G1-cf	75 dropped	MAA 3:1	FM 50 %	Biotin	1	30-60	photo, wall	RWGL 0.7 J RWGL 2.0- >5.0
Fig. 3B, Trask '91	Xq28	F G1-cf	75 dropped	MAA 3:1	FM 50 %	Biotin Dig	2	30-60	photo, wall	RWGL 1.0-3.0
Fig. 3, v.d. Engh '92 or Fig. 5A, Trask '93	4p16.3	F G1-cf	75 dropped	MAA 3:1	FM 50 %	Biotin Dig	2	?	photo, d-board	$L_S \leq 0.1$ for $GS < 0.5 < RWGL > 5.0$
Fig. 5B, Trask '93	6p21	F G1-cf	75	MAA 3:1	FM 50-70 %	Biotin Dig	2	?	photo, d-board	$L_S \leq 0.1$ for $GS < 1.0 < RWGL 1.0-5.0$
Fig. 5, Senger '93	MHC 6p21.31	HFF G1-cf	?	?	FM 50 %	Biotin	1	> 30	photo, wall	MLS L_S & $LI_S = 0.12-0.25$ RWGL 0.1-0.5
Fig. 5, Senger '93	MHC 6p21.31	HFF G1-cf	?	?	FM 50 %	Biotin Dig	2	> 30	photo, wall	MLS $L_S = 0.1$ $LI_S = 0.18$ RWGL 0.1-0.5
Fig. 1, Warrington '94	4p16.3	F G1-cf	75	MAA 3:1	FM 50 %	Biotin Dig	2	?	?	RWGL > 5.0
Tab. 1, Warrington '94	5q31-33	L	?	?	?	?	?	?	CLSM BioRad	RWGL > 5.0
Fig. 2B, Yokota '95	4p16.3	F G1-cf	40 dropped	MAA 3:1	FM 70 %	Biotin Dig	2	40-360	photo, d-board	RWGL 2.0-4.0
Fig. 3B, Yokota '95	4p16.3	F G1-cf	-	PFA 4 %	FM 70 %	Biotin Dig	2	40-350	photo, d-board	MLS L_S & $LI_S = 0.1-0.125$

Study	Location	Preparation of Cells			FISH			Microscopy		Fit to model
		Cell cycle	KCl [nM]	Fixative	Melting	Label	Colours	# of nuclei	Image acquisition	
Fig. 2A, Yokota '97	4p16.3 R-band	F G1-cf	40 dropped	MAA 3:1	FM 70 %	Biotin Dig	2	37-178	photo, d-board	RWGL 2.0-3.0
Fig. 2B, Yokota '97	6p21.3 R-band	F G1-o	40 dropped	MAA 3:1	FM 70 %	Biotin Dig	2	37-178	photo, d-board	RWGL 4.0-5.0
Fig. 2C, Yokota '97	21q22.2 G-band	F G1-o	40 dropped	MAA 3:1	FM 70 %	Biotin Dig	2	37-178	photo, d-board	RWGL 1.0-2.0
Fig. 2D, Yokota '97	Xp21.3 G-band	F G1-o	40 dropped	MAA 3:1	FM 70 %	Biotin Dig	2	37-178	photo, d-board	RWGL 0.5-0.9
Fig. 2D, Yokota '97	Xq28 R-band	F G1-of	40 dropped	MAA 3:1	FM 70 %	Biotin Dig	2	37-178	photo, d-board	RWGL 1.0-5.0j
Fig. 2A, Yokota '97	Xp21.3 G-band	F	-	PFA 4 %	FM 70 %	Biotin Dig	2	37-178	photo, d-board	RWGL 0.25 MLS $L_S = 0.126$ $LI_S = 0.200$
Fig. 2A, Yokota '97	Xq28 R-band	F	-	PFA 4 %	FM 70 %	Biotin Dig	2	37-178	photo, d-board	RWGL 1.0
Fig. 4B, Yokota '97	Xp21.3 G-band	HeLa	40 dropped	MAA 3:1	FM 70 %	Biotin Dig	2	37-178	photo, d-board	RWGL 0.25 MLS $L_S = 0.126$ $LI_S = 0.200$
Fig. 4B, Yokota '97	Xq28 R-band	HeLa	40 dropped	MAA 3:1	FM 70 %	Biotin Dig	2	37-178	photo, d-board	RWGL 1.0
Monier '97	11q13	F	-	PFA 4 %	FM 70 %	Biotin Dig	1	22-69	CLSM	MLS $L_S = 0.126$ $LI_S = 180$
Monier '97	11q13	L	-	PFA 4 %	FM 70 %	Biotin Dig	1	22-69	CLSM	MLS $L_S = 0.1$ $LI_S = 0.18-0.24$
Knoch '98/ Rauch '99	15q11-21	F	-	PFA 4 %	FM 70 %	Biotin Dig	1 & 2	60-120	CLSM	MLS $L_S = 0.1$ $LI_S = 0.06-0.125$

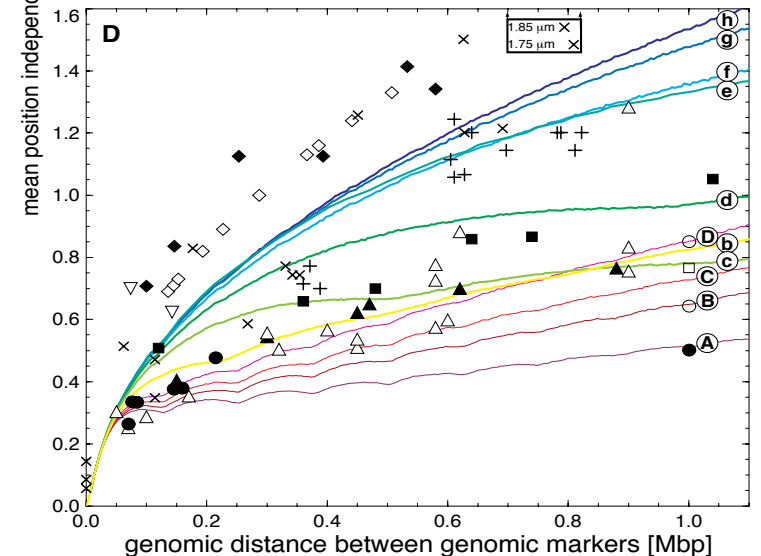
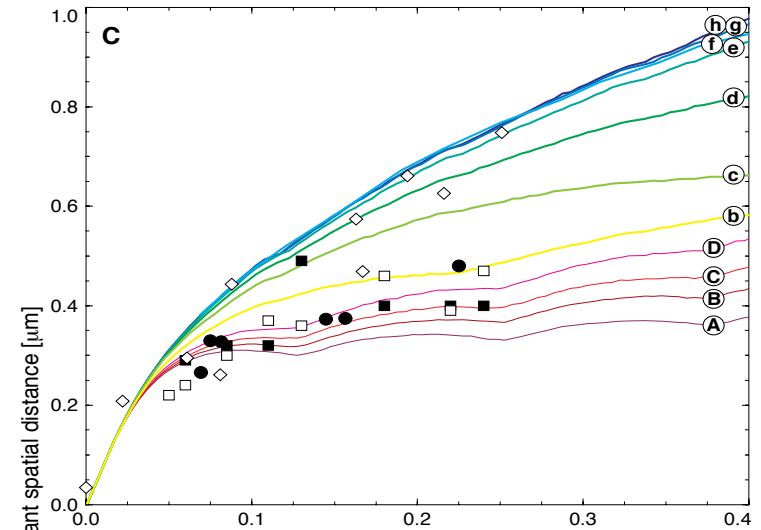
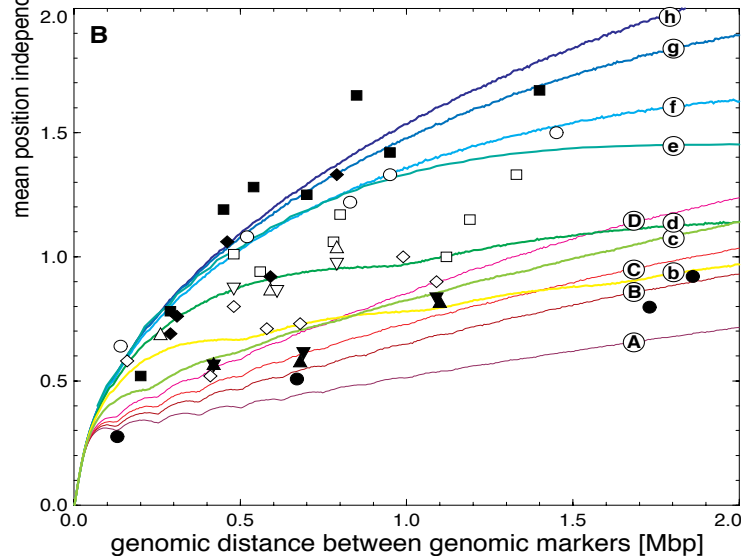
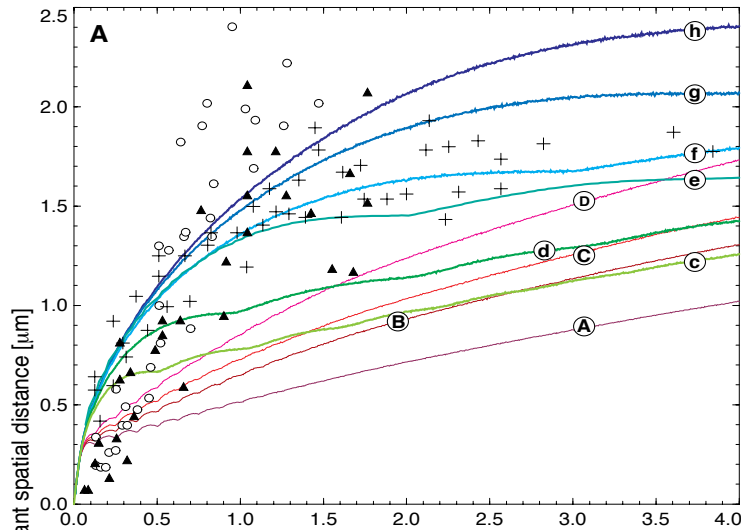


“Synoptic” 3D Architecture of Various Loci

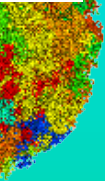
A history “synoptic” comparison of the spatial distance mapping from their original background and aim, FISH methodological protocols, via microscopic imaging and restoration analysis procedures, to their interpretation, reveals that with time Multi-Loop Subcompartment models are favoured.



Study
Fig. 3B, Tr '89
Fig. 3B, Lawrence '91
Fig. 3A, Tr '91
Fig. 3B, Tr '91
Fig. 3, v.d. '92 or Fig. Trask '93
Fig. 5B, Tr '93
Fig. 5, Senger '93
Fig. 5, Senger '93
Fig. 1, Warrington
Tab. 1, Warrington
Fig. 2B, Ye '95
Fig. 3B, Ye '95

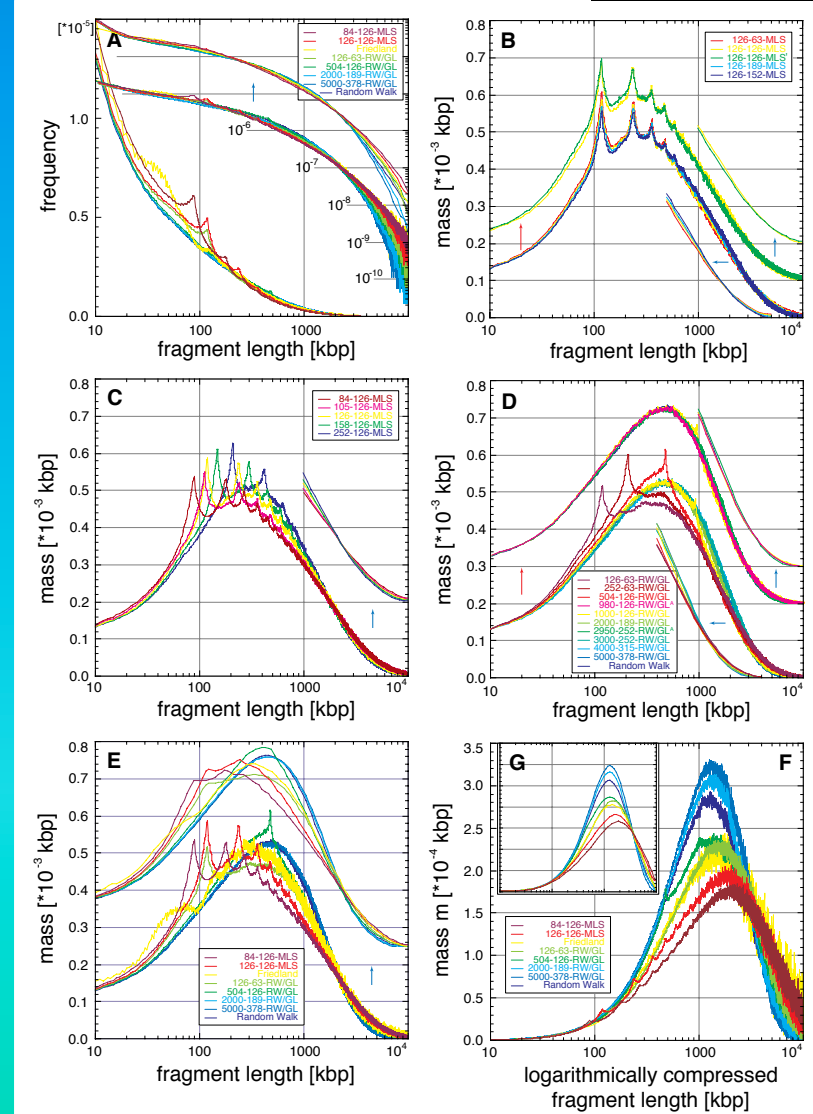
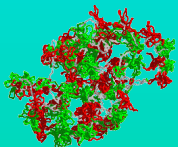
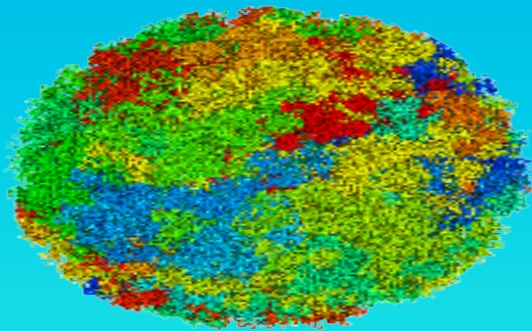


to model
L 2.0-3.0
L 4.0-5.0
L 1.0-2.0
L 0.5-0.9
L 1.0-5.0j
L 0.25
L _S =0.126
0.200
L 1.0
L 0.25
L _S =0.126
0.200
L 1.0
L _S =0.126
180
L _S =0.1
0.18-0.24
L _S =0.1
0.06-0.125



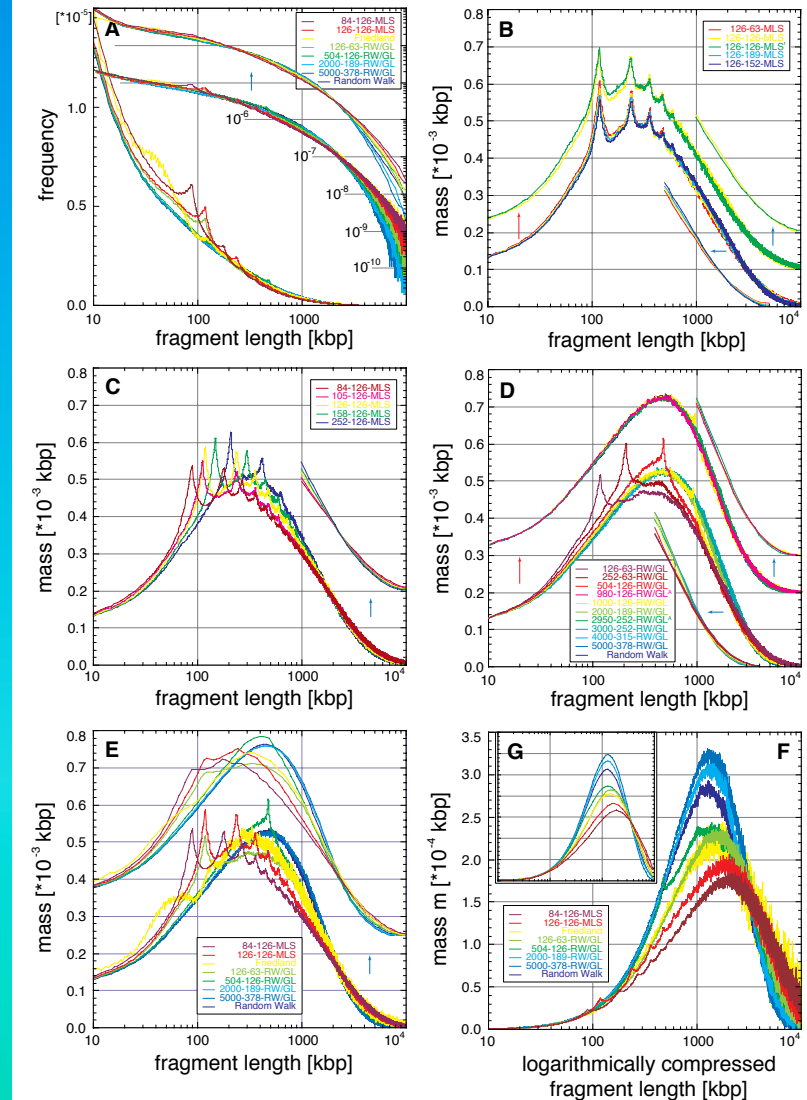
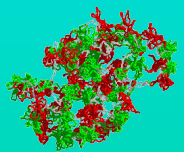
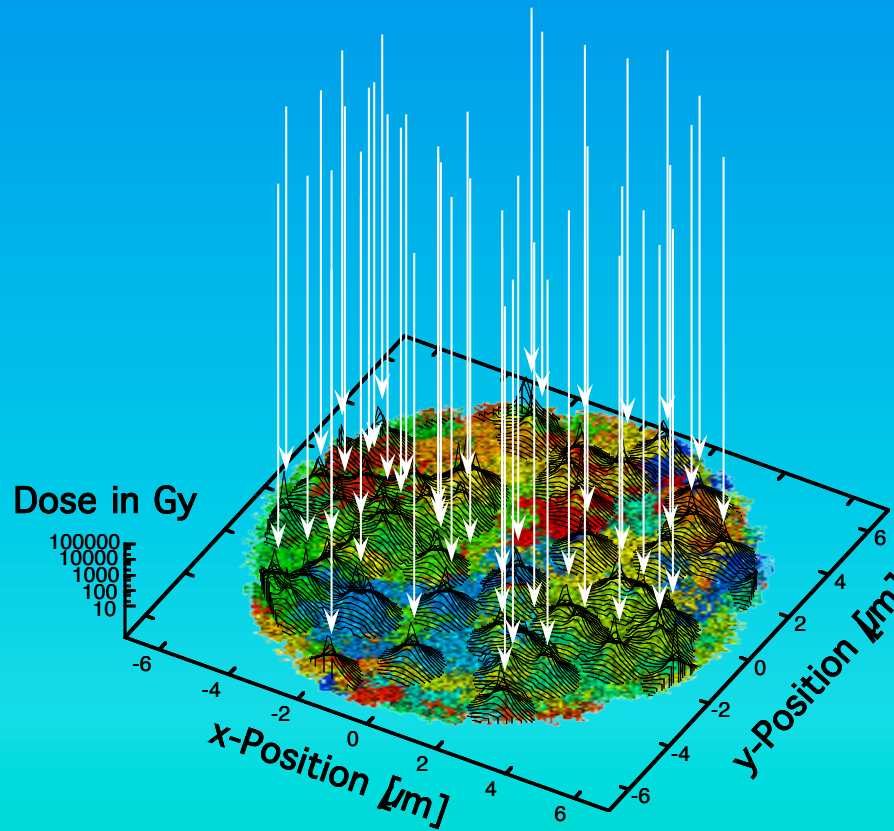
DNA Fragment Distribution after Ione-Irradiation

The length distribution of DNA fragments after irradiation with e. g. C or Ca with an inhomogeneous spatial double strand breakage probability depends on the detailed folding topology of the chromatin fiber and the RW/GL and MLS models differ largely.



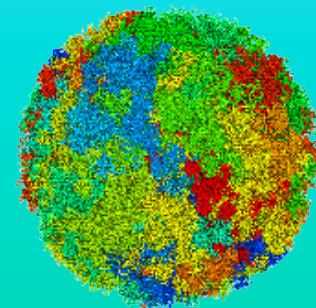
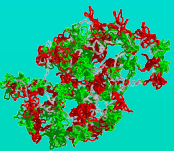
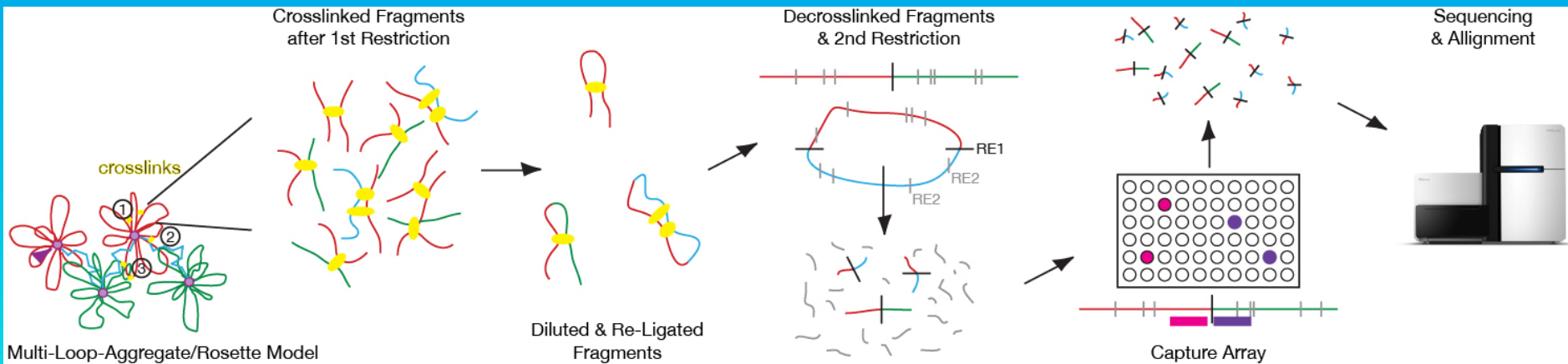
DNA Fragment Distribution after Ione-Irradiation

The length distribution of DNA fragments after irradiation with e. g. C or Ca with an inhomogeneous spatial double strand breakage probability depends on the detailed folding topology of the chromatin fiber and the RW/GL and MLS models differ largely.



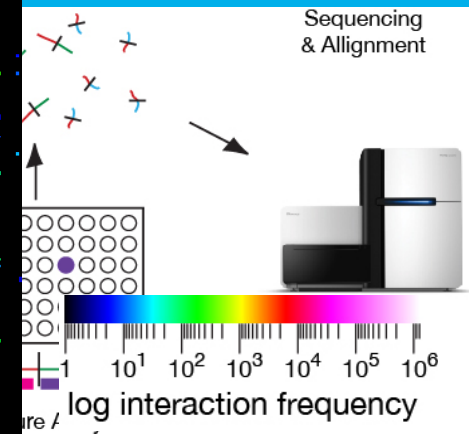
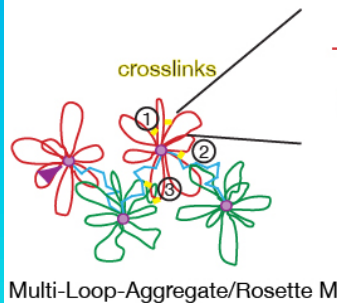
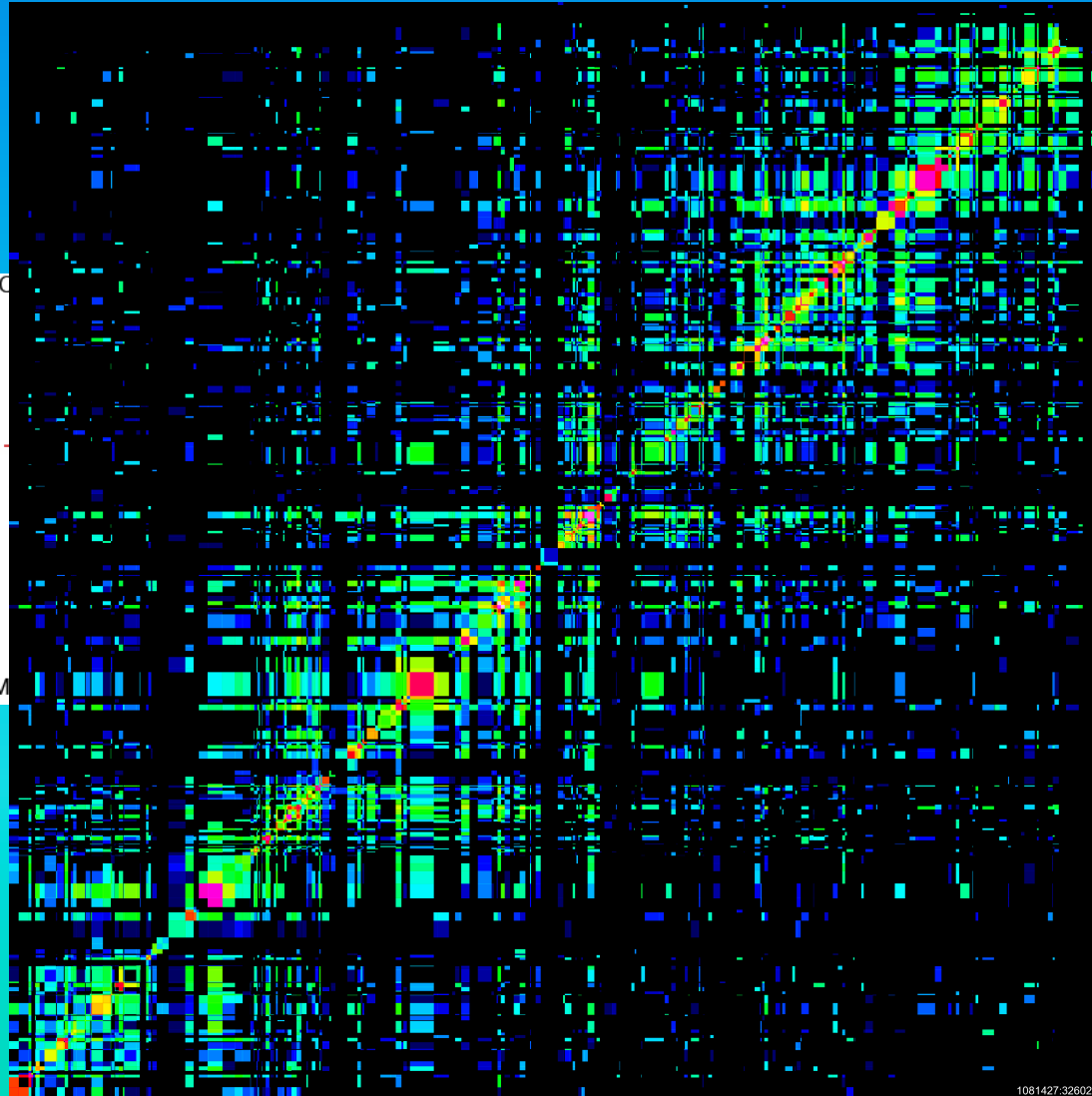
Selective Chromosome Interaction Capture (T2C)

T2C is a novel selective high-resolution high-throughput chromosome interaction capture, in which the relation between, region size, resolution, interaction frequency range, and sequencing depth can be designed towards the goal of the experiment. T2C reaches the limit of the “genomic” uncertainty principle and statistical mechanics.

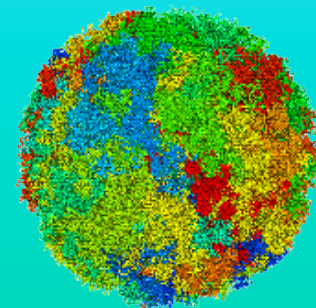
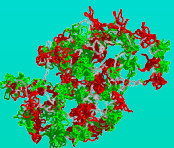


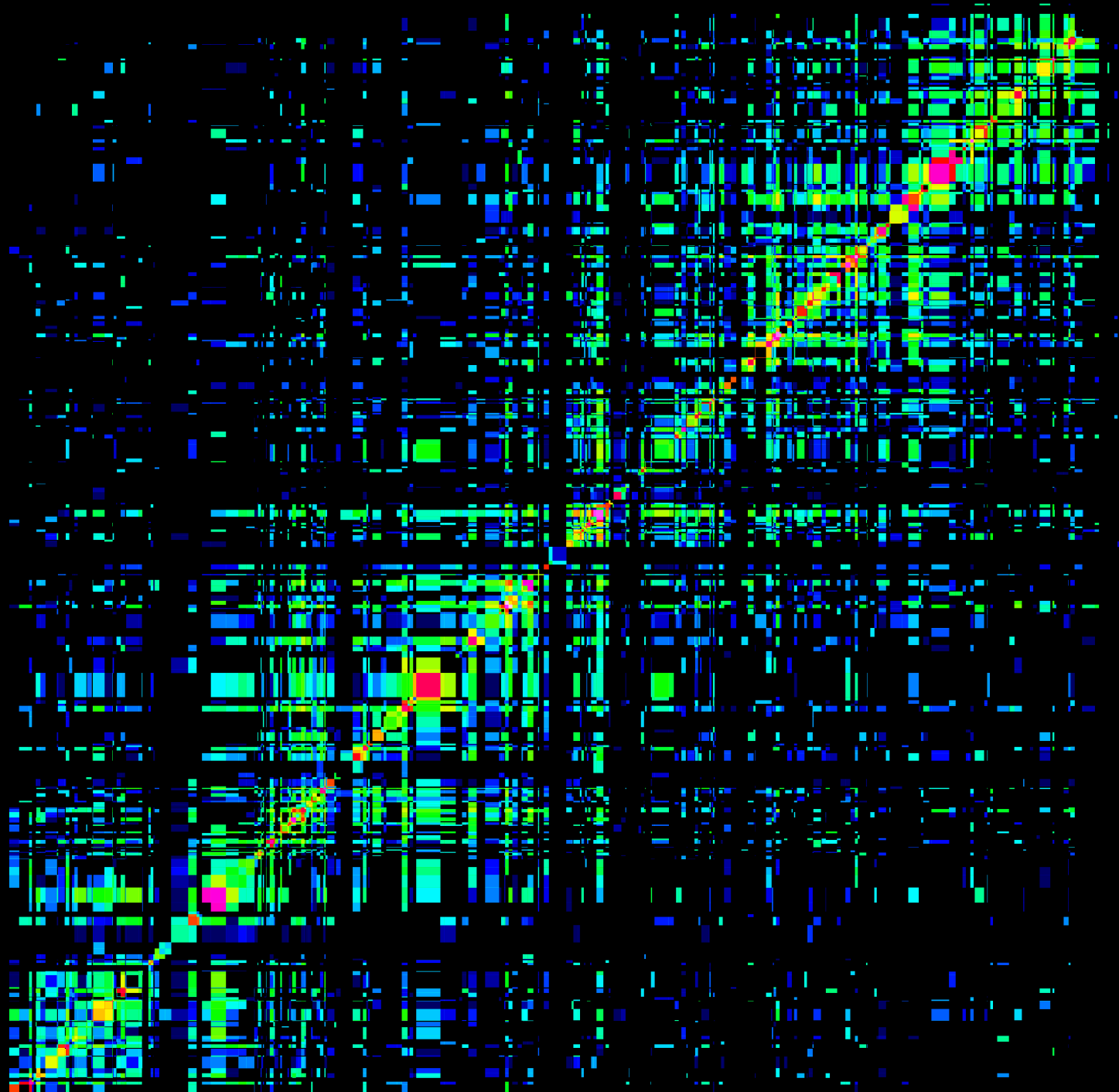
Selective Chromosome Interaction Capture (T2C)

T2C is a novel selective high-resolution high-throughput chromosome interaction capture, in which the relation between, region size, resolution, interaction frequency range, and sequencing depth can be designed towards the goal of the experiment. T2C reaches the limit of the “genomic” uncertainty principle and statistical mechanics.



HS IGF locus
~2.1 Mbp



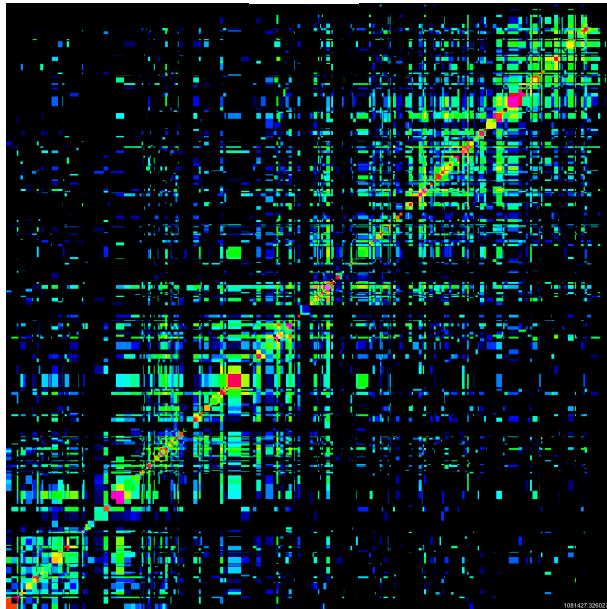


Stable Consensus Architecture of Genomes

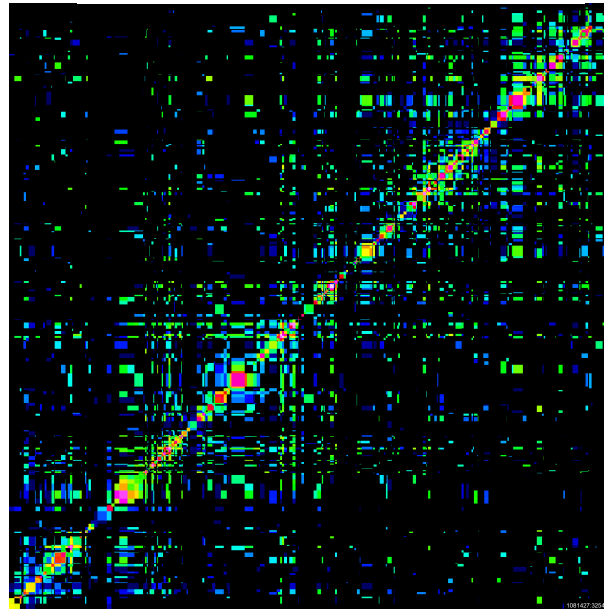
Due to the high signal-to-noise ratio of T2C reaching 5-6 orders of magnitude interaction maps reveal definitely an extremely high degree of similarity between different species, cell types, or functional states, thus functional differences are variation of a stable theme persisting through the cell cycle



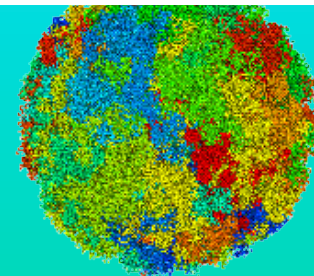
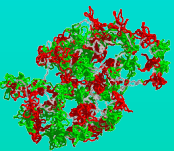
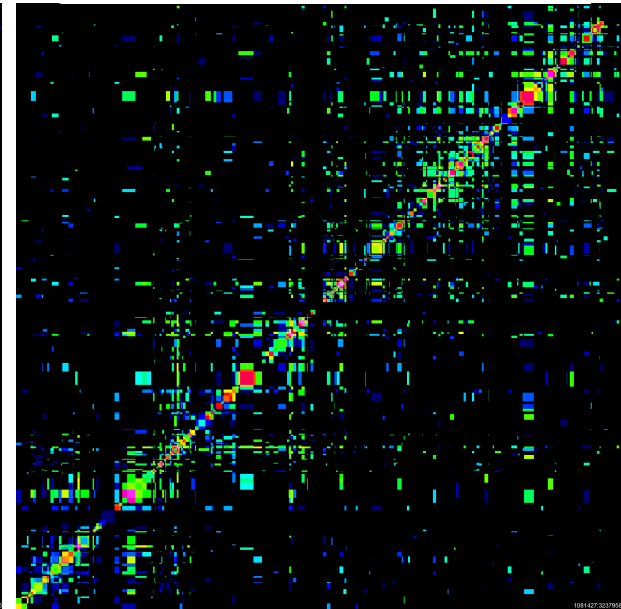
HB2



TEV-HEK293T cohesin intact



HRV-HEK293T cohesin cleaved

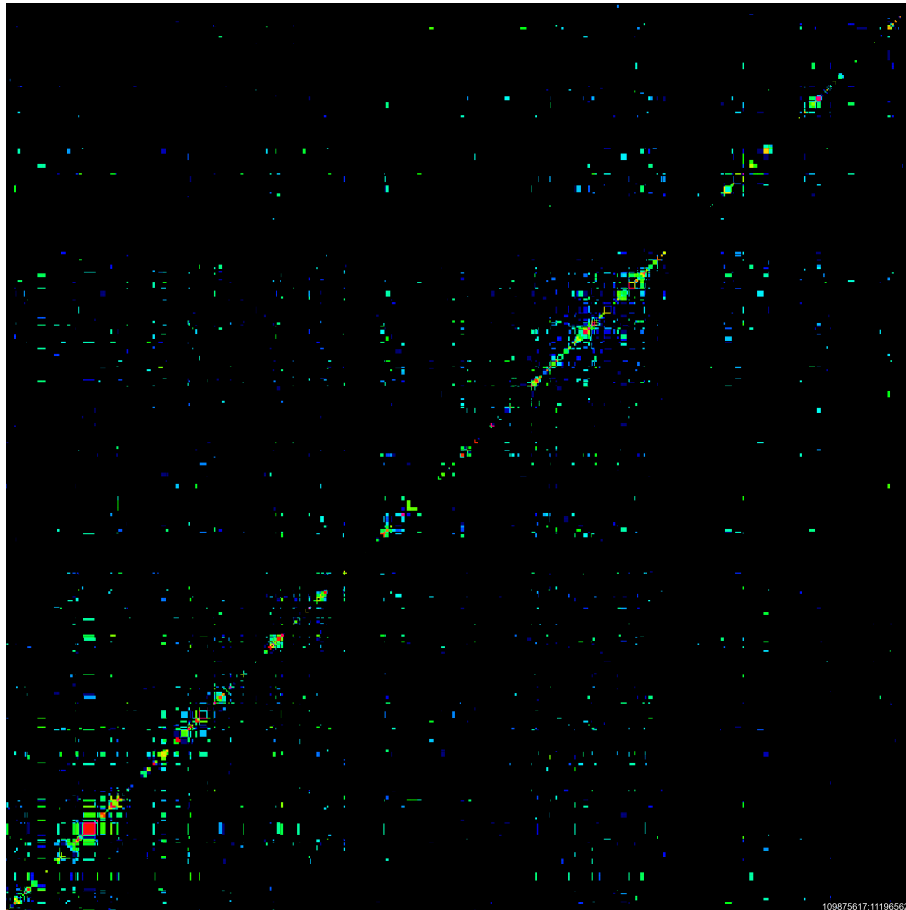


Stable Consensus Architecture of Genomes

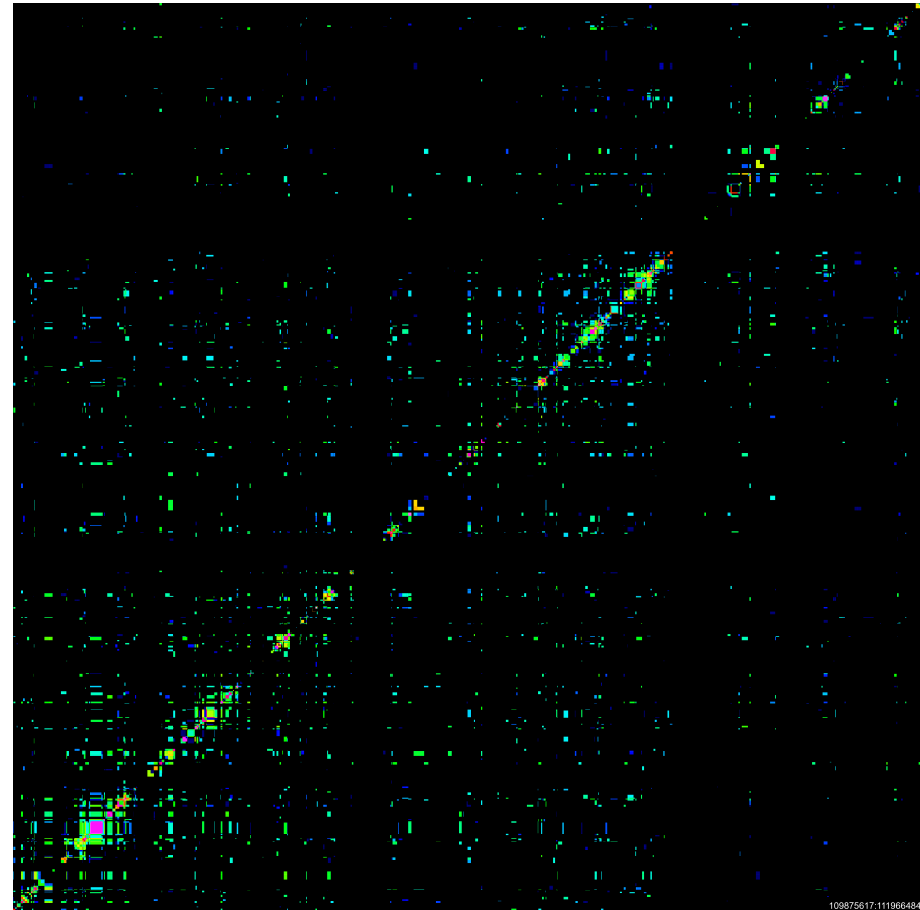
Due to the high signal-to-noise ratio of T2C reaching 5-6 orders of magnitude interaction maps reveal definitely an extremely high degree of similarity between different species, cell types, or functional states, thus functional differences are variation of a stable theme persisting through the cell cycle



Fetal Brain (inactive β -Globin)



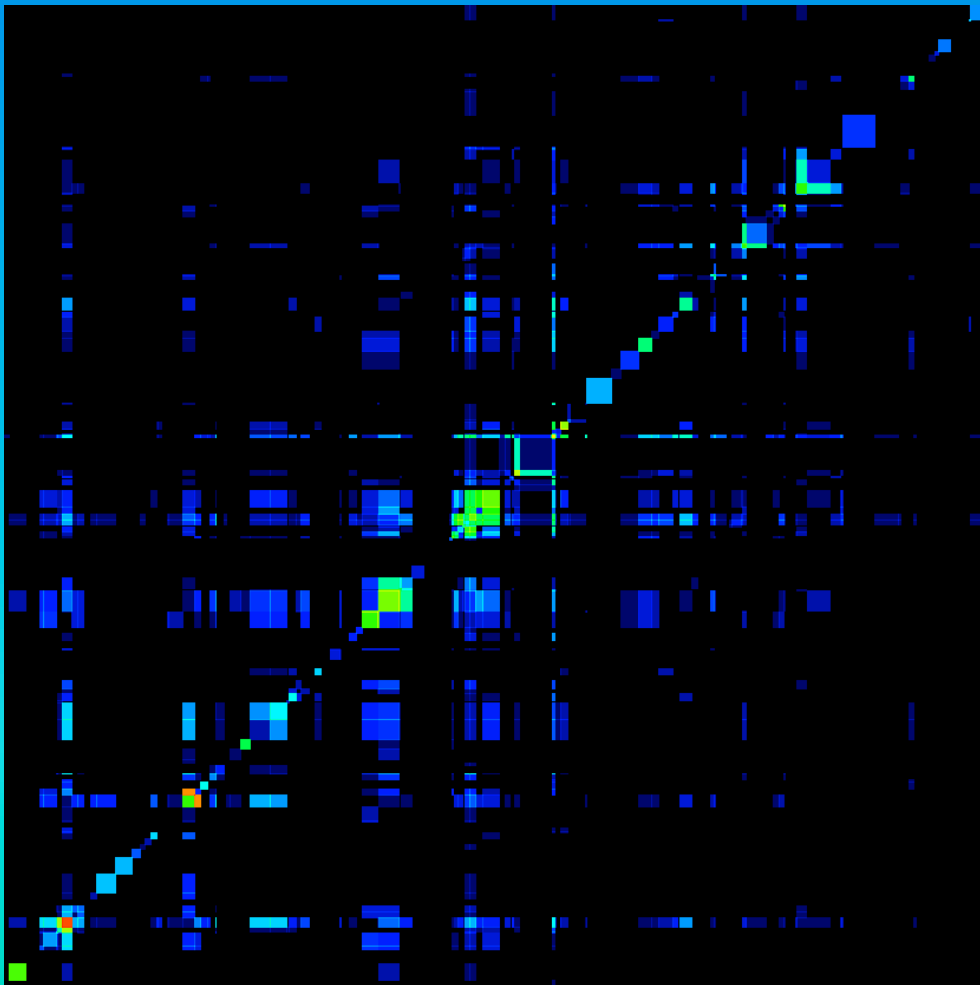
Fetal Liver (active β -Globin)



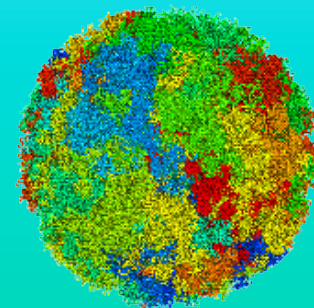
MM β -Globin 2.1 Mbp

Fine Structure of Loop Aggregates/Rosettes

Depending on the resolution, the loops within a domain and their arrangement in loop aggregates/rosettes can be shown as well as the details of how the loops are organized at their base as well as their aggregated rosette core: parallel loop fibres exist at the loop base with ~6kbp and these form the core.

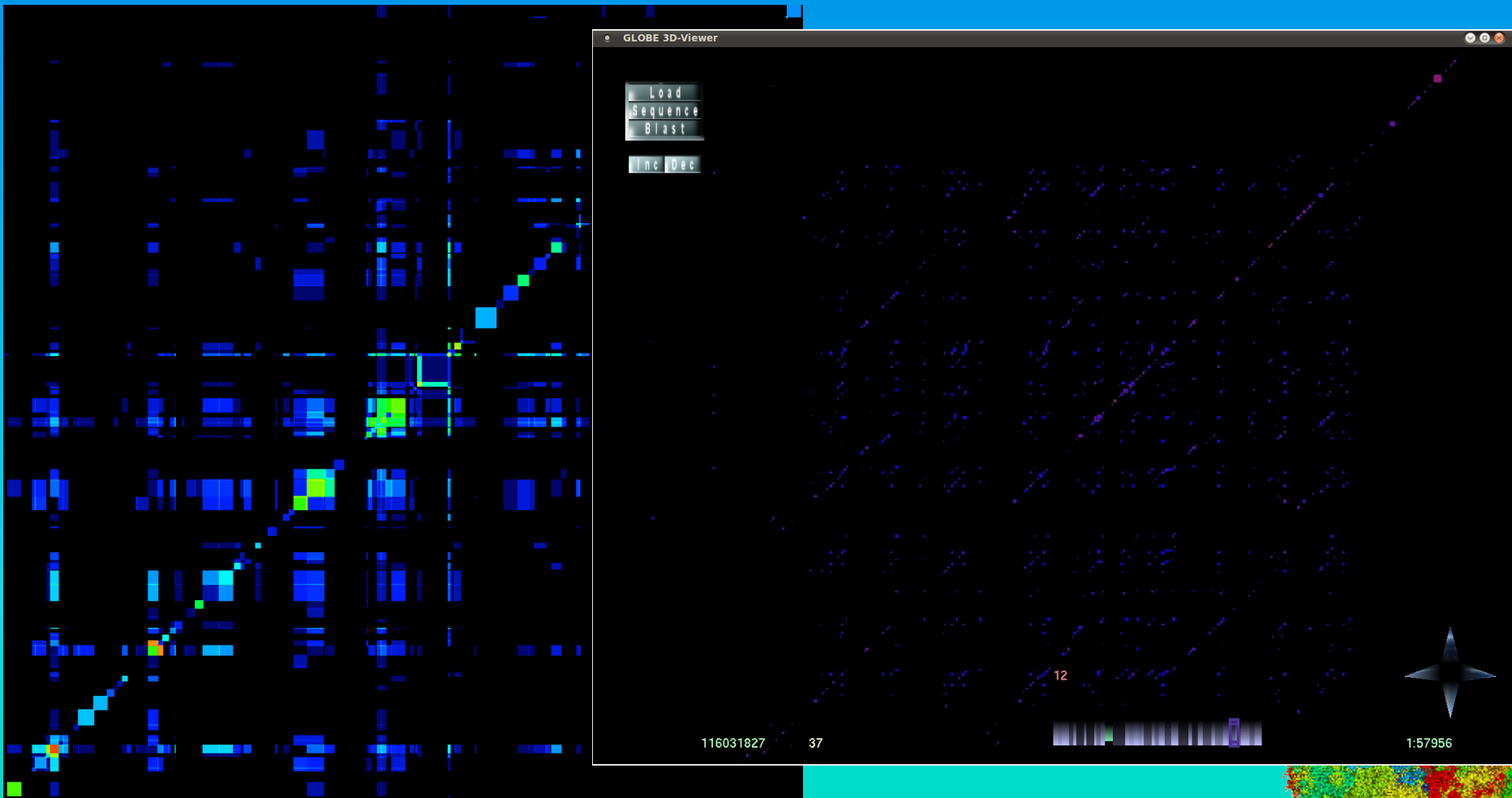


~ 400 kbp

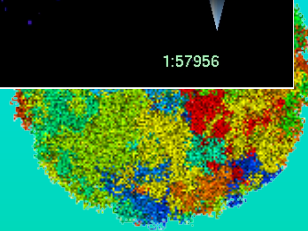


Fine Structure of Loop Aggregates/Rosettes

Depending on the resolution, the loops within a domain and their arrangement in loop aggregates/rosettes can be shown as well as the details of how the loops are organized at their base as well as their aggregated rosette core: parallel loop fibres exist at the loop base with ~6kbp and these form the core.

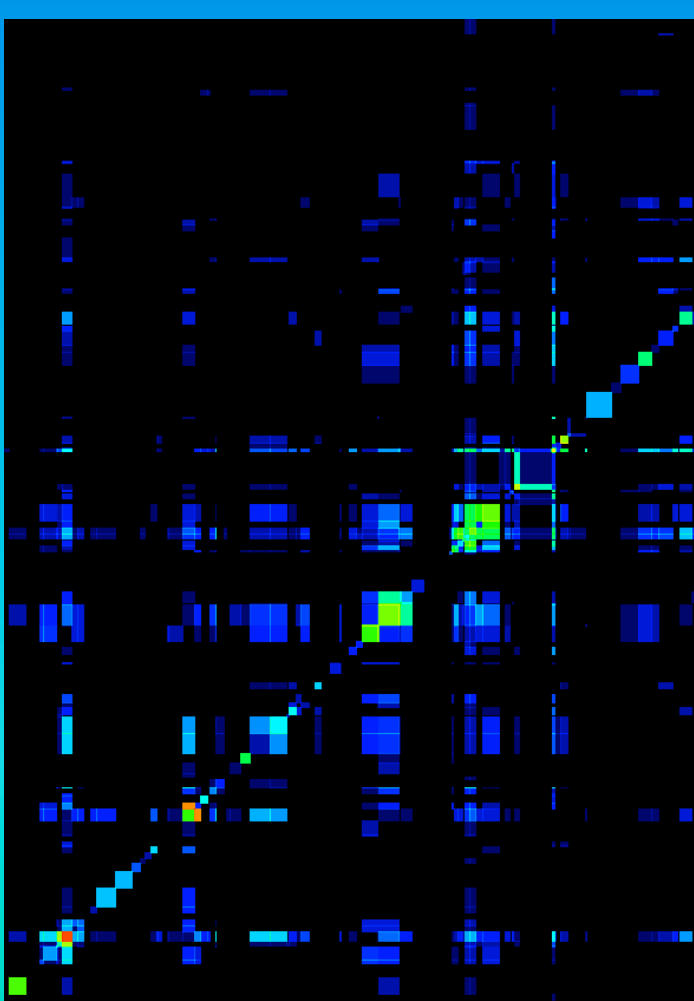


~ 400 kbp

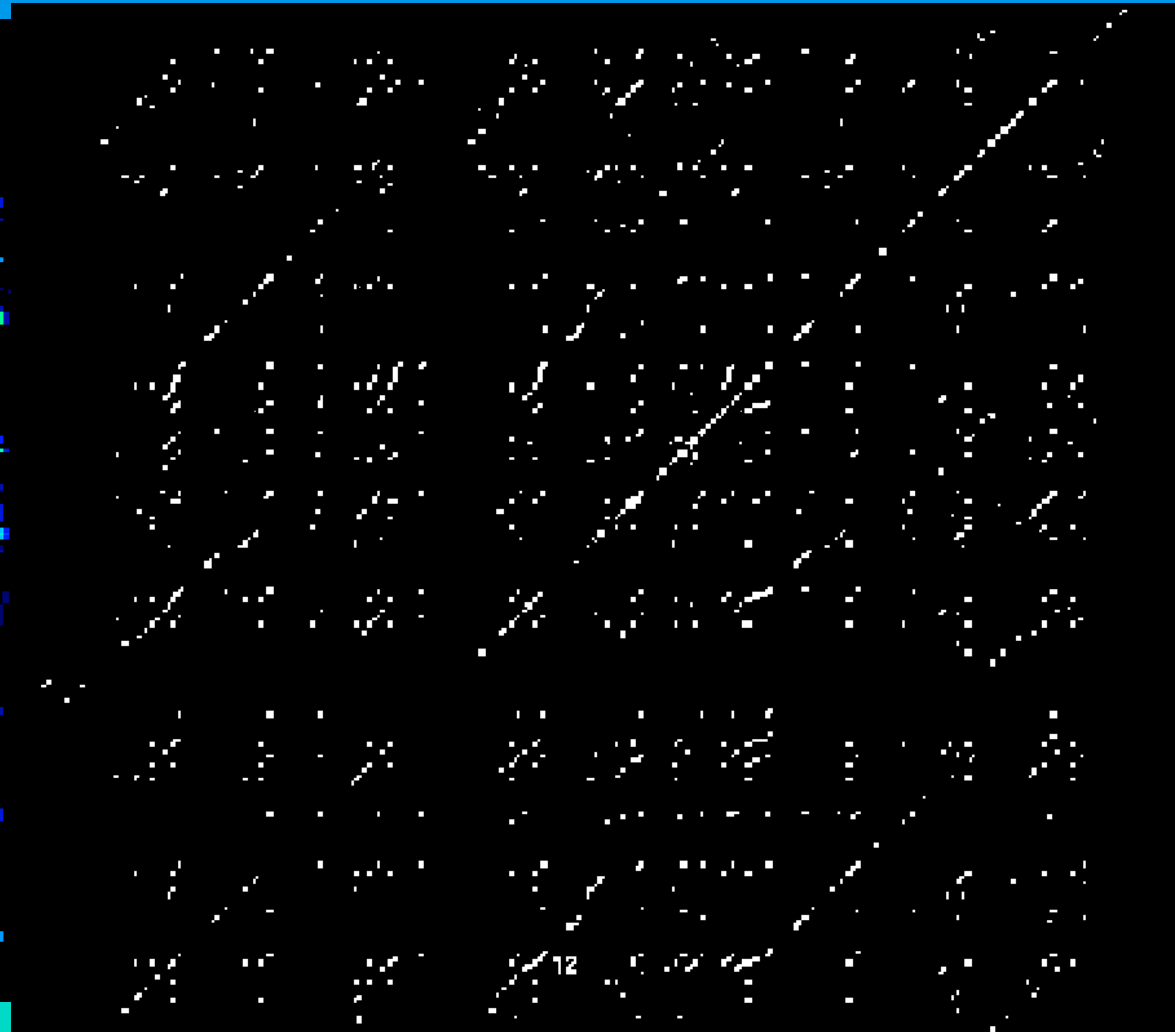


Fine Structure of Loop Aggregates/Rosettes

Depending on the resolution, the loops within a domain and their arrangement in loop aggregates/rosettes can be shown as well as the details of how the loops are organized at their base as well as their aggregated rosette core: parallel loop fibres exist at the loop base with ~6kbp and these form the core.



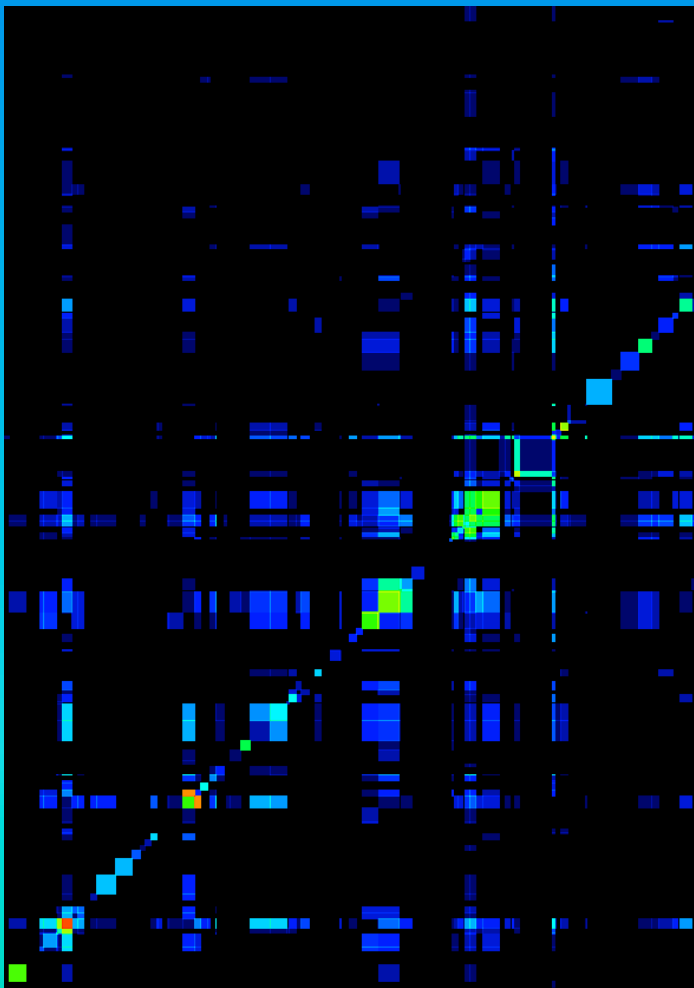
~ 400 kbp



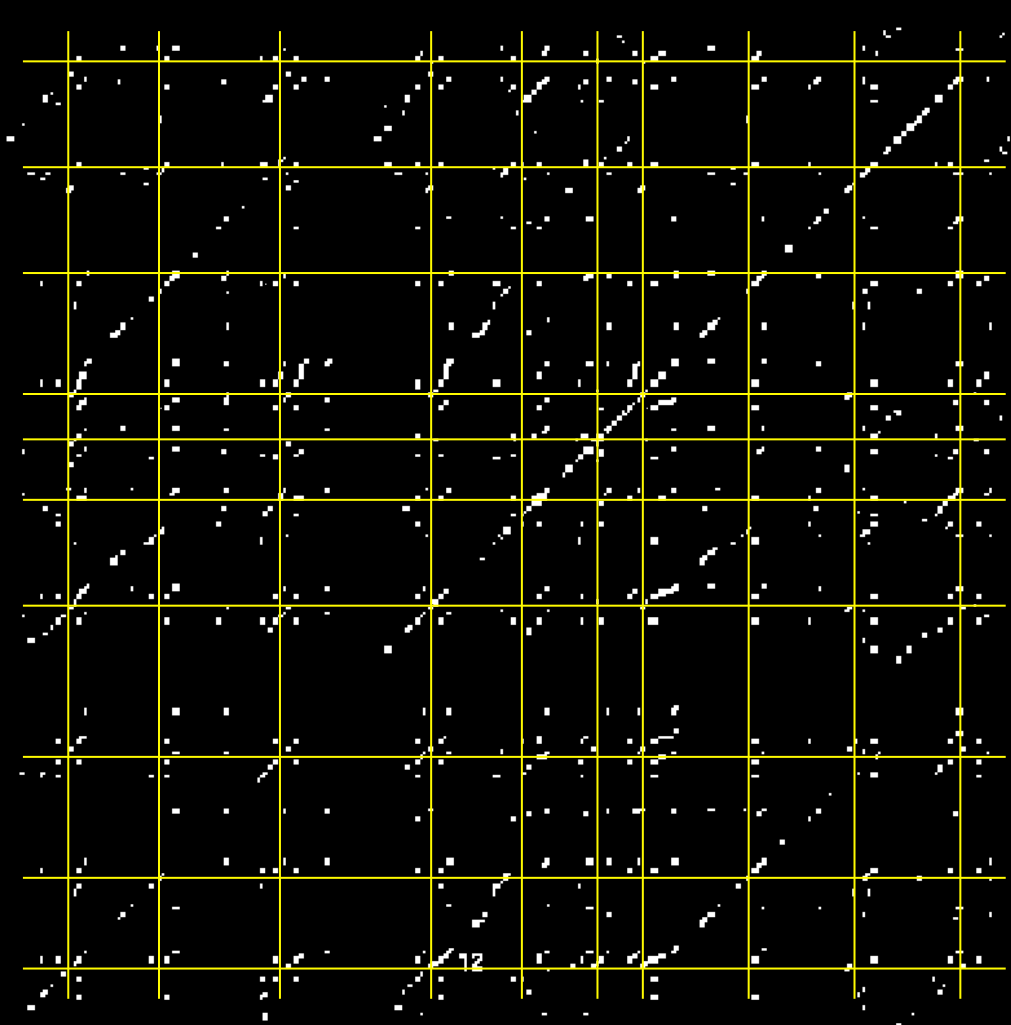
~ 380 kbp

Fine Structure of Loop Aggregates/Rosettes

Depending on the resolution, the loops within a domain and their arrangement in loop aggregates/rosettes can be shown as well as the details of how the loops are organized at their base as well as their aggregated rosette core: parallel loop fibres exist at the loop base with ~6kbp and these form the core.



~ 400 kbp



~ 380 kbp

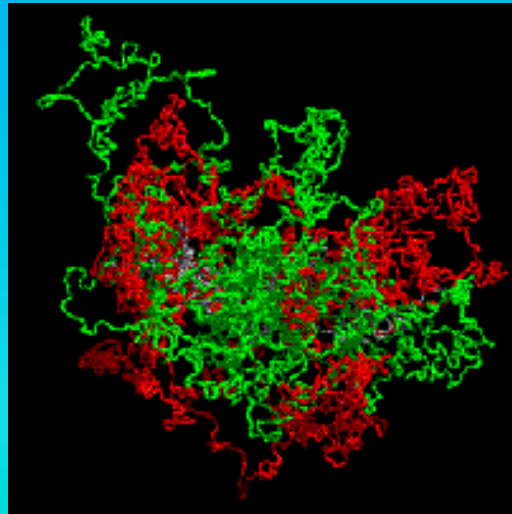
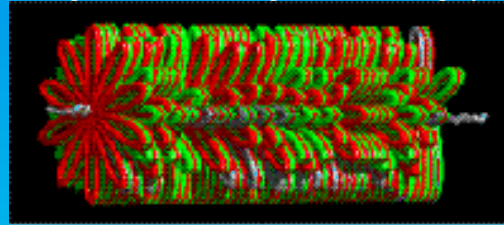
Simulation of Single Chromosomes

The 30 nm chromatin fiber is modeled as a polymer chain with stretching, bending, and excluded volume interactions. Monte Carlo and Brownian Dynamic methods lead to thermodynamical equilibrium configurations.

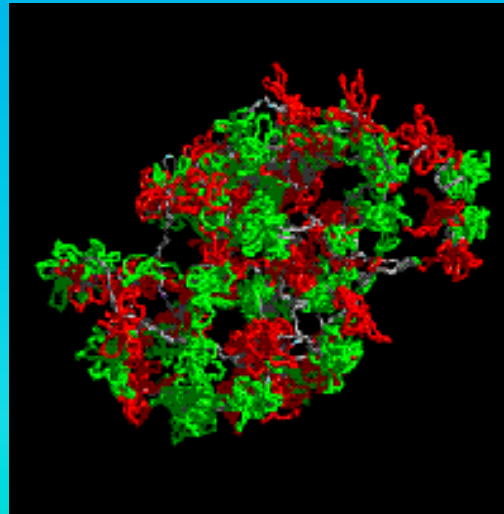
All models form chromosome territories with big voids and different chromatin morphologies. Experimental territory and subcompartment diameters agree best with an MLS model with 80 to 120 kbp loops and linkers.



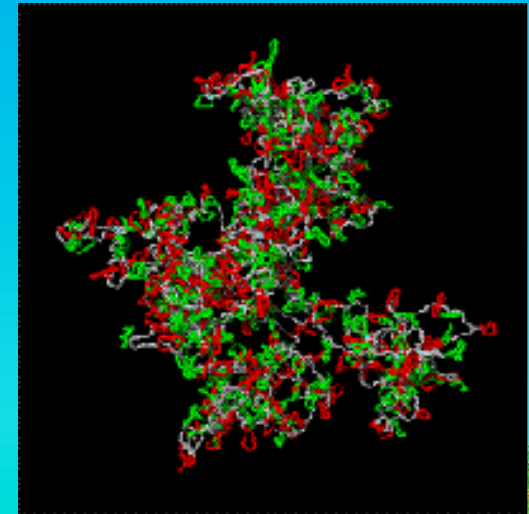
Metaphase starting configuration with ideogram bands in red/green, linker in grey.



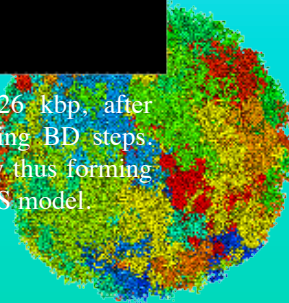
RW/GL model, loop size 5 Mbp, after ~80.000 MC and 1000 relaxing BD steps. Large loops intermingle freely and reach out of the chromosome territory, thus forming no distinct features like in MLS model.



MLS model, loop size 126 kbp, linker size 126 kbp, after ~50.000 MC and 1000 relaxing BD steps. Here rosettes form subcompartments as separated organizational and dynamic entities.



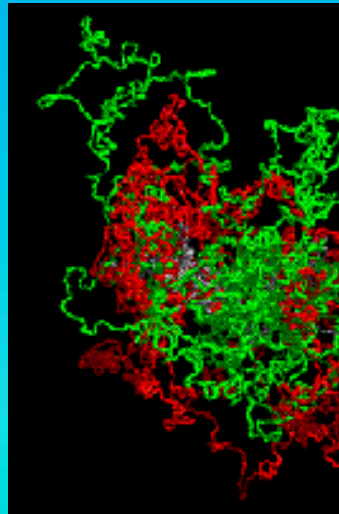
RW/GL model, loop size 126 kbp, after ~80.000 MC and 1000 relaxing BD steps. Large loops intermingle freely thus forming no distinct features like in MLS model.



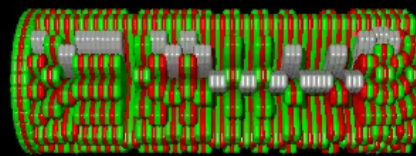
Simulation of Single Chromosomes

The 30 nm chromatin fiber is modeled as a polymer chain with stretching, bending, and excluded volume interactions. Monte Carlo and Brownian Dynamic methods lead to thermodynamical equilibrium configurations.

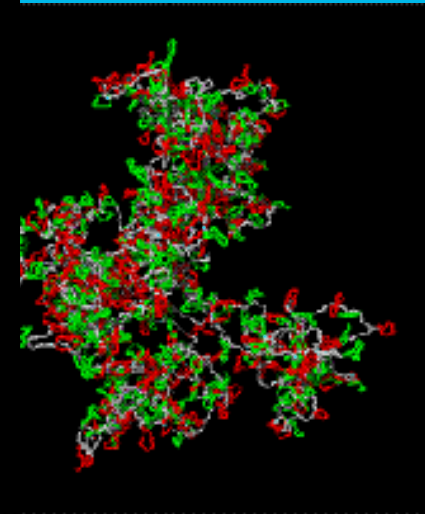
All models form chromosome territories with big voids and different chromatin morphologies. Experimental territory and subcompartment diameters agree best with an MLS model with 80 to 120 kbp loops and linkers.



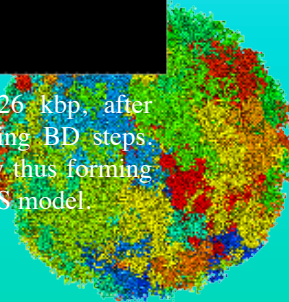
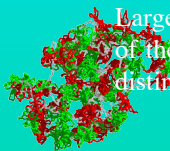
RW/GL model, loop size ~80.000 MC and 1000 relaxing BD steps. Large loops intermingle freely and reach out of the chromosome territory, thus forming no distinct features like in MLS model.



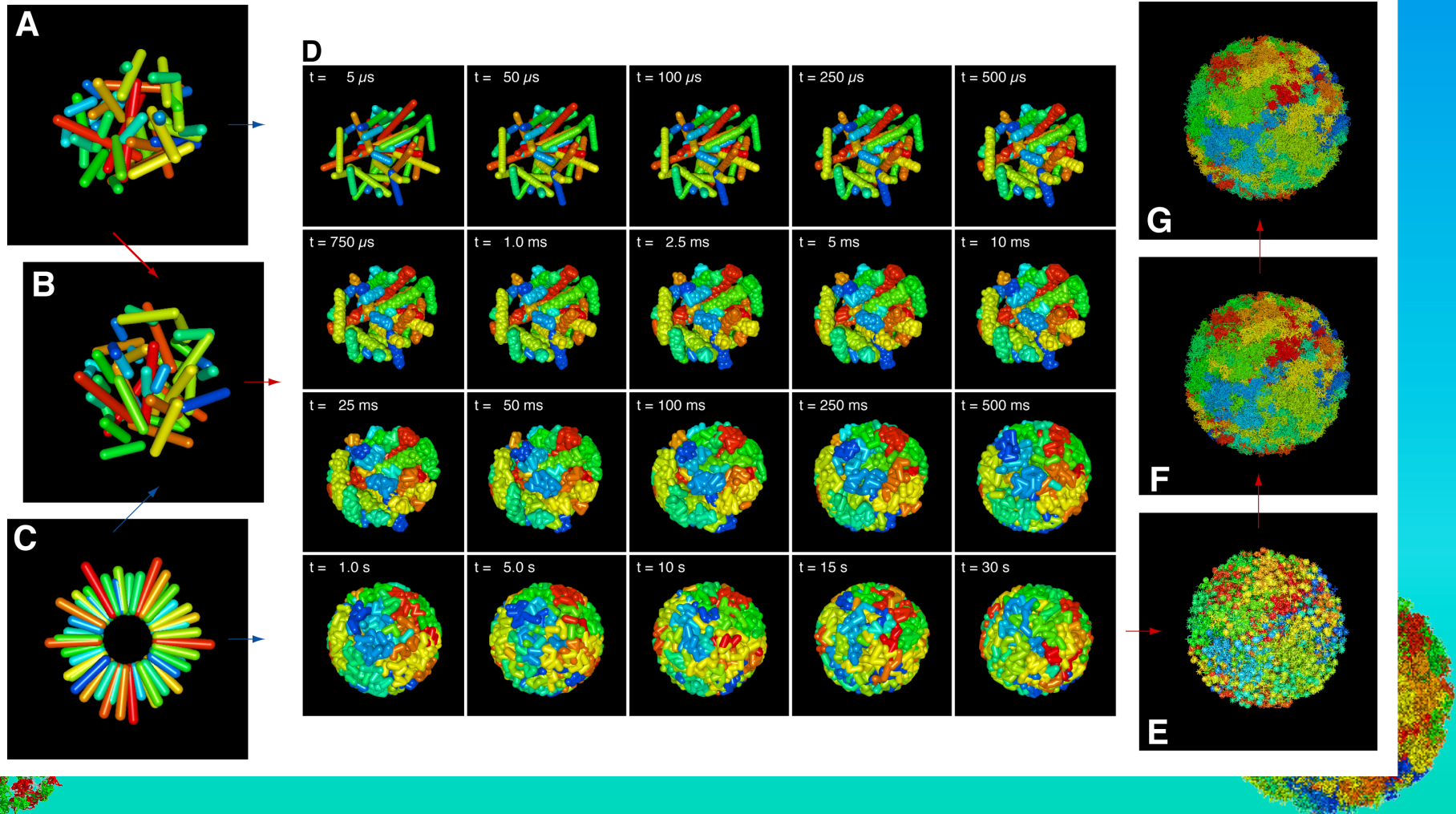
120 kbp, after ~50.000 MC and 1000 relaxing BD steps. Here rosettes form subcompartments as separated organizational and dynamic entities.



model, loop size 126 kbp, after ~80.000 MC and 1000 relaxing BD steps. Large loops intermingle freely thus forming no distinct features like in MLS model.

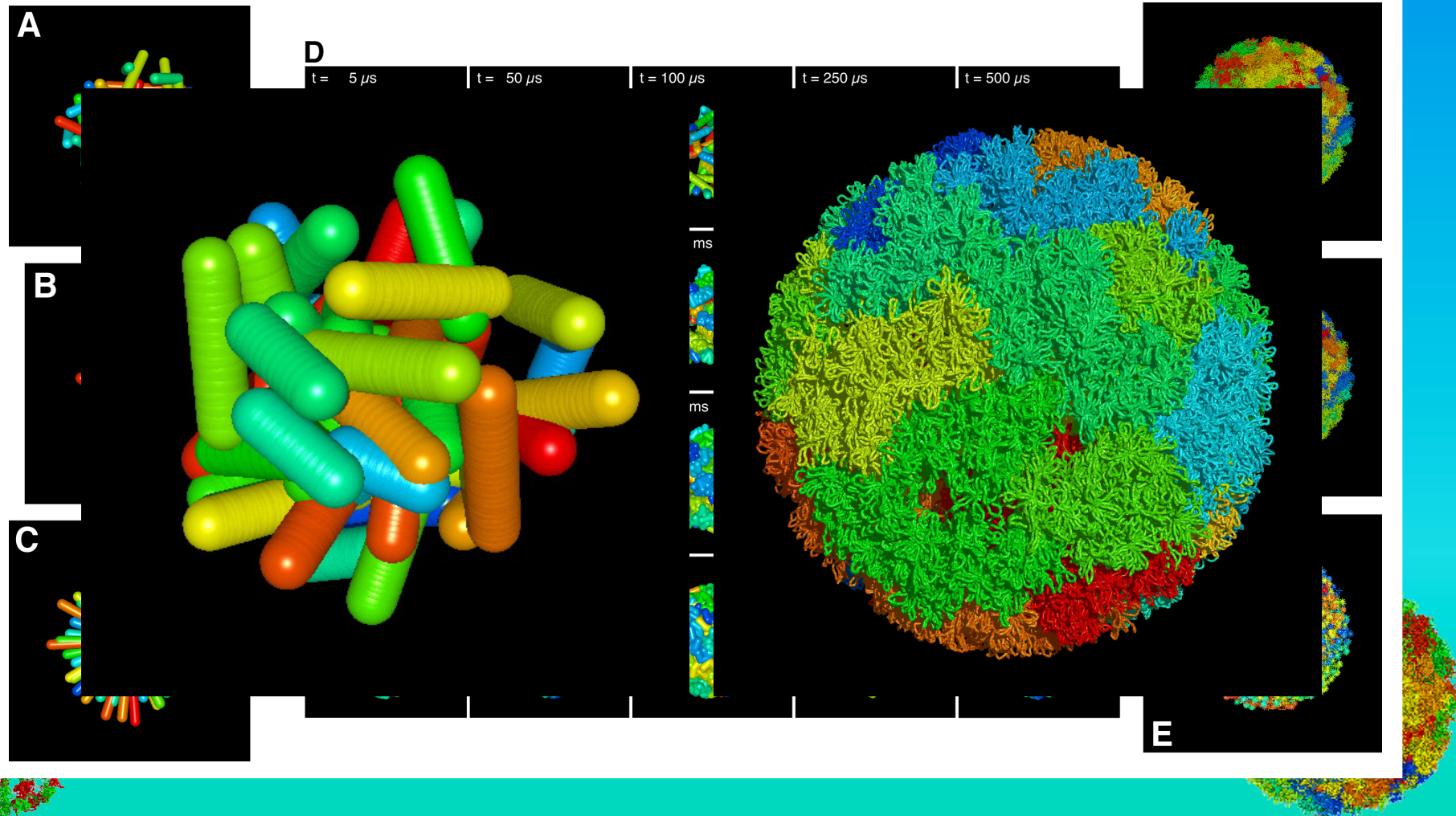


The chromosome territory position depends on their metaphase position and is reasonably stable.



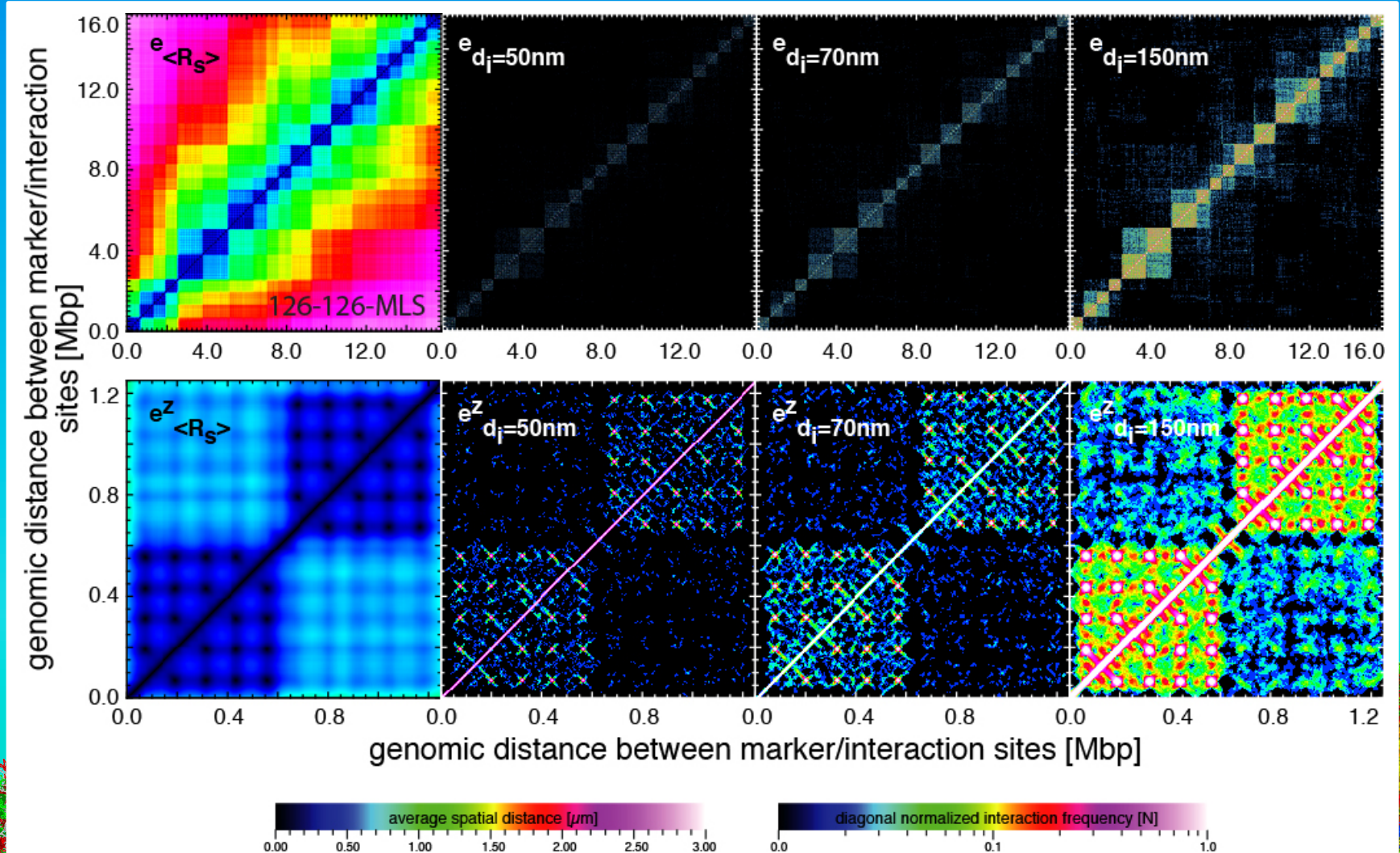
[illegible]

The chromosome territory position depends on their metaphase position and is reasonably stable.



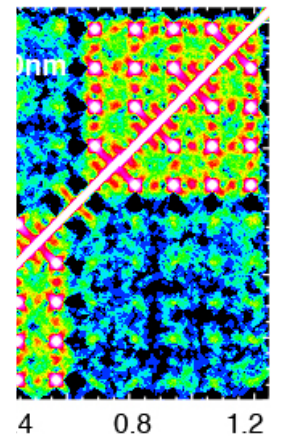
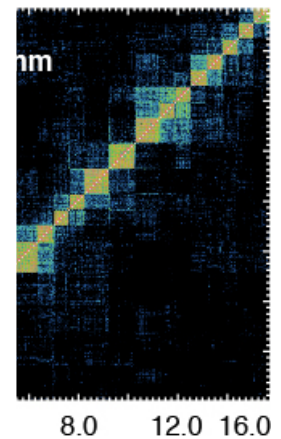
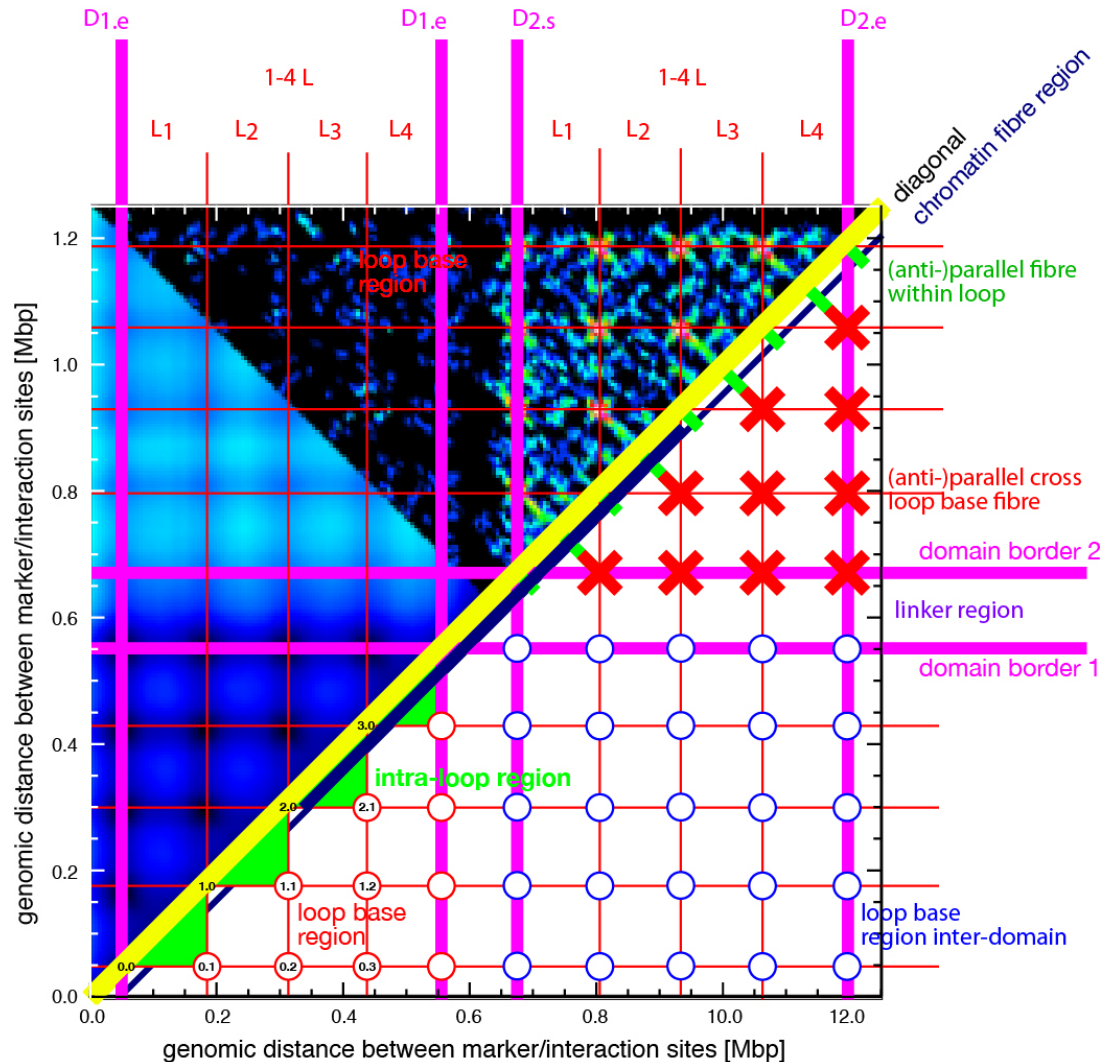
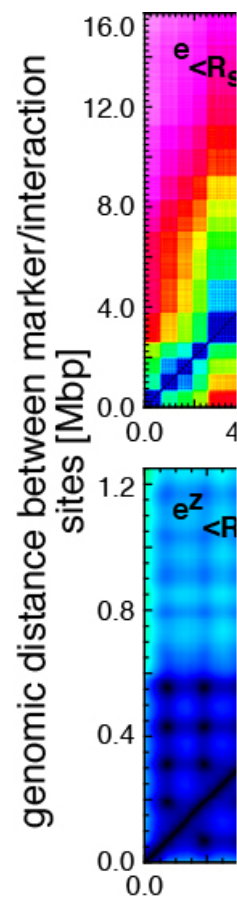
Simulated Interaction Maps

Simulated spatial distance maps as well as simulated interaction maps result in the representation of every parameter variation, and also exhibit the fine-structure describing the loop base as well as rosette core. Thus from the quasi-fibre to the entire chromosome the architecture can be understood in detail.



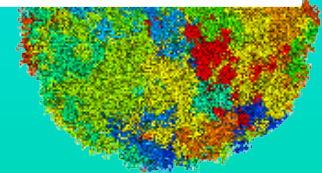
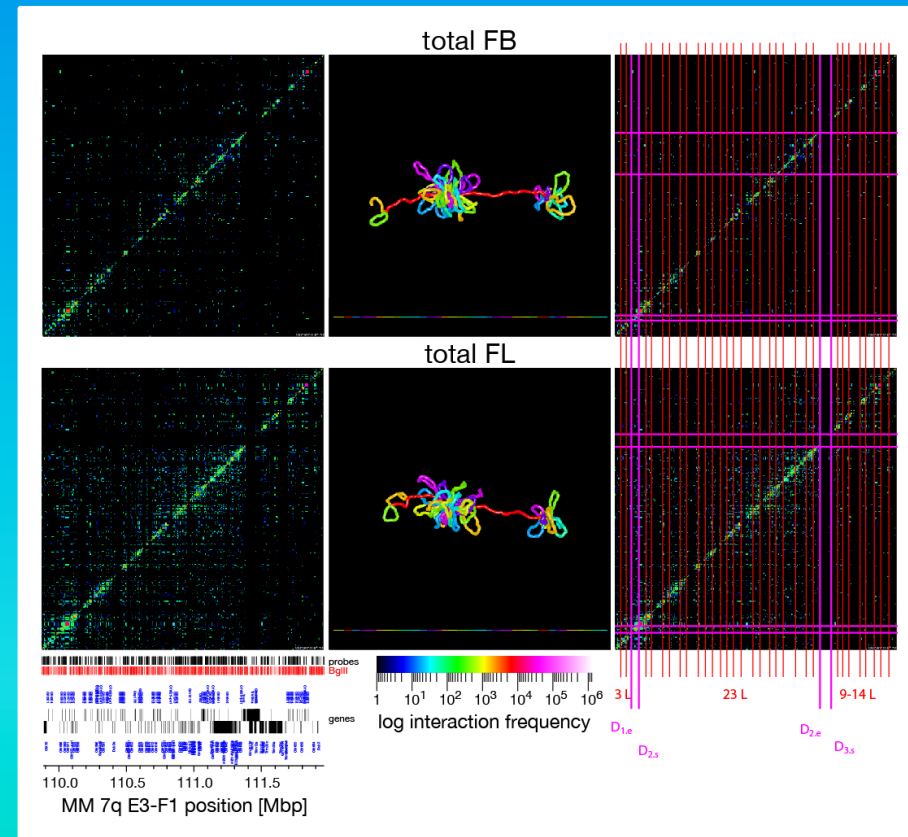
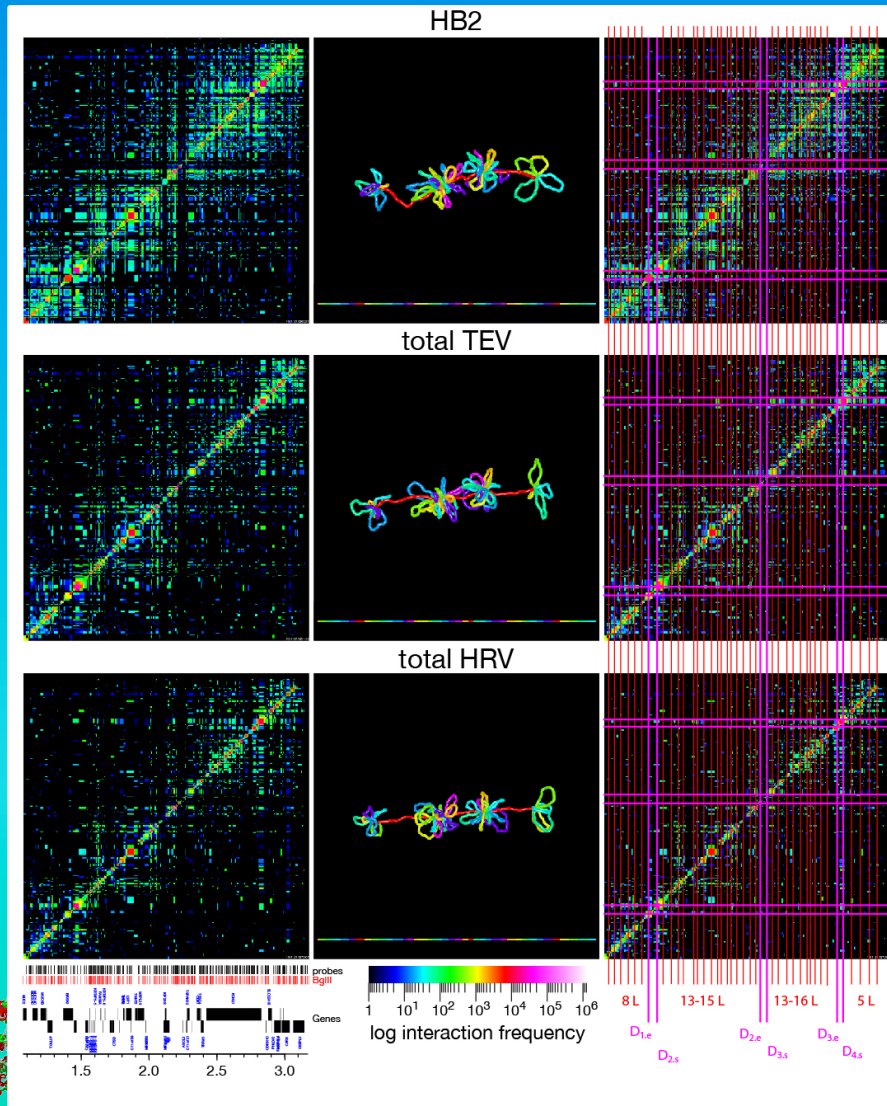
Simulated Interaction Maps

Simulated spatial distance maps as well as simulated interaction maps result in the representation of every parameter variation, and also exhibit the fine-structure describing the loop base as well as rosette core. Thus from the quasi-fibre to the entire chromosome the architecture can be understood in detail.



Variation of a Consensus Architecture Scheme

The difference between different cell types, functional states or even species is minor despite depending on the region. From this, the chromatin fibre conformation, loop position, and their association into loop aggregates/rosettes can be derived, simulated by polymer models and finally visualized.

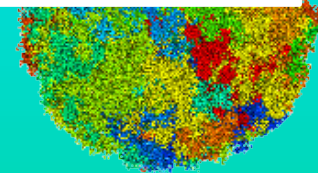
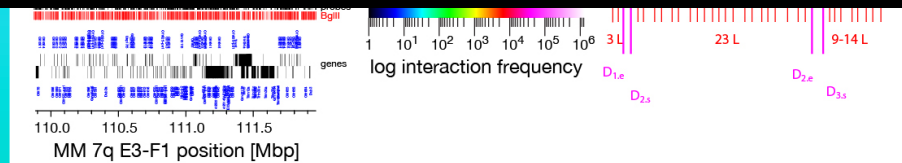
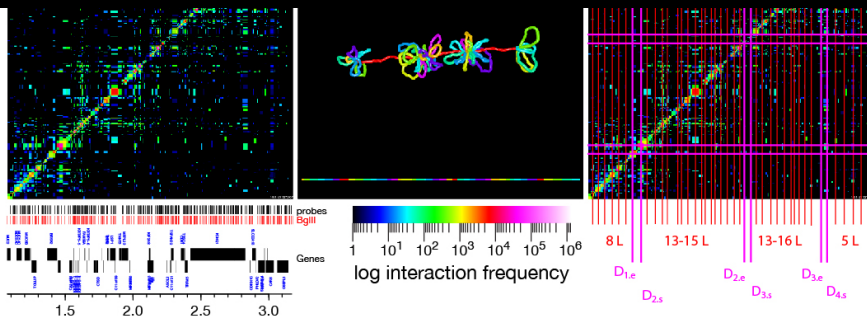


Variation of a Consensus Architecture Scheme

The difference between different cell types, functional states or even species is minor despite depending on the region. From this, the chromatin fibre conformation, loop position, and their association into loop aggregates/rosettes can be derived, simulated by polymer models and finally visualized.

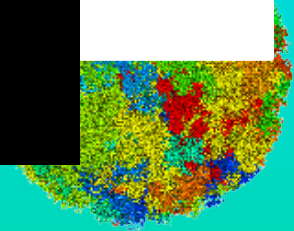
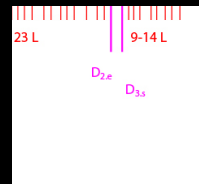
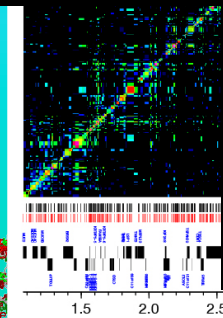


HB2



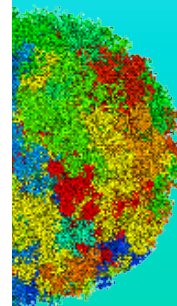
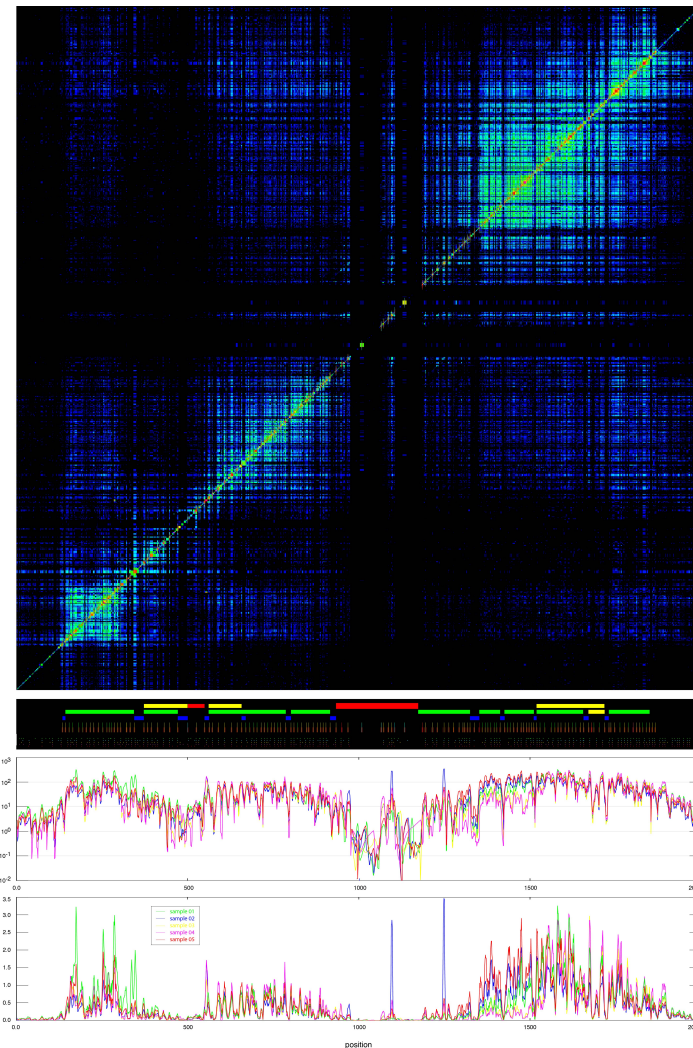
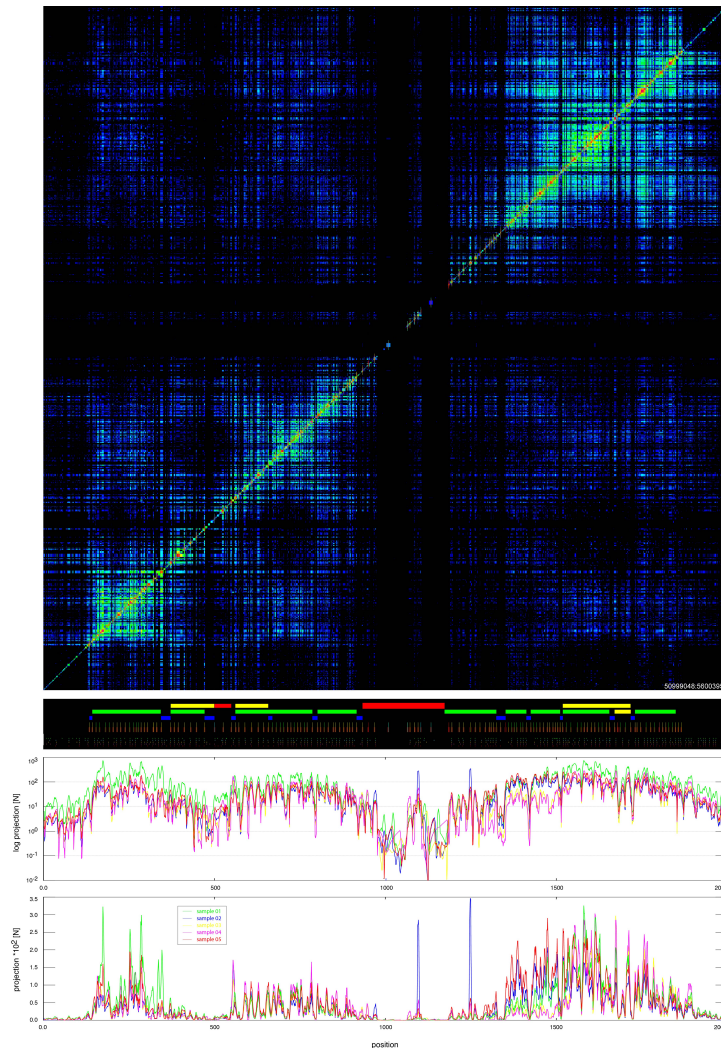
Variation of a Consensus Architecture Scheme

The difference between different cell types, functional states or even species is minor despite depending on the region. From this, the chromatin fibre conformation, loop position, and their association into loop aggregates/rosettes can be derived, simulated by polymer models and finally visualized.



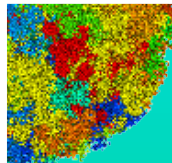
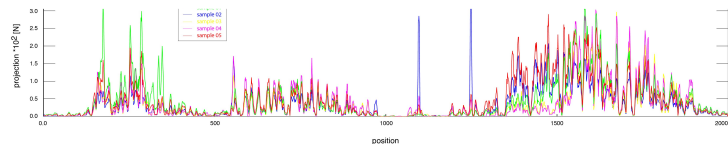
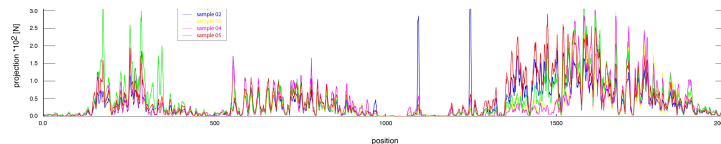
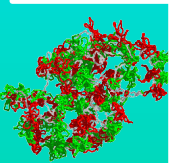
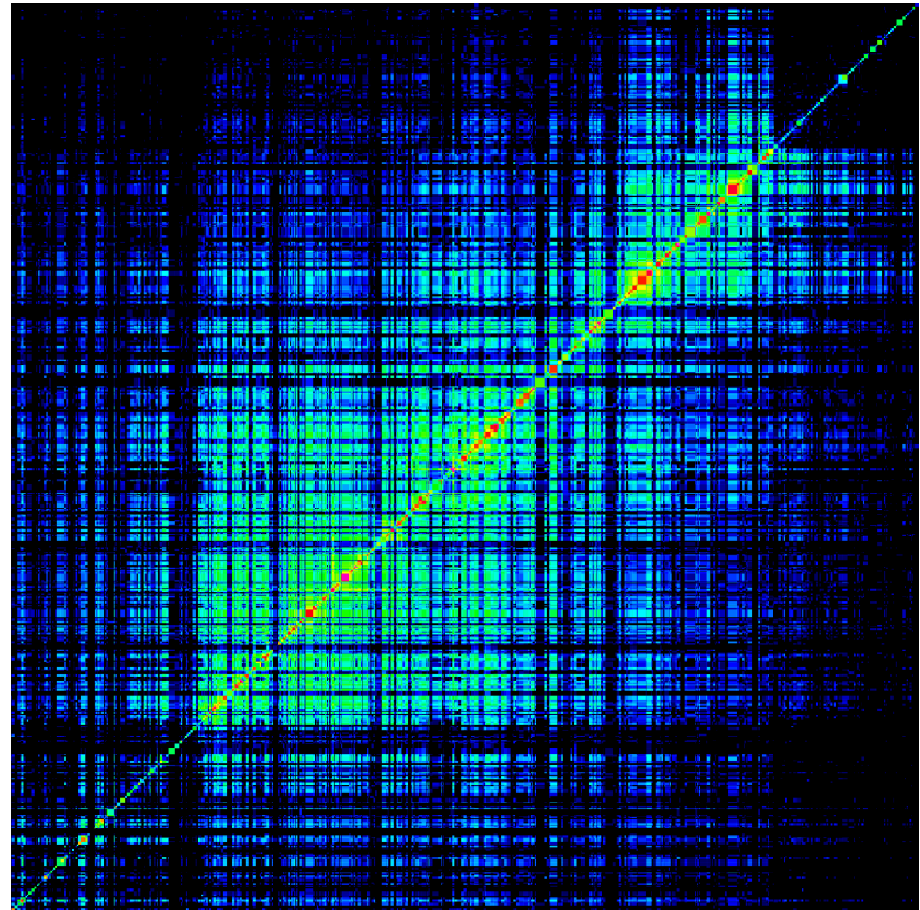
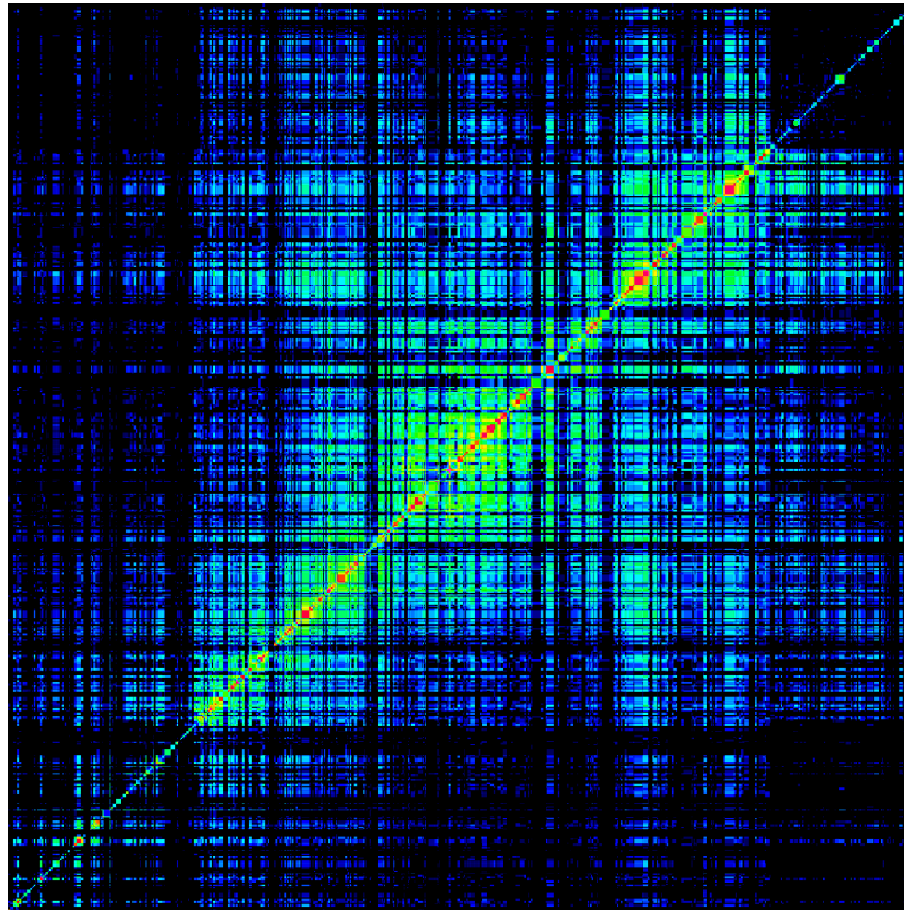
Clinical Epigenetic Functional 3D Architecture Context

Although the ground state architecture remaining the same, depending on the local functional status of genetic regions, the quasi-fibre compaction, loop and their arrangement in loop aggregates/rosettes allow for different functional interaction dynamics and thus regulation of a genetic regions represented by characteristic interaction map changes. If the variation is beyond the evolutionary bandwidth the system turns into malfunctional or disease states.



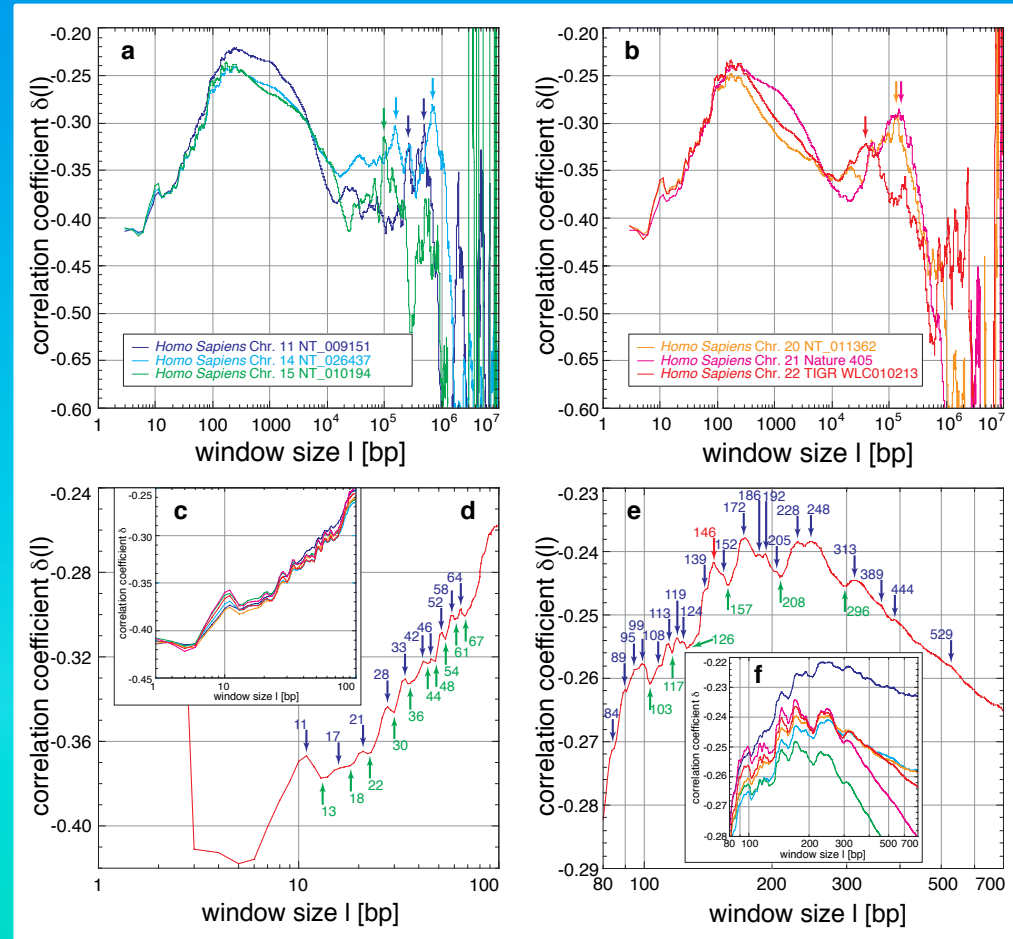
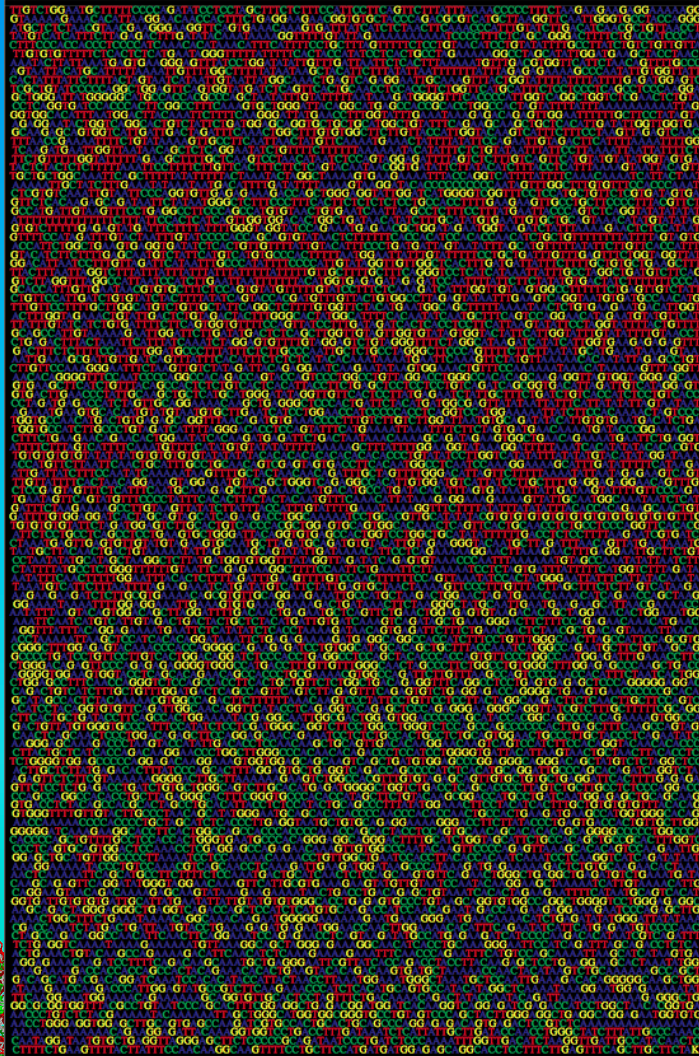
Clinical Epigenetic Functional 3D Architecture Context

Although the ground state architecture remaining the same, depending on the local functional status of genetic regions, the quasi-fibre compaction, loop and their arrangement in loop aggregates/rosettes allow for different functional interaction dynamics and thus regulation of a genetic regions represented by characteristic interaction map changes. If the variation is beyond the evolutionary bandwidth the system turns into malfunctional or disease states.



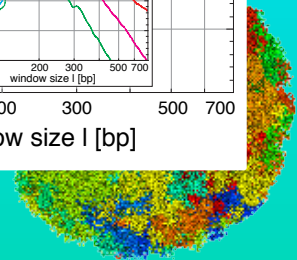
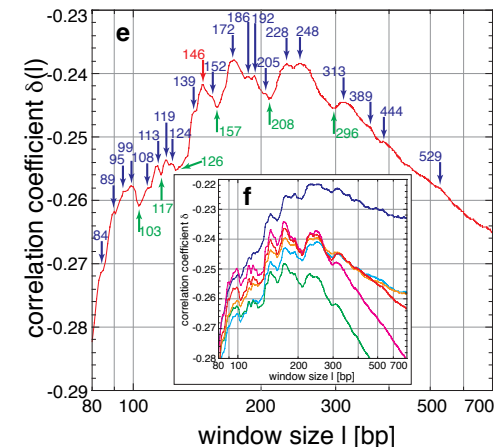
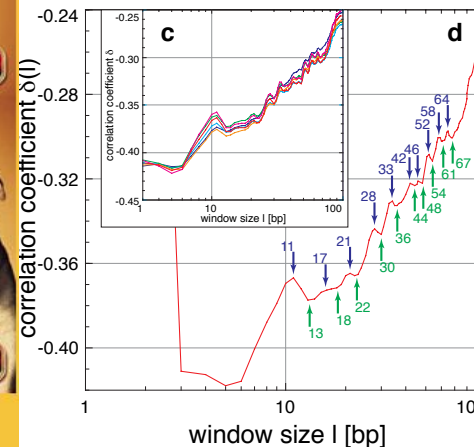
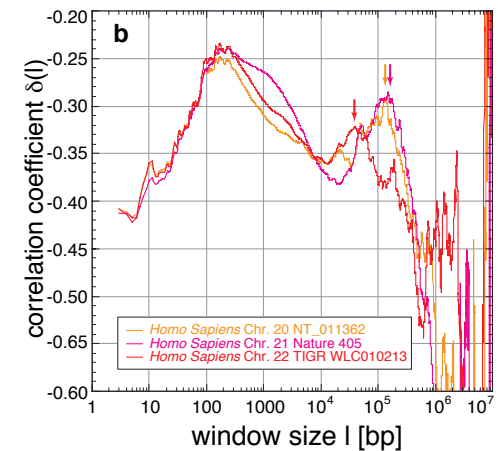
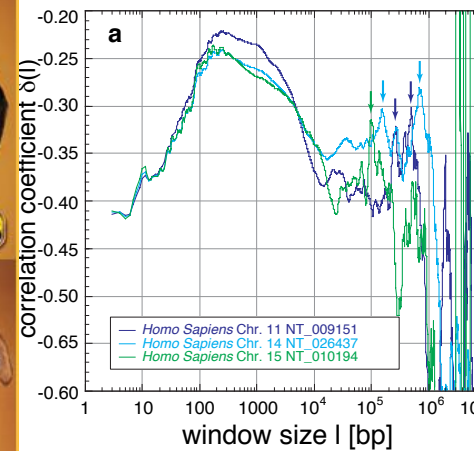
DNA Sequence Organization

Determination of the concentration fluctuation function $C(l)$ and its local slope the correlation coefficient $\delta(l)$ are an indication for the i) degree of long-rang scaling behaviour, ii) general multi-scaling, and iii) fine-structure features, which all are connected to all levels of genome organization and especially also the three-dimensional genome architecture.



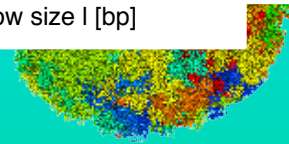
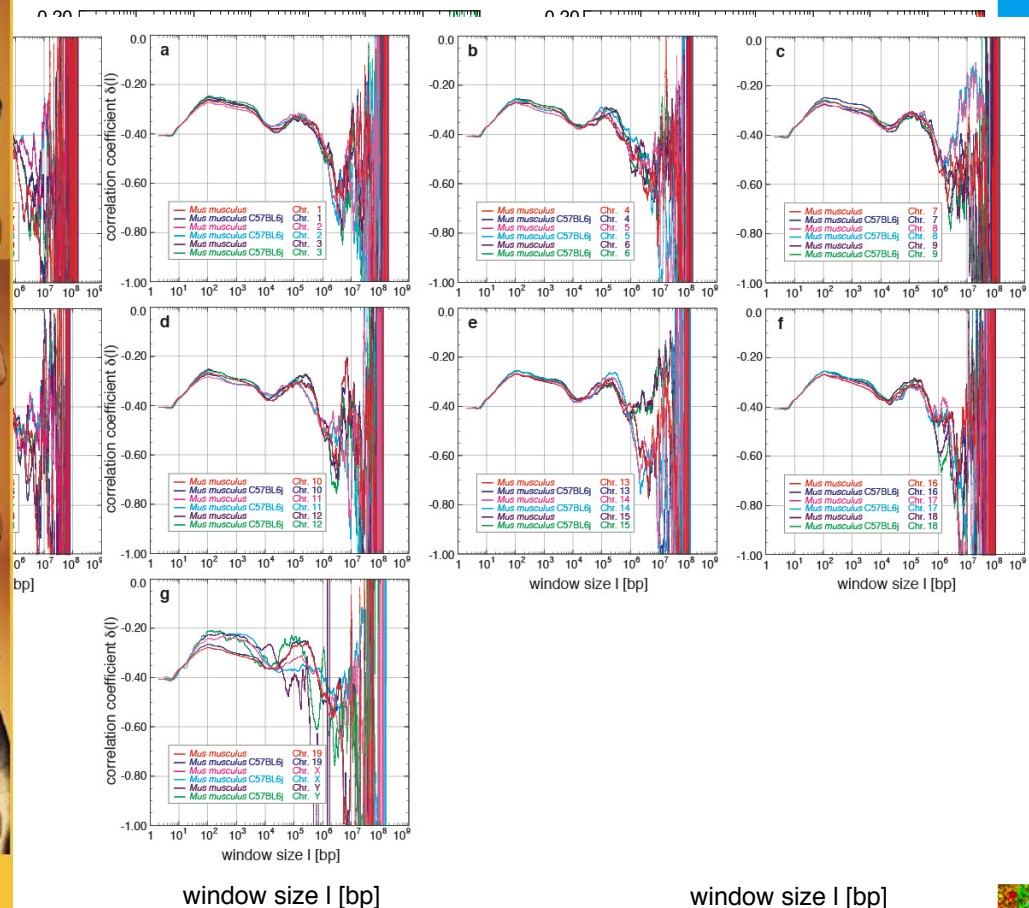
DNA Sequence Organization

Determination of the concentration fluctuation function $C(l)$ and its local slope the correlation coefficient $\delta(l)$ are an indication for the i) degree of long-range scaling behaviour, ii) general multi-scaling, and iii) fine-structure features, which all are connected to all levels of genome organization and especially also the three-dimensional genome architecture.



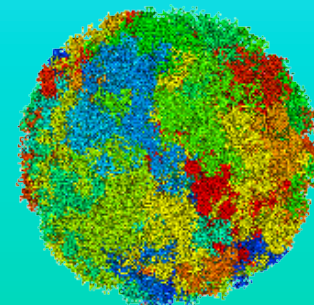
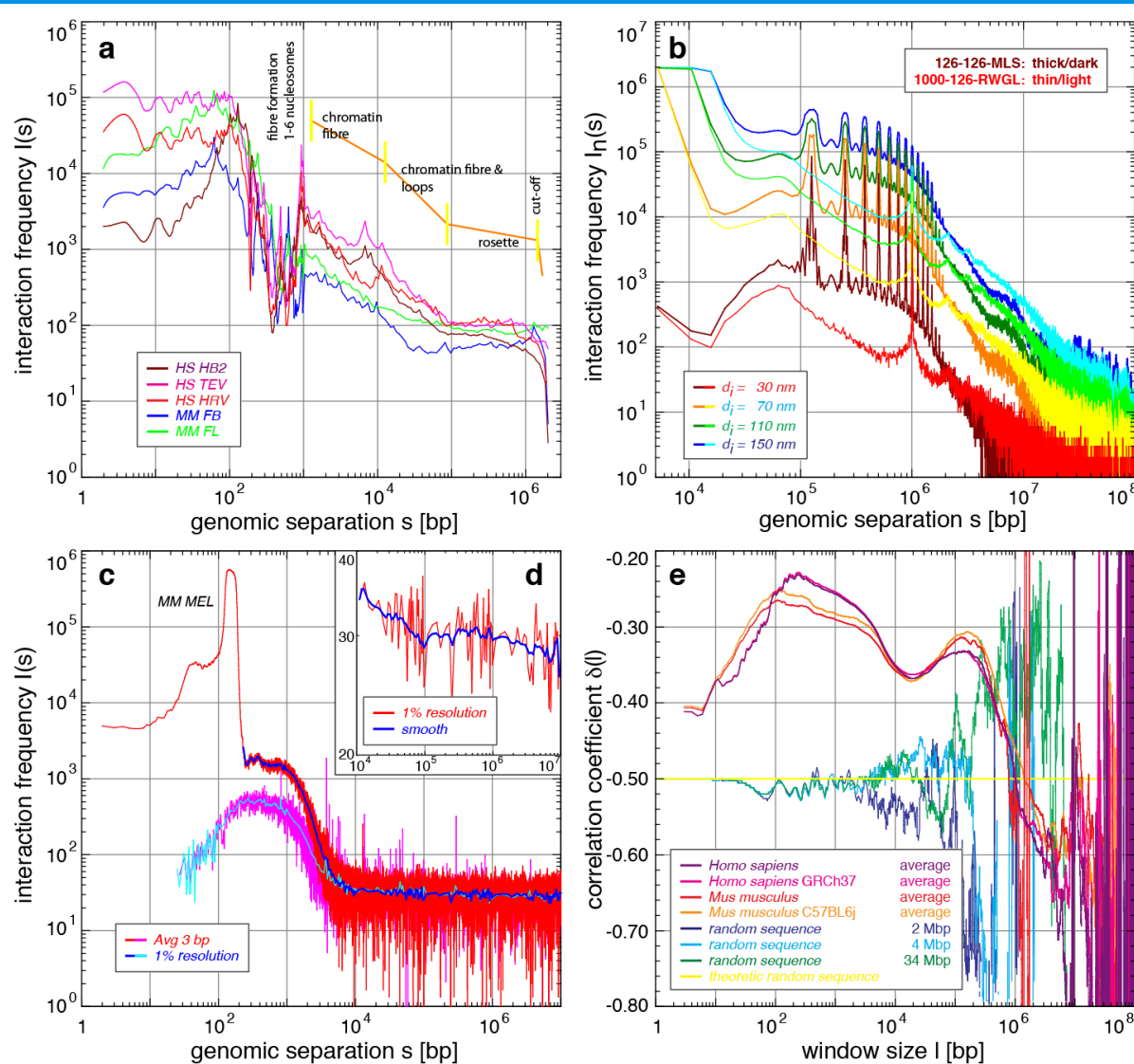
DNA Sequence Organization

Determination of the concentration fluctuation function $C(l)$ and its local slope the correlation coefficient $\delta(l)$ are an indication for the i) degree of long-rang scaling behaviour, ii) general multi-scaling, and iii) fine-structure features, which all are connected to all levels of genome organization and especially also the three-dimensional genome architecture.



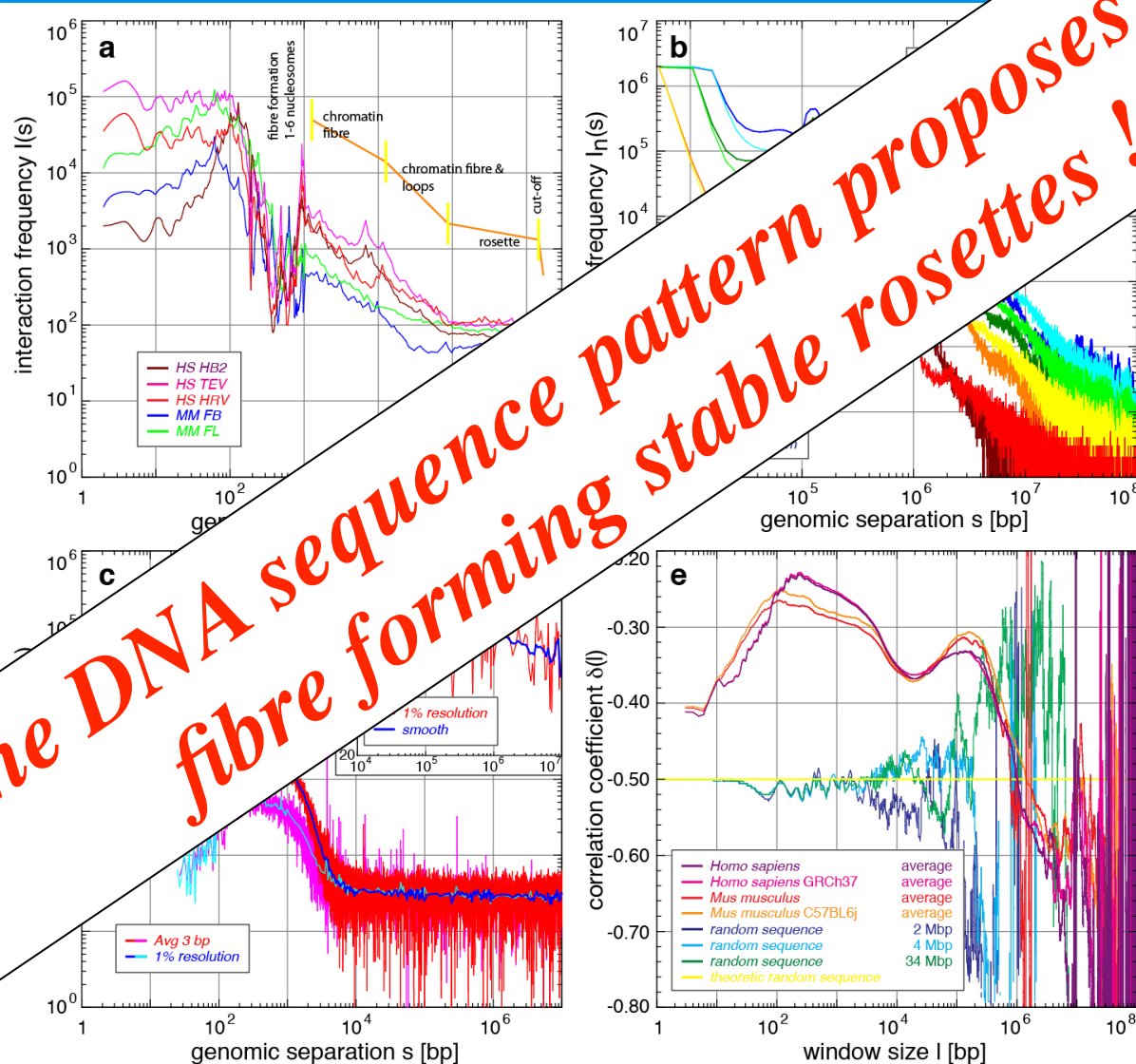
Scaling Analysis

Scaling analysis show again the entire bandwidth of architectural effects in an aggregated manner. Beyond, they show the scale bridging of the structures and the evolutionary holistic entanglement between the 3D architecture and the DNA sequence organization itself.

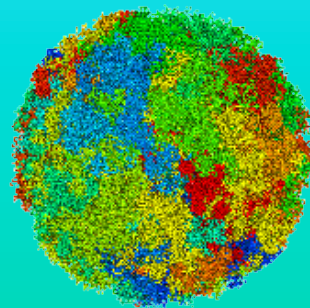


Scaling Analysis

Scaling analysis show again the entire bandwidth of architectural effects in an aggregated manner. Beyond, they show the scale bridging of the structures and the evolutionary holistic entanglement between the 3D architecture and the DNA sequence organization itself.



Also the DNA sequence pattern proposes a quasi-fibre forming stable rosettes !

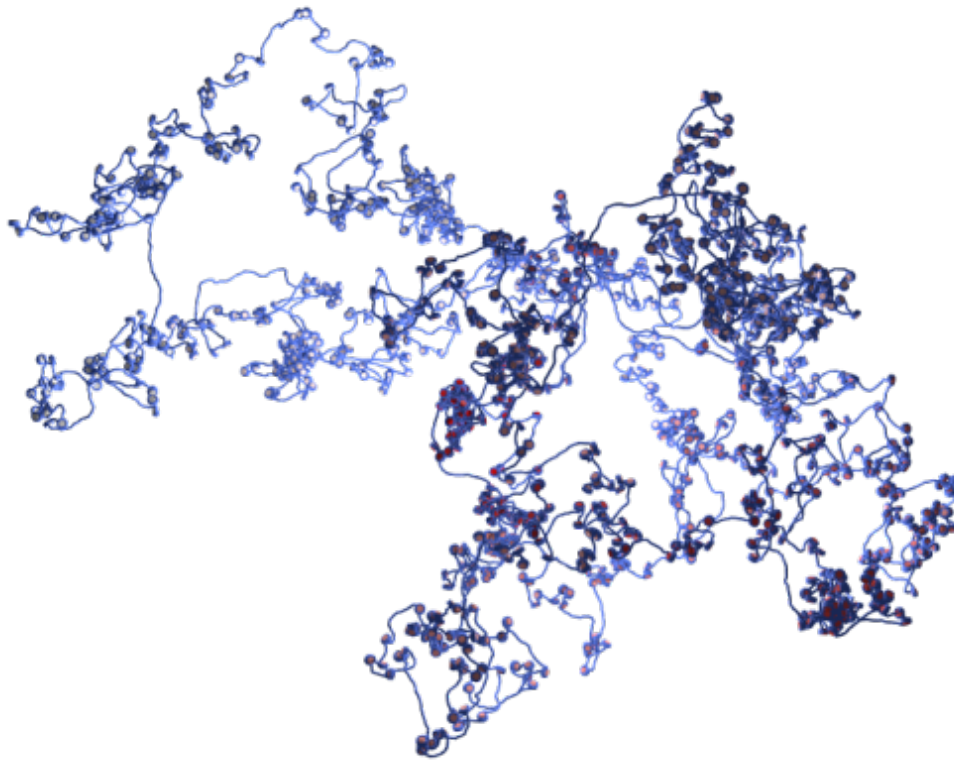


Simulation of Chromatin Quasi-Fibres

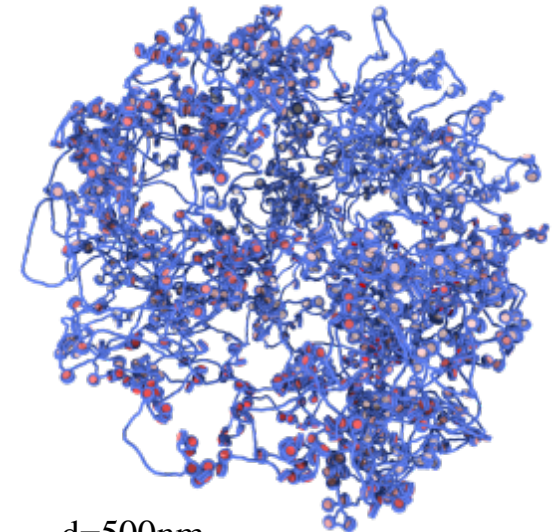
The position of nucleosomes influence greatly the structure of chromatin fibers done on super-computers. Here a dedicated workflow is applied, with which overlapping nucleosome populations can be analyzed and the best positioning of nucleosomes by Monte Carlo simulated annealing can be achieved. For an actual locus in a spherical confinement then a 3D independent nucleosome fiber conformation can be simulated.



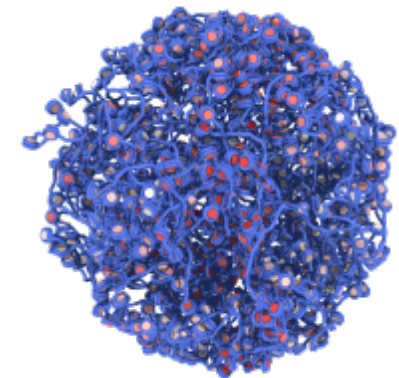
Monte Carlo Simulation of SAMD4A Mouse ES Cells



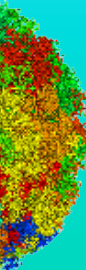
d=1000nm



d=500nm



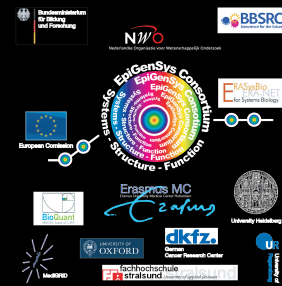
d=200nm



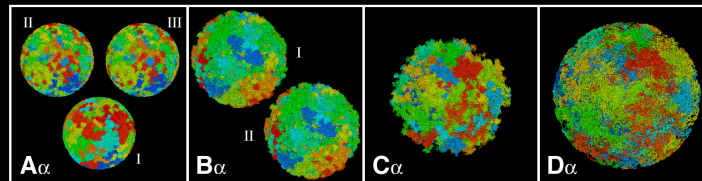
From Fiber Topology to Nuclear Morphology

Chromosome territories form in the RW/GL and the MLS model. However, only the MLS model leads distinct subcompartments and low chromosome and subcompartment overlap. Best agreement is reached for an MLS model with 80 to 120 kbp loops and linkers in nuclei with 8 to 10 μm diameter.

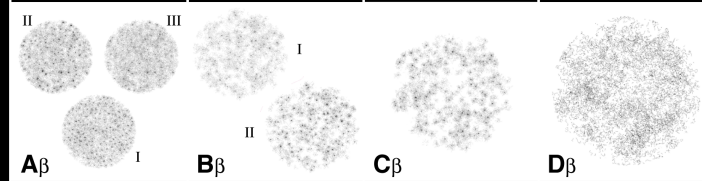
The simulated nuclear morphology reflects the chromosome fiber topology of different models in detail.



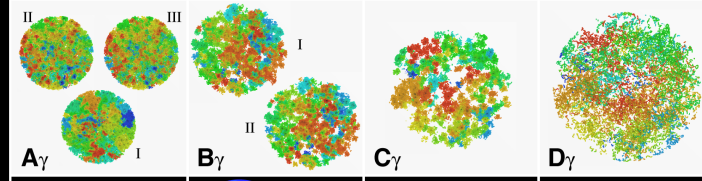
rendering



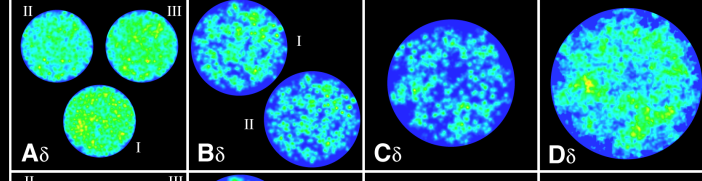
electron microscopy



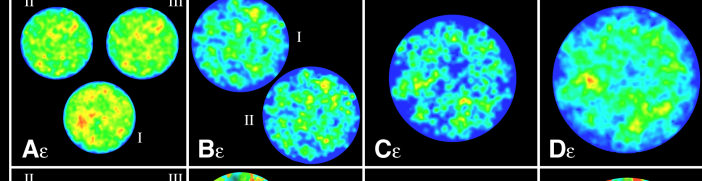
electron microscopy territory painting



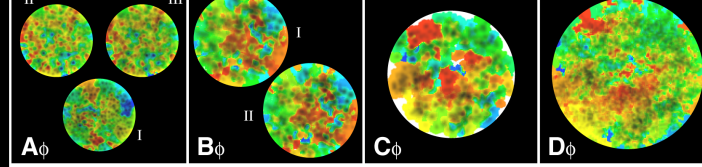
confocal microscopy
100x objective, theoretic resolution



confocal microscopy
63x objective, real resolution



confocal microscopy territory painting

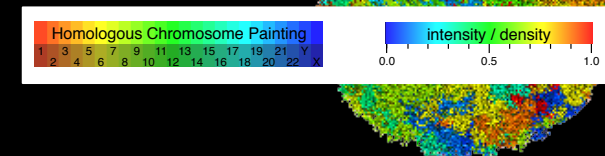
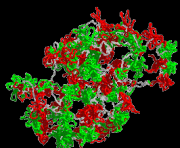


A: MLS in 6 μm nucleus
I: 63 kbp loops, 63 kbp linkers
II: 63 kbp loops, 252 kbp linkers
III: 126 kbp loops, 252 kbp linkers

B: MLS in 8 μm nucleus
I: 126 kbp loops, 126 kbp linkers
II: 84 kbp loops, 126 kbp linkers

C: MLS in 10 μm nucleus
126 kbp loops, 126 kbp linker,
not totally relaxed

D: RW/GL in 12 μm nucleus
5 Mbp loops
not totally relaxed



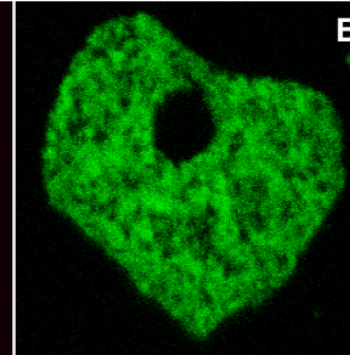
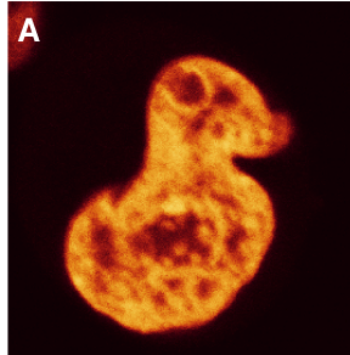
In vivo Morphology & Chromatin Distribution

The stable expression of fusions between histones and autofluorescent proteins and the integration into nucleosomes allows the minimal invasive investigation of the structure and dynamics of chromatin.

The clustered morphology in detail favour an MLS like chromatin topology.

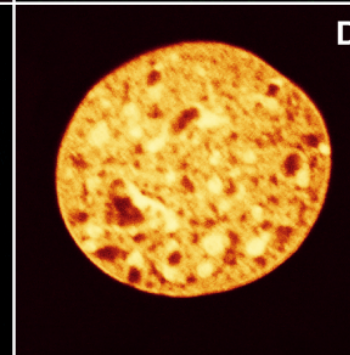
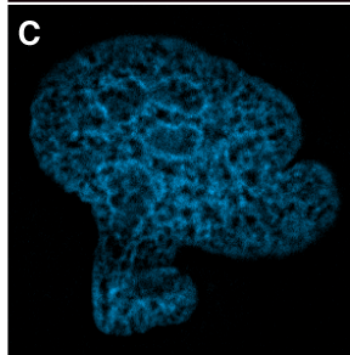


HeLa, H2A-YFP



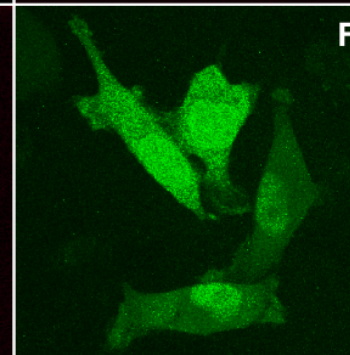
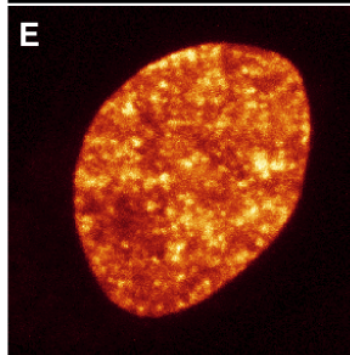
Cos7, H1.0-GFP

LCLC 103H, H2A-CFP

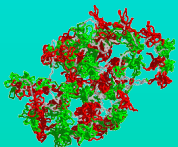
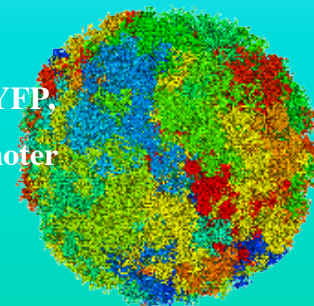


ID13, H2A-YFP

HeLa, mH2A1.2-YFP

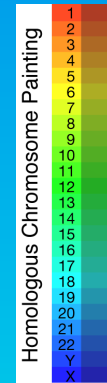
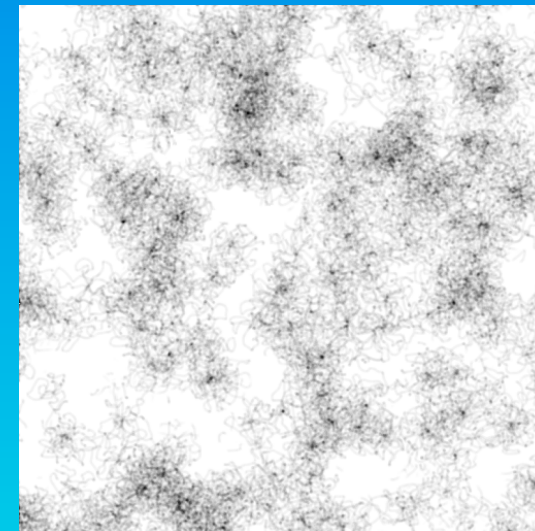
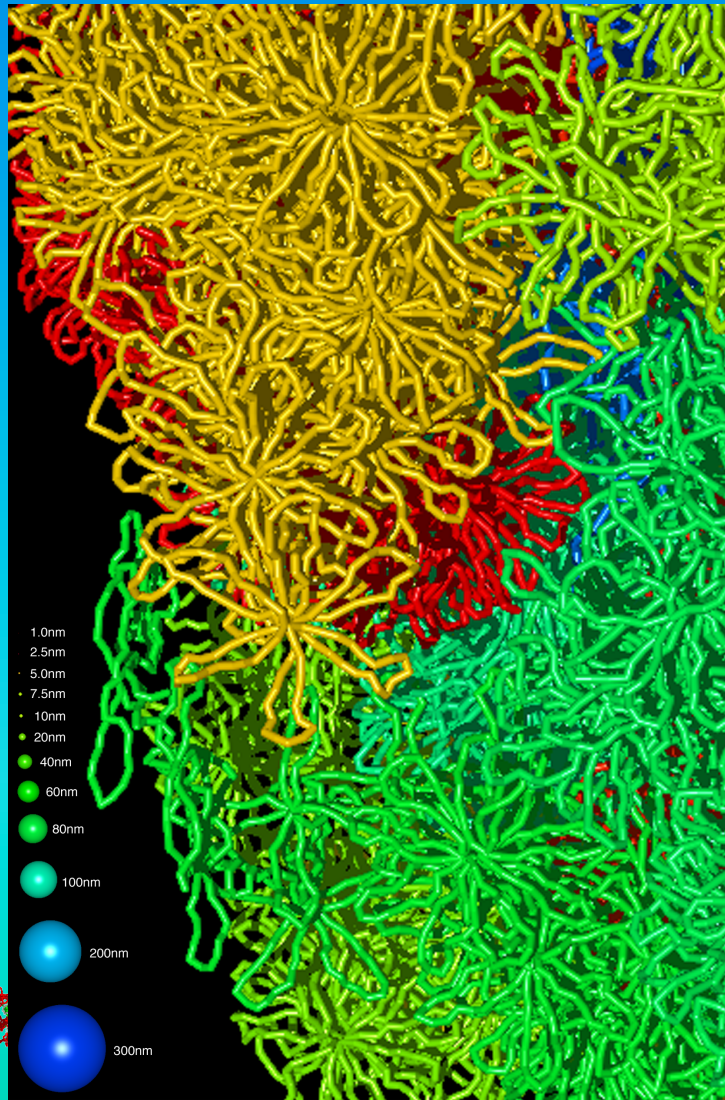


HeLa, H2A-YFP,
natural promoter

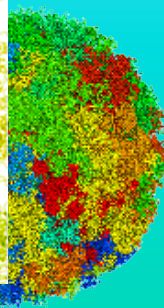
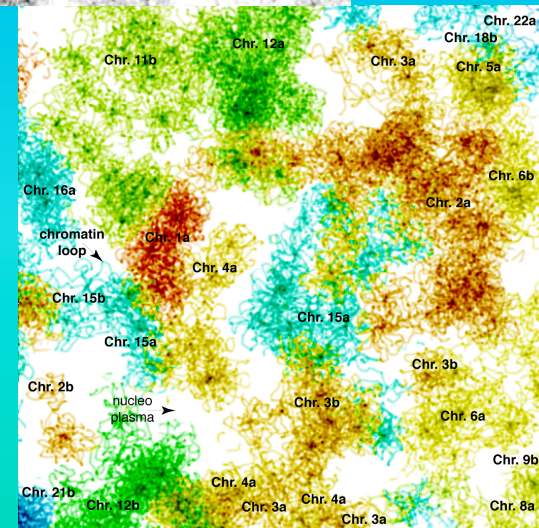


Fine Morphology of Nuclei

High resolution rendering and simulated electron microscopy including territory painting reveal not only again the model details but also that any location in the nucleus is accessible to biological molecules <15 nm in diameter and that even the Extended Interchromosomal Domain hypothesis is oversimplified.

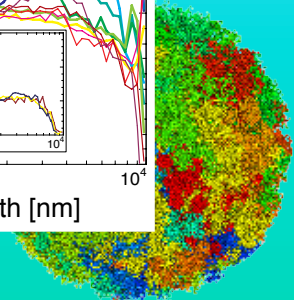
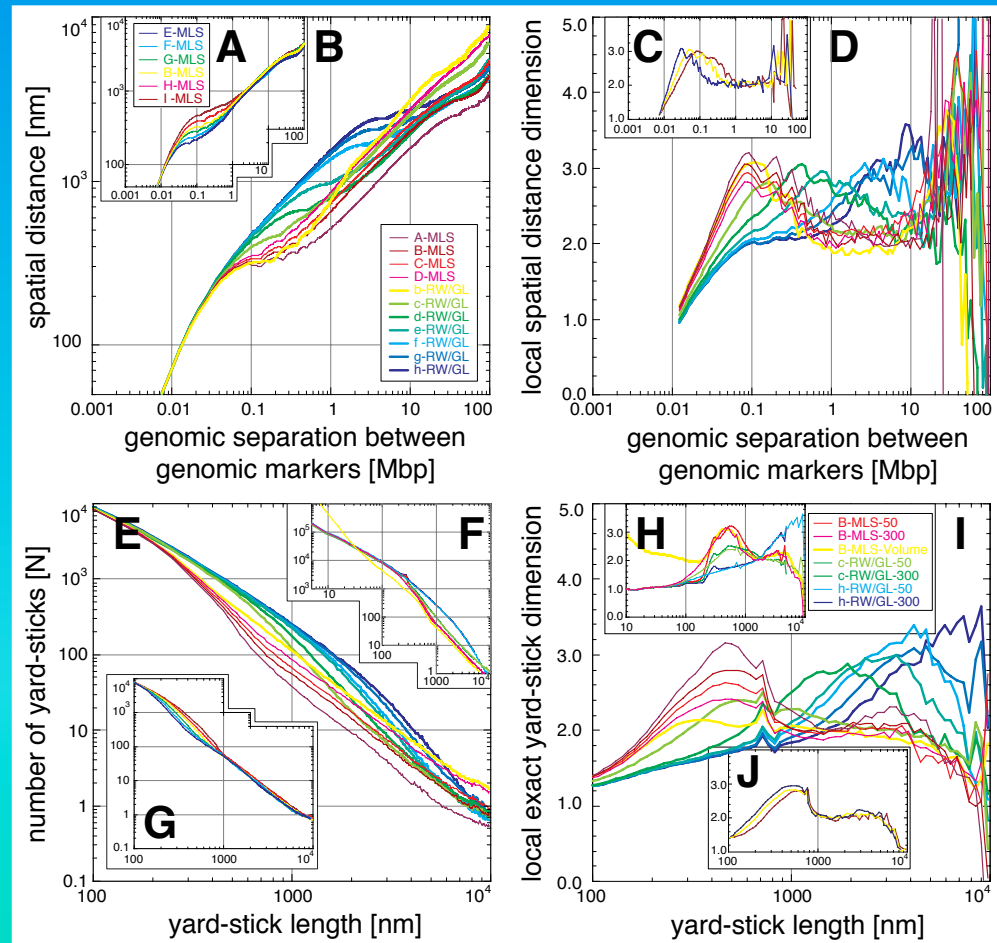
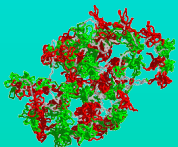
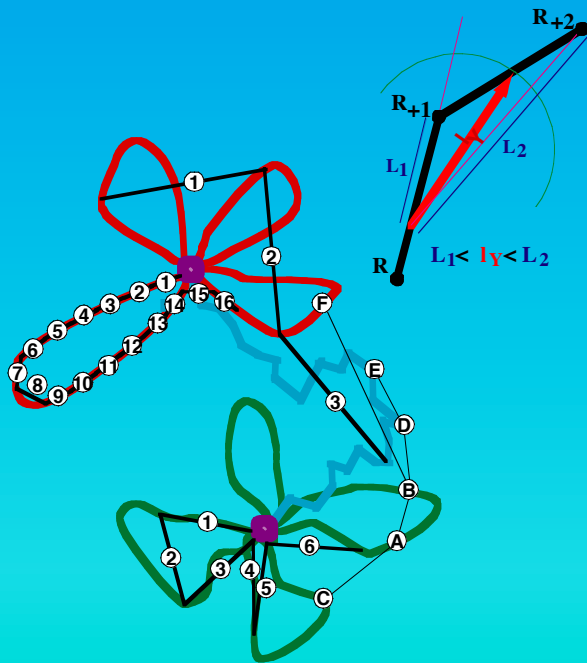


MLS models model with 126 kbp loops and linkers in a 10 μ m nucleus.



Scaling of the Chromatin Fiber Topology

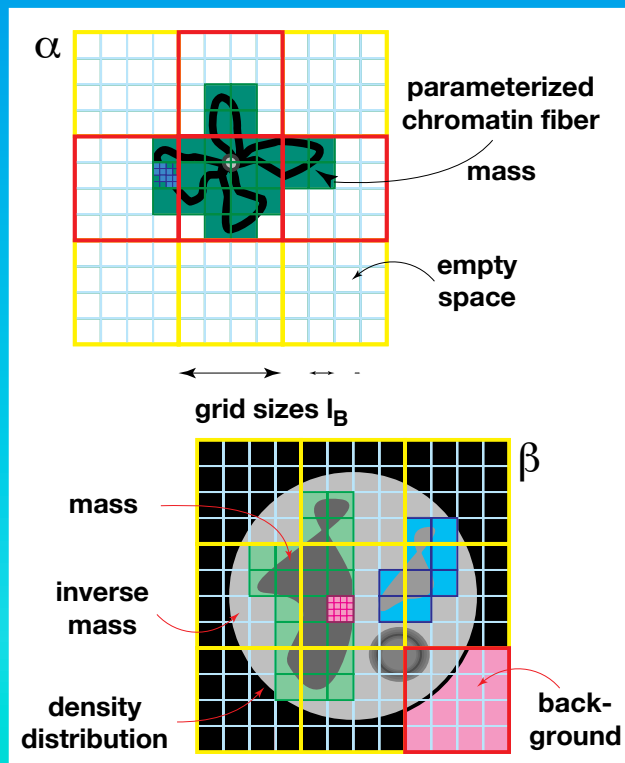
The spatial-distance and exact yard-stick dimension distinguish between the simulated models in detail. The MLS model shows a globular and fine-structured multi scaling behaviour due to the loops forming rosettes. This agrees with DNA fragmentation by Carbon ion irradiation and the appearance of fine-structured multi-scaling long-range correlations found in the sequential organization of genomes.



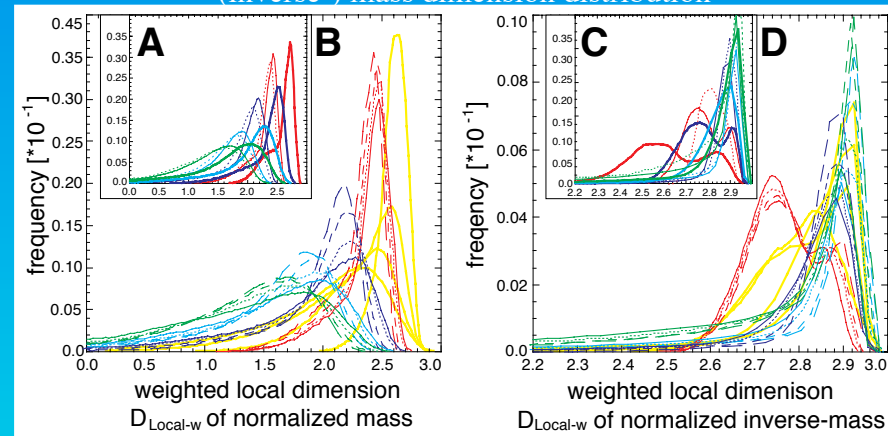
Scaling of the Chromatin Morphology & Distribution

The local (inverse-) mass dimension distribution distinguishes between the models in detail and show also a multi-scaling behaviour with globular feature for the MLS model like the scaling of the fiber topology. With the mass dimension as function of image intensity separates very well between different nuclei *in vivo*.

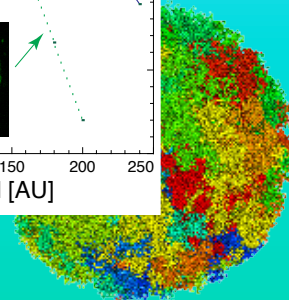
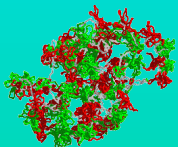
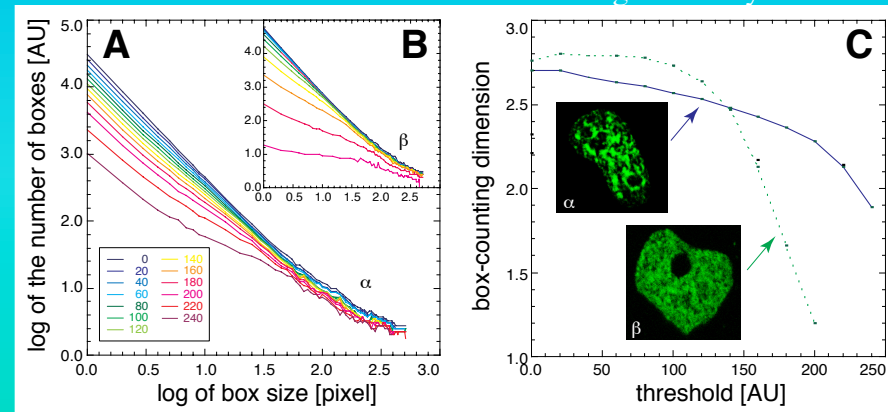
Consequently, the chromatin morphology is causally and quantitatively connected to the fiber topology.



(inverse-) mass dimension distribution

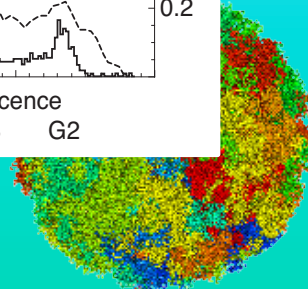
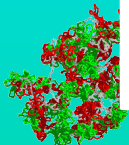
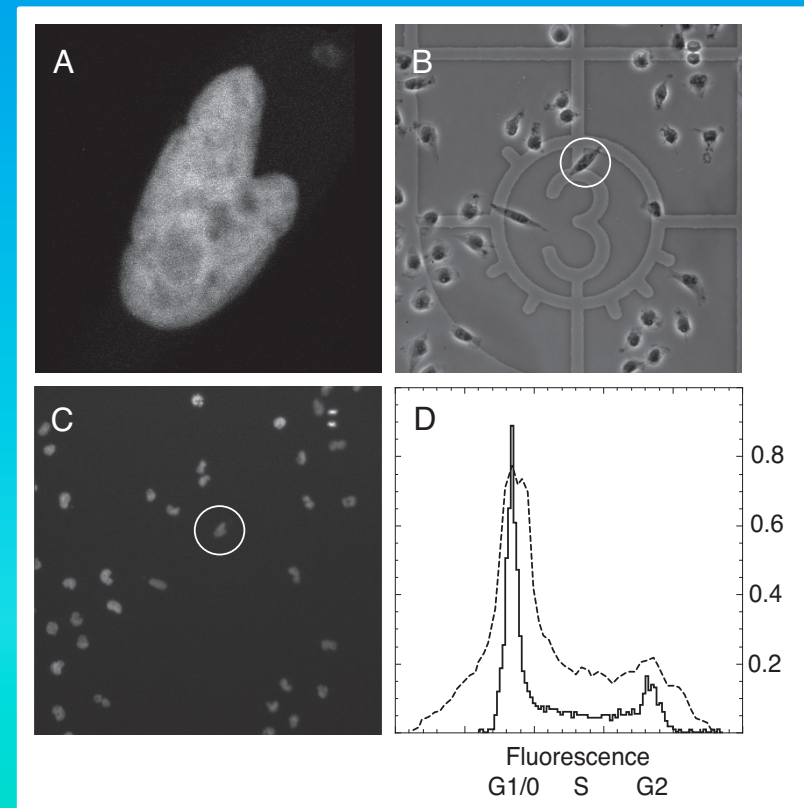
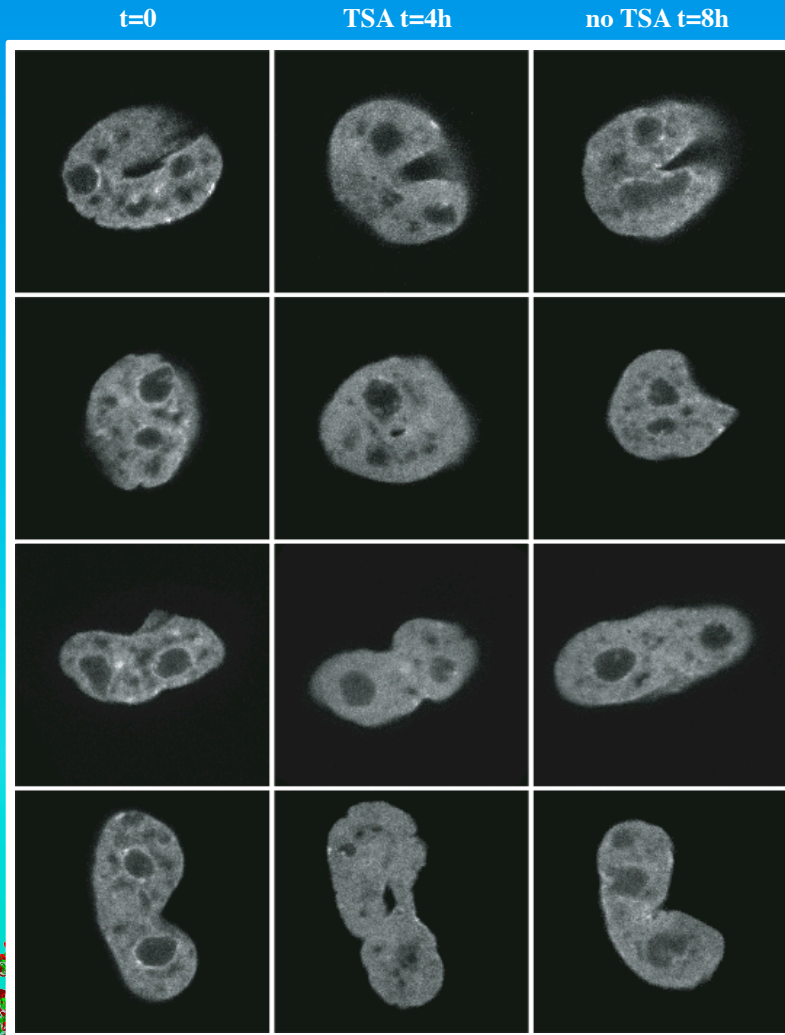


mass dimension as function of image intensity



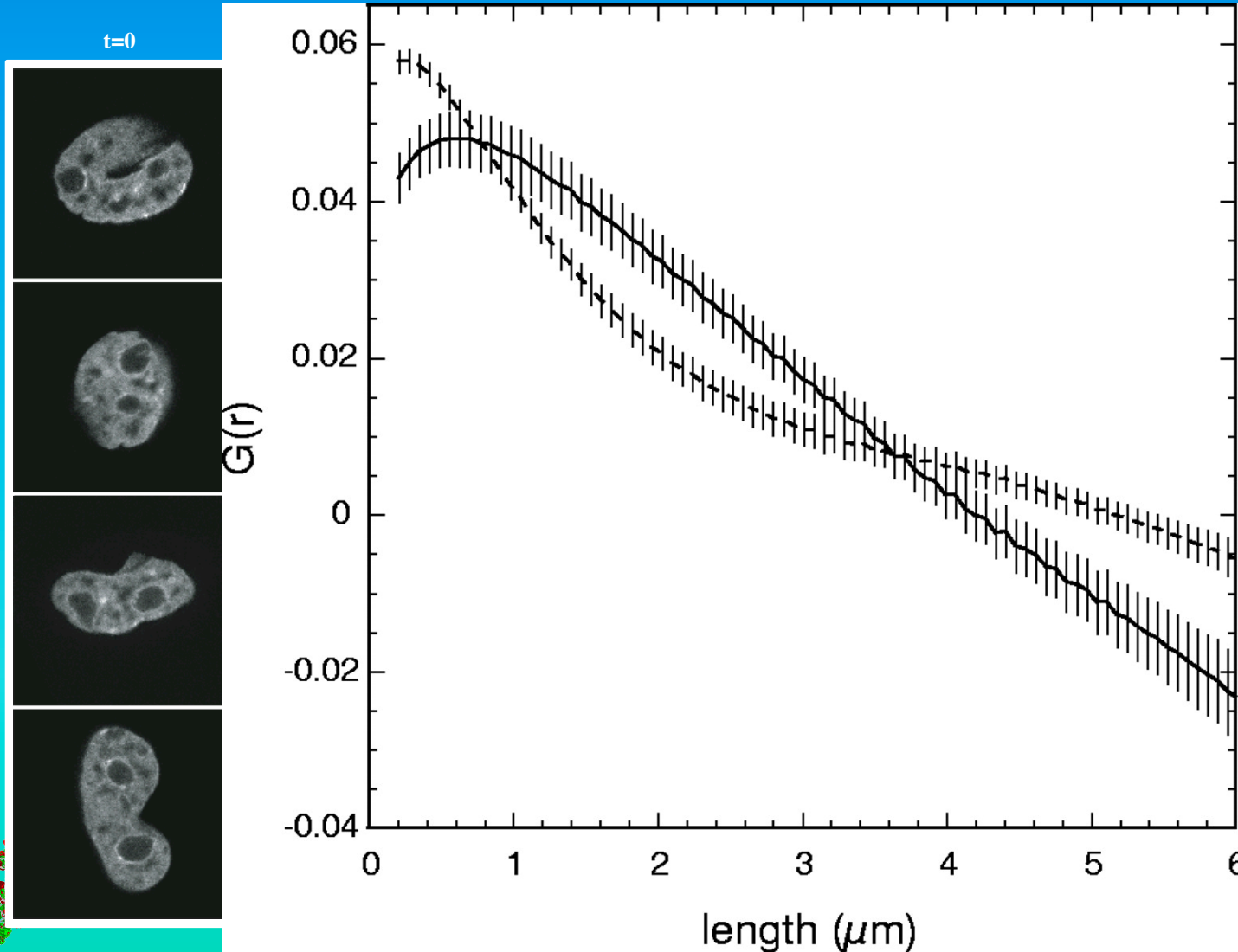
Quantified TSA induced Morphology Changes

Trichostatin A induced histone acetylation can be quantified by *in vivo* H2A-GFP confocal images and image correlation spectroscopy (iFCS), which is a scaling analysis, and reveals the opening of chromatin, and thus reorganization changes on scales from 0.2 to $\sim 1\mu\text{m}$, consistent with MLS models.



Quantified TSA induced Morphology Changes

Trichostatin A induced histone acetylation can be quantified by *in vivo* H2A-GFP confocal images and image correlation spectroscopy (iFCS), which is a scaling analysis, and reveals the opening of chromatin, and thus reorganization changes on scales from 0.2 to $\sim 1\mu\text{m}$, consistent with MLS models.



Diffusion of Particles in the Nucleus

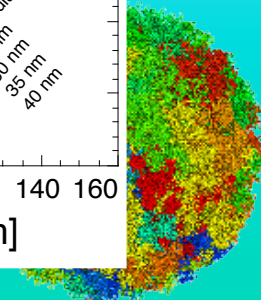
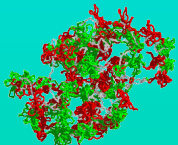
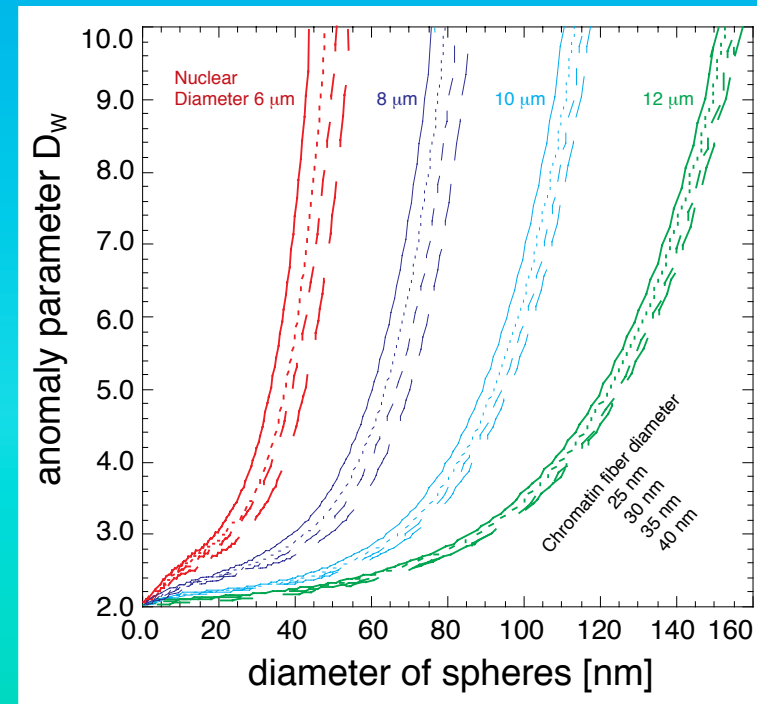
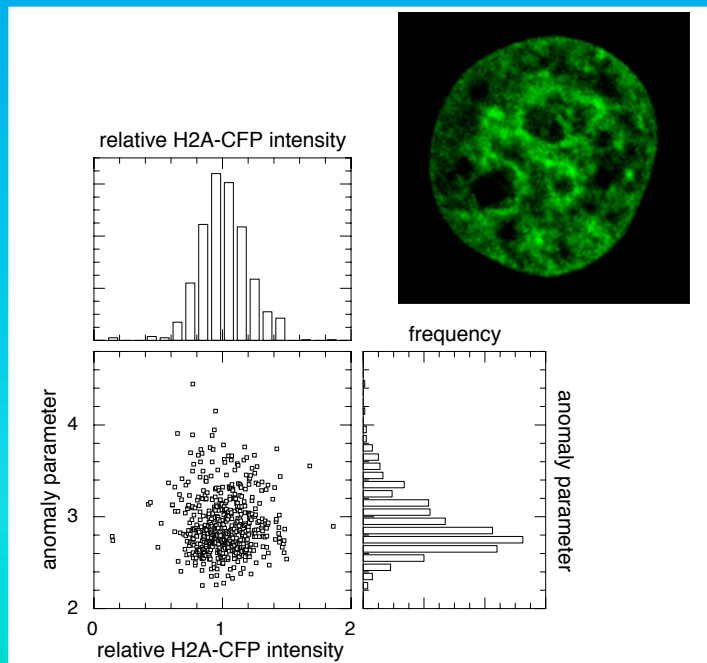
Due to the volume and spatial relationships in the nucleus typical particles reach almost any location in the nucleus by moderately obstructed diffusion: a 10 nm particle moves 1 to 2 μm within 10 ms.

The structural influence on the obstruction degree is random for Alexa 568 as function of the chromatin distribution visualized by H2A CFP in vivo and measured by fluorescence correlation spectroscopy (FCS)



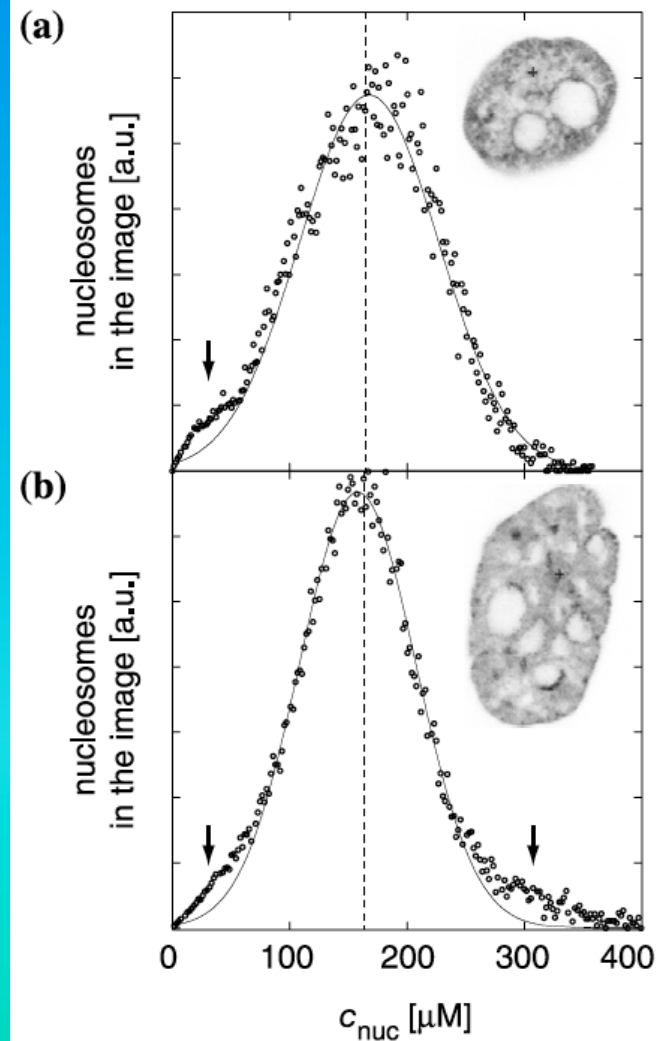
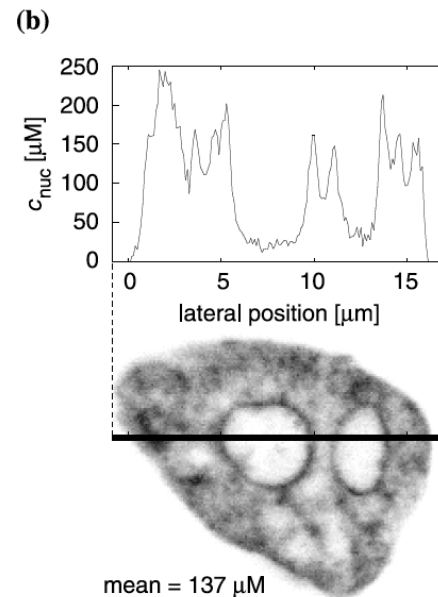
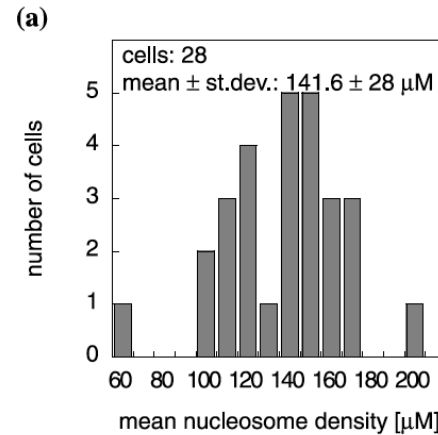
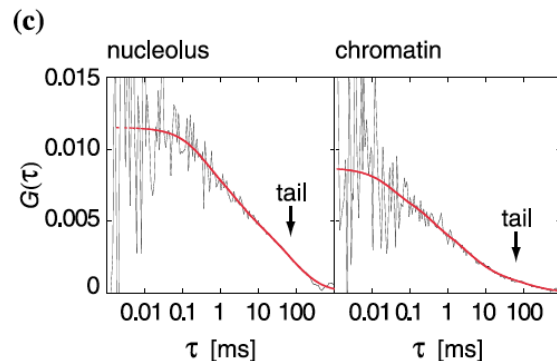
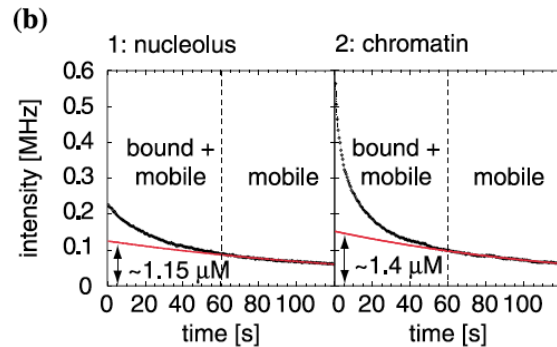
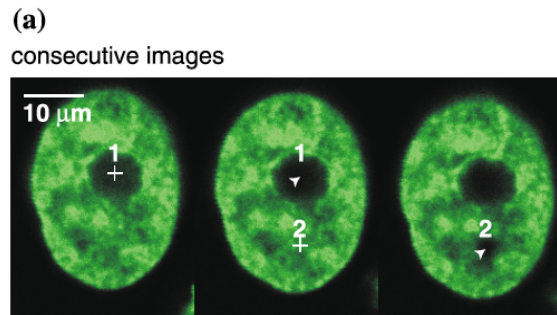
$$\langle r^2 \rangle \propto t^{2/D_w}$$

Nuclear diameter [μm]	Nuclear Volume [μm^3]	Mean Nucleosome Concentration [μM]	Chromatin Volume Fraction [%]	Mean Isotropic Mesh Spacing [nm]
6	115	251	20.1	41
8	268	107	8.6	64
10	523	55	4.4	90
12	904	32	2.6	117



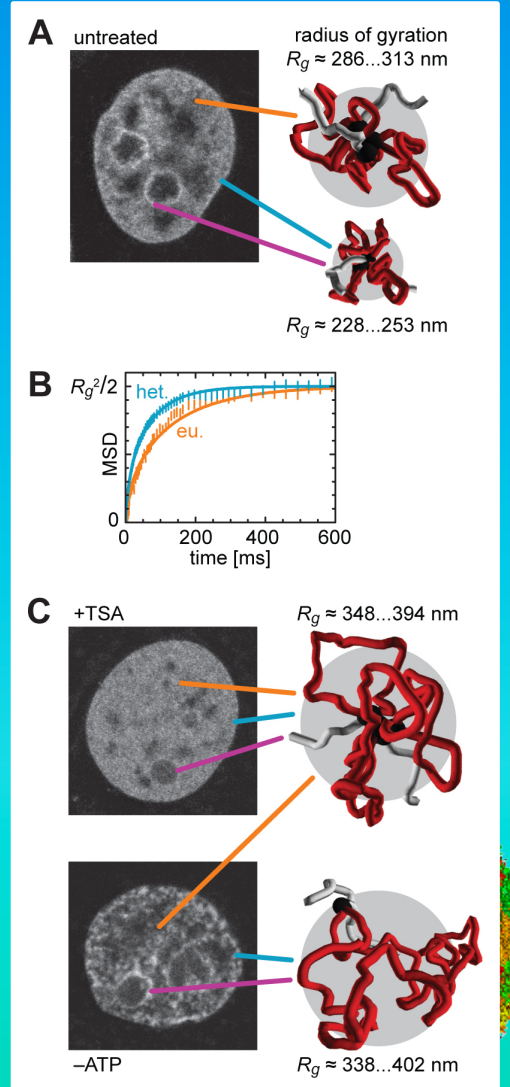
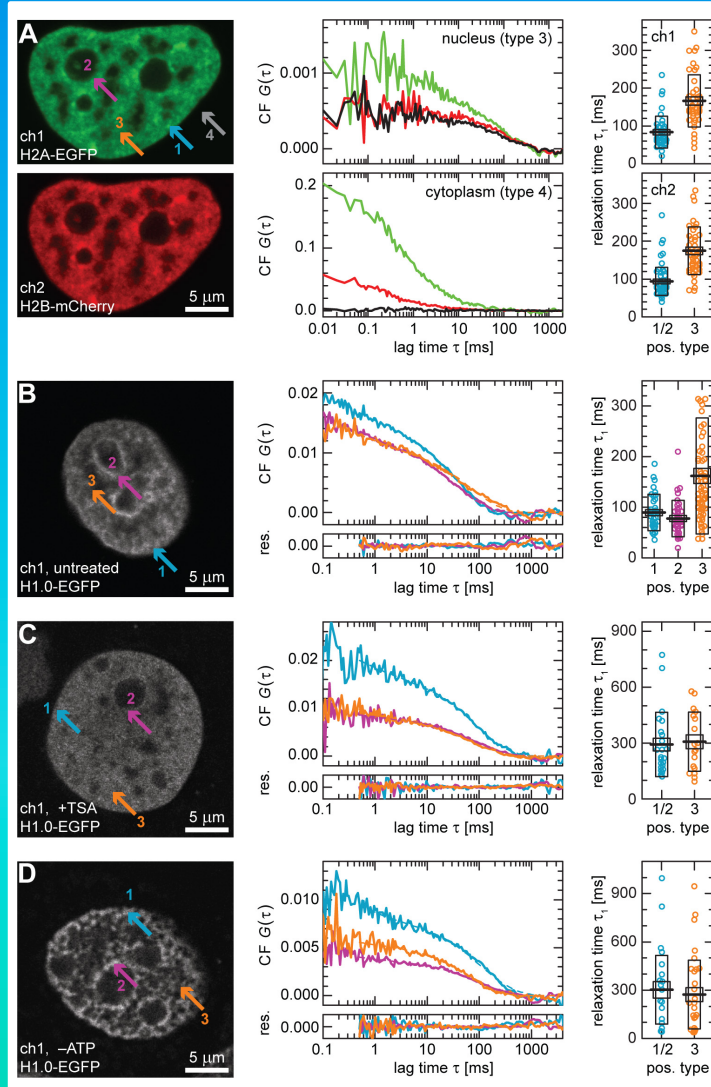
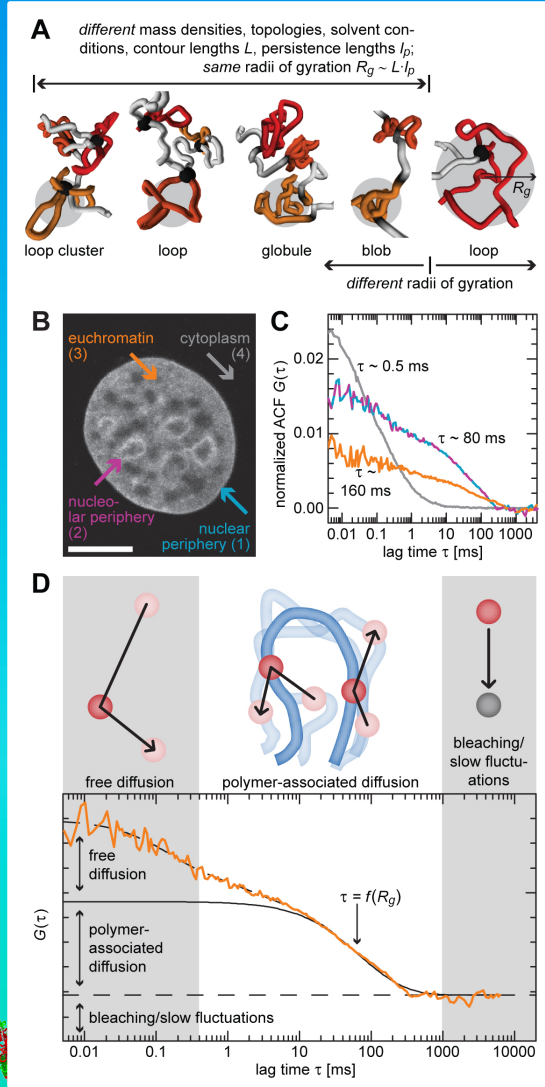
In Vivo Nucleosome Concentrations and 3D architecture

Counting nucleosomes in living cells with a combination of fluorescence correlation spectroscopy (FCS) and confocal laser scanning microscopy (CLSM) reveals the association of nucleosomes and their kinetics as well as again the typical expected distribution of a multi-loop aggregate/rosette.



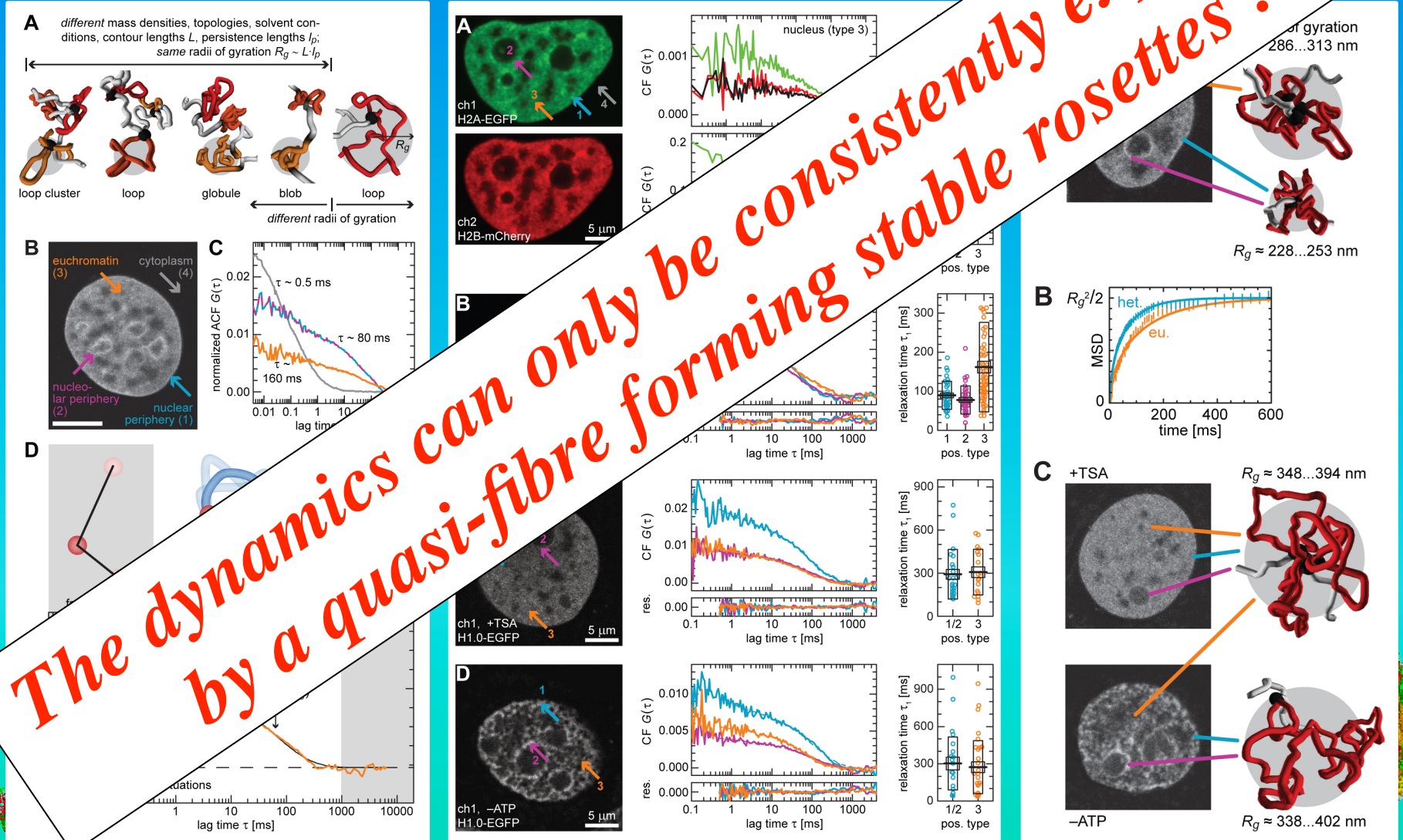
In Vivo Dynamics and 3D architecture

Fluorescence correlation spectroscopy (FCS) also reveals the dynamics of nucleosomes bound to DNA, i.e. FCS measures the movement of the chromatin quasi-fibre and its constraining architecture. This shows again a differentially compacted quasi-fibre folded into multi-loop aggregates/rosettes with functional differences as to e.g. hetero- and euchromatin or induced disturbances chromatin fiber (de-)condensation (+TSA, -ATP)



In Vivo Dynamics and 3D architecture

Fluorescence correlation spectroscopy (FCS) also reveals the dynamics of nucleosomes bound to DNA, i.e. FCS measures the movement of the chromatin quasi-fibre and its constraining architecture. This shows again a differentially compacted quasi-fibre folded into multi-loop aggregates/rosettes with functional differences, e.g. hetero- and euchromatin or induced disturbances chromatin fiber (de-)condensation (+TSA)



Conclusion

The compacted chromatin quasi-fibre, folds into stable loop-aggregates connected by a linker !

Every structural level of nuclear organization including its dynamics is connected and represented in all the other levels in a holistic systems genomics manner.



Parameter/Observable			Simulation Single Chromosomes						Simulation Whole Nuclei							General Comparison	
Architectural Level	Observable Class	Spec. Feature	Applic. & Quality	Topological Parameter Dependence				Modell	Applic. & Quality	Topological Parameter Dependence					Modell	Experiment vs. Simulation	
				L ₅ /R ₅	LI ₅	C _{VOL}	EV			L ₅ /R ₅	LI ₅	NUC _{VOL}	EV	Chrom ₅		Comp. Degree	Modell
Morphology: Chromatin Fibre to Nucleus	Morphology	Rendering	+++	+++	+++	+++	+++	MLS	+++	+++	+++	+++	+++	-	MLS	+	MLS
		EM	ND; but similar to the simulation of whole <u>nulcei</u> .						+	+	+	+++	+	-	~MLS	+	~MLS +
		FISH-EM							++	++	++	+++	++	+++	~MLS	+	~MLS +
		CLSM							+	+	++	+++	+	-	MLS	++	MLS ++
		FISH-CLSM							++	++	+++	+++	++	+++	MLS	+++	MLS +++
Nucleus	Radial Distribution Nuclei	Mass							+++	+	+	+++	++	+++	≈MLS	+	≈MLS
		Density							+++	+	+	+++	++	+++	≈MLS	+	≈MLS
	CLSM-Image Distribution	Intensity							+++	+	+	+++	++	-	MLS	+++	MLS +++
		Mass							+++	+	+	+++	++	-	MLS	+++	MLS +++
	Chromosome Position	Distance Mass Centre							+++	+	++	+++	++	+++	~MLS	+	~MLS +
Chromosome	Radial Distribution Chromosomes	Mass	+++	++	+++	+++	++	MLS	+++	++	+++	++	+	+++	MLS	+	MLS +
		Density	+++	++	+++	+++	++	MLS	+++	++	+++	++	+	+++	MLS	+	MLS +
	Territory Shape	Roundness	ND; but similar to the simulation of whole <u>nulcei</u> .						++	+	+++	++	+	+++	MLS	++	MLS ++
	Territory Distance	Nearest							+++	+	++	+++	+	+++	MLS	++	MLS ++
		Arbitrary							+++	+	++	+++	+	+++	MLS	++	MLS ++
	Territory CLSM/Interaction	Volume CLSM							+++	+	++	+++	++	+++	MLS	+++	MLS +++
		Overlap CLSM							+++	+	++	+++	++	+++	MLS	+++	MLS +++
Subchromosomal Domain	SD Radial Distribution	Mass	+++	+++	+	+	+	MLS	+++	+++	+	+	~+	-	MLS	+++	MLS +++
		Density	+++	+++	+	+	+	MLS	+++	+++	+	+	~+	-	MLS	+++	MLS +++
	SD Distance	Genetically Adjacent	+++	++	+++	+	+	MLS	+++	++	+++	+	~+	-	MLS	+++	MLS +++
		Spatial Arbitrary	+++	+	+	++	++	MLS	+++	+	+	+++	~+	-	MLS	+++	MLS +++
		Spatial Nearest	+++	++/+	+++/+	++	++	MLS	+++	++/+	+++/+	++/+	~+	-	MLS	+++	MLS +++
	SD CLSM/Interaction	Volume CLSM	ND; but similar to the simulation of whole <u>nulcei</u> .						+++	+++	+	+	~+	-	MLS	+++	MLS +++
		Overlap CLSM							+++	+++	+	+++	~+	-	MLS	+++	MLS +++
Chromatin Loop/Fibre	Spatial Distance	Position Independent	+++	+++	+++	-/+	++	MLS	+++	+++	+++	-/+	+	-/+	MLS	+++	MLS +++
		Position Dependent	++++	+++	+++	-/+	++	MLS	++++	+++	+++	-/+	+	-/+	MLS	+++	MLS +++
		Marker Ensemble	++++	+++	+++	-/+	++	MLS	++++	+++	+++	-/+	+	-/+	MLS	+++	MLS +++

Evolutionary Architecture Perspective

Only a compacted chromatin quasi-fibre, folded into stable loop-aggregates connected by a linker allows to guaranty the functional informational requirements of genomes:

i) storage stability/flexibility, ii) readout, and iii) replication !



➤ Storage stability/flexibility:

The packaging ratio/scale into a quasi-fibre and stable loops forming rosettes is optimal for the physical stability of genomes, while it is flexible enough to allow functional differences as well as react to entropic and other damages.

➤ Readout:

The dynamics this architecture allows expression/regulation by self-organization into (in-)active units already in proximity, and guaranties at the same time accessibility to and from the information for factors as well transcripts.

➤ Replication:

The 2D knot-free topology as well as the packaging ratio/scale into a quasi-fibre and stable loops forming rosettes, allows concatenation free replication with low error/damage rate due to the easy block-wise proximity organization as well as the easy physical (de-)condensation during cell division.

Form follows function and function follows form!

Evolutionary Architecture Perspective

Only a compacted chromatin quasi-fibre, folded into stable loop-aggregates connected by a linker allows to guaranty the functional informational requirements of genomes:

i) storage stability/flexibility, ii) readout, and iii) replication !

➤ **Storage stability/flexibility:**

The packaging ratio/scale into a quasi-fibre and stable loops is optimal for the physical stability of genomes, while it is flexible to adapt to environmental differences as well as react to entropic and other damages.

➤ **Readout:**

The dynamics this architecture allows by self-organization into (in-)active units already in proximity, and the accessibility to and from the information for factors as well transcription.

➤ **Replication:**

The 2D structure of the packaging ratio/scale into a quasi-fibre and stable loops forms a template for error free replication with low error/damage rate due to the easy access to the information as well as the easy physical (de-)condensation during cell division.

Genomes are an Evolutionary Holistic Form-Function Entanglement !

Form follows function and function follows form!

Clinical Epigenetic Context

Only a compacted chromatin quasi-fibre, folded into stable loop-aggregates connected by a linker allows to guaranty the functional informational requirements of genomes:

i) storage stability/flexibility, ii) readout, and iii) replication !



➤ Clinical Epigenetic Context of Storage Stability/Flexibility:

Epigenetic alteration of the packaging ratio/scale into a quasi-fibre and stable loops forming rosettes alters the optimum ground state of the physical stability of genomes. While this ground state is flexible enough to allow for functional differences as well as react to entropic and other damages, functional alterations beyond this flexibility turns into malfunction and disease.

➤ Clinical Epigenetic Context of the Readout:

Epigenetic variation of the dynamics of this architecture alters the expression/regulation preset by self-organization into (in-)active units already in proximity, and thus changes at the same time the guaranteed accessibility to and from the information for factors as well transcripts. Beyond, the evolutionary limits this also leads to malfunction and disease.

➤ Clinical Epigenetic Context of Replication:

Epigenetic changes influence the 2D knot-free topology as well as the packaging ratio/scale into a quasi-fibre and stable loops forming rosettes, and thus changes the degree of concatenation free replication with low error/damage rate due to the easy block-wise proximity organization as well as the easy physical (de-)condensation during cell division. Again, beyond the limits, this results in malfunction and disease.

Form Follows Function and Function Follows Form

ONLY within the Limits of Evolutionary Preset Multilism between Genotype and Phenotype!

Clinical Epigenetic Context

Only a compacted chromatin quasi-fibre, folded into stable loop-aggregates connected by a linker allows to guaranty the functional informational requirements of genomes:

i) storage stability/flexibility, ii) readout, and iii) replication !

➤ Clinical Epigenetic Context of Storage Stability/Flexibility:

Epigenetic alteration of the packaging ratio/scale into a stable loop-aggregate, forming rosettes, alters the optimum ground state of the physical system. This ground state is flexible enough to allow for functional differentiation. Beyond this flexibility, functional alterations beyond this flexibility result in disease.

➤ Clinical Epigenetic Context of the Readout:

Epigenetic variation of the dynamics of the system alters the expression/regulation preset by self-organization into (in-)stable loop-aggregates, and thus changes at the same time the guaranteed accessibility for factors as well transcripts. Beyond, the evolutionary limits, this results in disease.

➤ Clinical Epigenetic Context of Replication:

Epigenetic alteration of the knot-free topology as well as the packaging ratio/scale into a stable loop-aggregate, forming rosettes, and thus changes the degree of concatenation free organization. This results in a higher damage rate due to the easy block-wise proximity organization as well as in a higher condensation during cell division. Again, beyond the limits, this results in disease.

Genomes are an Evolutionary Holistic Form-Function Entanglement !

Form Follows Function and Function Follows Form

ONLY within the Limits of Evolutionary Preset Multilism between Genotype and Phenotype!

Acknowledgements

Thanks go to all the lab local lab members, those people who supported this work in the last decades, the institutions providing their infrastructure, and the national and international computing infrastructures.

Special thanks go to the reviewers, the EraSysBio+ initiative and the national and EU funding bodies.



Erasmus MC

Nick Kepper
Michael Lesnussa
Anis Abuseiris
A.M. Ali Imam

Cell Biology & Biophysics

EMBL

Malte Wachsmuth

EpiGenSys

EraSysBio+ Consortium Labs

Petros Kolovos
Harmen J. G. van de Werken
Jessica Zuin
Christel E. M. Kockx
Rutger W. W. Brouwer
Wilfred F. J. van Ijken
Kerstin S. Wendt
Frank G. Grosveld

Pathology

New York University

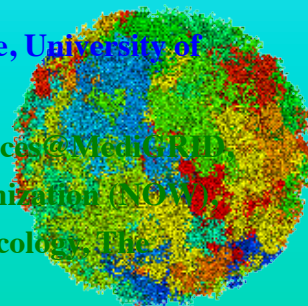
Julie Chaumeil
Jane Skok

Peter R. Cook
Gernot Längst
Tobias A. Knoch
Karsten Rippe
Gero Wedemann

Erasmus Medical Center and BioQuant & German Cancer Research Center

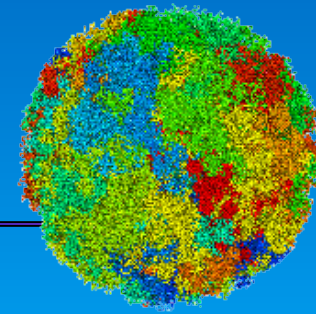
High-Performance Computing Center Stuttgart, University of Stuttgart; Supercomputing Center Karlsruhe, University of Karlsruhe; Computing Center, Deutsches Krebsforschungszentrum Heidelberg (DKFZ)

Erasmus Medical Center, Hogeschool Rotterdam, The Fraunhofer Society, The German MediGRID and Services@MediGRID
The German D-Grid Initiatives, The German Ministry for Science and Technology, The Dutch Science Organization (NOW)
The European EGEE Initiative, The European EDGES Consortium, The German Society for Human Ecology, The
International Society for Human Ecology, The European Commission



Acknowledgements

Thanks go also to all those people who supported this work in the last decades,
the institutions providing their infrastructure, and the national and international computing infrastructures.

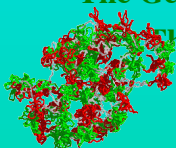


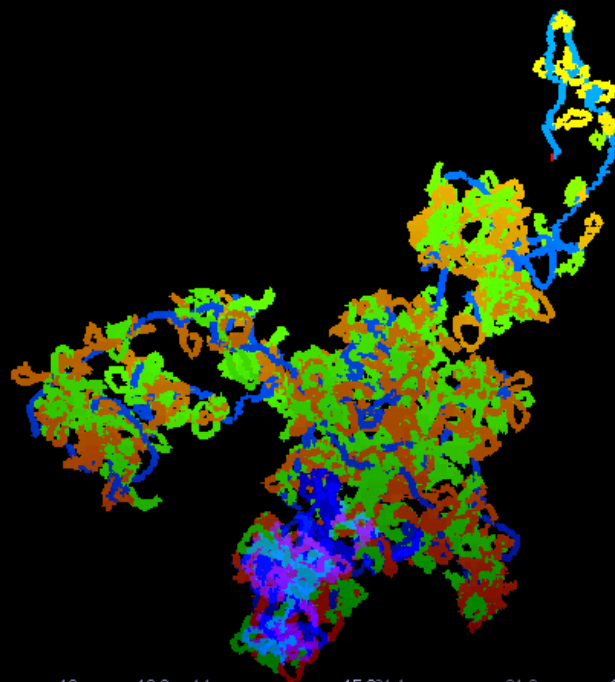
	Biophysical Genomics, Cell Biology, Erasmus MC	Biological Sciences, UCSD Suchit Jhunjunwala	The Cremer Labs Joachim Rauch	
Cell Biology & Biophysics EMBL Malte Wachsmuth	Petros Kolovos Anis Abuseiris Michael Lesnussa	Menno van Zelm Cornelis Murre	Irina Solovei Michael Hausmann Christoph Cremer Thomas Cremer	Biophysics of Macromolecules DKFZ Gabriele Müller Waldemar Waldeck Jörg Langowski
Biophysics, LMU Thomas Weidemann	Rob de Graaf Nick Kepper Frank Grossveld	Clinical Genetics Erasmus MC Bert Eussen Annelies de Klein		
CALTECH Katalin Fejes-Toth	LMU Munich Peter Quicken Anna Friedl	University Braunschweig Markus Göker	Molecular Genetics DKFZ Karsten Richter Peter Lichter	Supercomputing Center Karlsruhe Rudolph Lohner
Genome Org & Function BioQuant/DKFZ Karsten Rippe				

Erasmus Medical Center and BioQuant & German Cancer Research Center

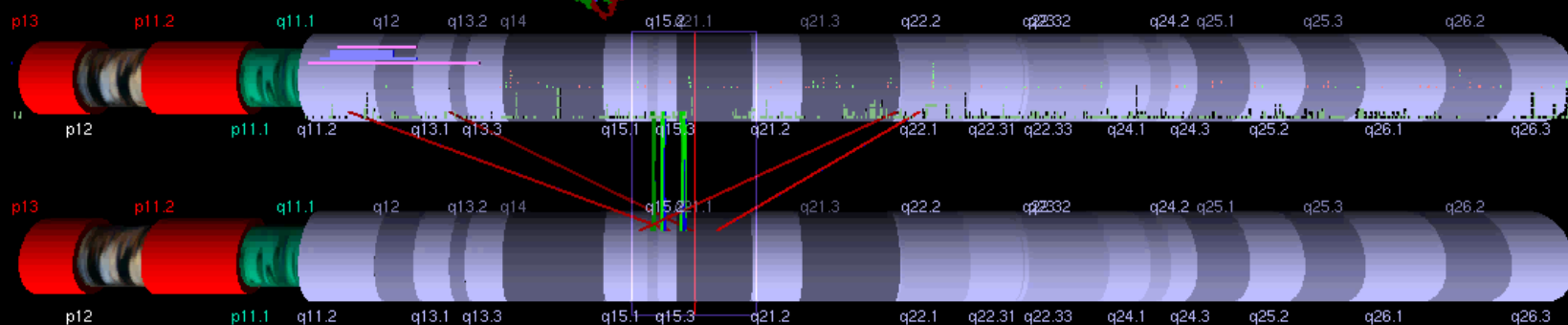
High-Performance Computing Center Stuttgart, University of Stuttgart; Supercomputing Center Karlsruhe, University of
Karlsruhe; Computing Center, Deutsches Krebsforschungszentrum Heidelberg (DKFZ)

Erasmus Medical Center, Hogeschool Rotterdam, The Fraunhofer Society, The German MediGRID and Services@MediGRID,
The German D-Grid Initiatives, The German Ministry for Science and Technology, The Dutch Science Organization (NOW),
The European EGEE Initiative, The European EDGES Consortium, The German Society for Human Ecology, The
International Society for Human Ecology,
The European Commission





15
 Decipher
 Affy100KXba
 Refseqb36



43750000

15

1:500000

**Decoding
the
3D Multi-Loop Aggregate/Rosette Chromatin Architecture, Dynamics,
and
Functional Epigenetics of Genomes**

Knoch, T. A.

2nd Annual Epigenetics Discovery Congress, Heathrow Marriott Hotel, London, United Kingdom, 8th – 9th September, 2016.

Abstract

The dynamic three-dimensional chromatin architecture of genomes and the obvious co-evolutionary connection to its function – the storage and expression of genetic information – is still debated after ~170 years. With a systems genomics approach combining a novel selective high-throughput chromosomal interaction capture (T2C) with quantitative polymer simulations and scaling analysis of architecture and DNA sequence, we determined and cross-proved the final architecture of genomes with unprecedented molecular resolution and dynamic range from single base pairs to entire chromosomes: for a variety of genetic loci of different species, cell type, cell cycle, functional states and system distortion a chromatin quasi-fibre exists with 5 ± 1 nucleosome per 11 nm, which folds into stable(!) 40-100 kbp loops forming stable(!) aggregates/rosettes which are connected by a ~50 kbp chromatin linker. Modifications on all these organizational levels are variations of the aforementioned scheme. Beyond, functional variations on various levels are reflected also on others. Spatial isotropy breaking is also found. Polymer simulations using Monte Carlo and Brownian dynamics approaches confirm this and predict and explain additional experimental findings. Beyond, a novel fluorescence correlation spectroscopy (FCS) approach combined with analytical polymer models measures the architectural dynamics *in vivo* in the entire genome and agrees with the before mentioned conclusion using completely independent means. System distortions are reflected in the corresponding variations as well. Beyond, we find a fine-structured multi-scaling behaviour of both the architecture and the DNA sequence, showing for the first time directly the tight entanglement between architecture and sequence. All this agrees with the outcome of a synopsis e.g. with previous spatial distance measurement studies, *in vivo* morphology of entire cell nuclei, or electron microscopy of chromosome spreading studies, as well as the heuristics of the field in the last 170 years. This now complete architecture and dynamics of these genomes has fundamental consequences for the entire system of the storage and expression of genetic information, for its investigation in general as well as for clinical epigenetics: E.g. this architecture, its dynamics, and accessibility balance stability and flexibility ensuring genome integrity and variation enabling gene expression/regulation by self-organization of (in)active units already in proximity. Thus, both the T2C and FCS approaches open the door to “architectural and dynamic sequencing” of genomes at a resolution where a genome mechanics with corresponding uncertainty principles applies. Consequently, this will lead now to a detailed understanding of genomes with fundamental new insights and huge novel perspectives for diagnosis, treatment and genome engineering efforts in the future.

Corresponding author email contact: TA.Knoch@taknoch.org

Keywords:

Genome, genomics, genome organization, genome architecture, structural sequencing, architectural sequencing, systems genomics, coevolution, holistic genetics, genome mechanics, genome statistical mechanics, genomic uncertainty principle, multilism genotype-phenotype, genome function, genetics, gene regulation, replication, transcription, repair, homologous recombination, simultaneous co-transfection, cell division, mitosis, metaphase, interphase, cell nucleus, nuclear structure, nuclear organization, chromatin density distribution, nuclear morphology, chromosome territories, subchromosomal domains, chromatin loop aggregates, chromatin rosettes, chromatin loops, chromatin quasi fibre, chromatin density, persistence length, spatial distance measurement, histones, H1.0, H2A, H2B, H3, H4, mH2A1.2, DNA sequence, complete sequenced genomes, molecular transport, obstructed diffusion, anomalous diffusion, percolation, long-range correlations, fractal analysis, scaling analysis, exact yard-stick dimension, box-counting dimension, lacunarity dimension, local nuclear dimension, nuclear diffuseness, parallel super computing, grid computing, volunteer computing, polymer model, analytic mathematical model, Brownian Dynamics, Monte Carlo, fluorescence *in situ* hybridization (FISH), targeted chromatin capture (T2C) confocal laser scanning microscopy, fluorescence correlation spectroscopy, spatial precision distance microscopy, super-resolution microscopy, two dimensional fluorescence correlations spectroscopy (2D-FCS) auto-fluorescent proteins, CFP, GFP, YFP, DsRed, fusion protein, *in vivo* labelling, information browser, visual data base access, holistic viewing system, integrative data management, extreme visualization, three-dimensional virtual environment, virtual paper tool, human ecology, e-human grid ecology, society, social systems, e-social challenge, inverse tragedy of the commons, grid phenomenon, micro-sociality, macro-sociality, autopoietic tragedy of social sub-systems, micro subsystems, macro subsystems, micro operationality, macro operationality, grid psychology micro riskmanagement, macro riskmanagement.

Literature References

- Knoch, T. A.** Dreidimensionale Organisation von Chromosomen-Domänen in Simulation und Experiment. (Three-dimensional organization of chromosome domains in simulation and experiment.) *Diploma Thesis*, Faculty for Physics and Astronomy, Ruperto-Carola University, Heidelberg, Germany, 1998, and TAK Press, Tobias A. Knoch, Mannheim, Germany, ISBN 3-00-010685-5 and ISBN 978-3-00-010685-9 (soft cover, 2nd ed.), ISBN 3-00-035857-9 and ISBN 978-3-00-035885-0 (hard cover, 2nd ed.), ISBN 3-00-035858-7, and ISBN 978-3-00-035858-6 (DVD, 2nd ed.), 1998.
- Knoch, T. A., Münkkel, C. & Langowski, J.** Three-dimensional organization of chromosome territories and the human cell nucleus - about the structure of a self replicating nano fabrication site. *Foresight Institute - Article Archive*, Foresight Institute, Palo Alto, CA, USA, <http://www.foresight.org>, 1- 6, 1998.
- Knoch, T. A., Münkkel, C. & Langowski, J.** Three-Dimensional Organization of Chromosome Territories and the Human Interphase Nucleus. *High Performance Scientific Supercomputing*, editor Wilfried Jüling, Scientific Supercomputing Center (SSC) Karlsruhe, University of Karlsruhe (TH), 27- 29, 1999.
- Knoch, T. A., Münkkel, C. & Langowski, J.** Three-dimensional organization of chromosome territories in the human interphase nucleus. *High Performance Computing in Science and Engineering 1999*, editors Krause, E. & Jäger, W., High-Performance Computing Center (HLRS) Stuttgart, University of Stuttgart, Springer Berlin-Heidelberg-New York, ISBN 3-540-66504-8, 229-238, 2000.
- Bestvater, F., **Knoch, T. A.**, Langowski, J. & Spiess, E. GFP-Walking: Artificial construct conversions caused by simultaneous cotransfection. *BioTechniques* 32(4), 844-854, 2002.
- Gil-Parado, S., Fernández-Montalván, A., Assfalg-Machleidt, I., Popp, O., Bestvater, F., Holloschi, A., **Knoch, T. A.**, Auerswald, E. A., Welsh, K., Reed, J. C., Fritz, H., Fuentes-Prior, P., Spiess, E., Salvesen, G. & Machleidt, W. Ionomycin-activated calpain triggers apoptosis: A probable role for Bcl-2 family members. *J. Biol. Chem.* 277(30), 27217-27226, 2002.
- Knoch, T. A. (editor)**, Backes, M., Baumgärtner, V., Eysel, G., Fehrenbach, H., Göker, M., Hampl, J., Hampl, U., Hartmann, D., Hitzelberger, H., Nambena, J., Rehberg, U., Schmidt, S., Weber, A., & Weidemann, T. Humanökologische Perspektiven Wechsel - Festschrift zu Ehren des 70. Geburtstags von Prof. Dr. Kurt Egger. Human Ecology Working Group, Ruperto-Carola University of Heidelberg, Heidelberg, Germany, 2002.

- Knoch, T. A.** Approaching the three-dimensional organization of the human genome: structural-, scaling- and dynamic properties in the simulation of interphase chromosomes and cell nuclei, long- range correlations in complete genomes, *in vivo* quantification of the chromatin distribution, construct conversions in simultaneous co-transfections. *Dissertation*, Ruperto-Carola University, Heidelberg, Germany, and TAK†Press, Tobias A. Knoch, Mannheim, Germany, ISBN 3-00-009959-X and ISBN 978-3-00-009959-5 (soft cover, 3rd ed.), ISBN 3-00-009960-3 and ISBN 978-3-00-009960-1 (hard cover, 3rd ed.), ISBN 3-00-035856-9 and ISBN 978-3-00-010685-9 (DVD, 3rd ed.) 2002.
- Westphal, G., van den Berg-Stein, S., Braun, K., **Knoch, T. A.**, Dümmerling, M., Langowski, J., Debus, J. & Friedrich, E. Detection of the NGF receptors TrkA and p75NTR and effect of NGF on the growth characteristics of human tumor cell lines. *J. Exp. Clin. Canc. Res.* 21(2), 255-267, 2002.
- Westphal, G., Niederberger, E., Blum, C., Wollman, Y., **Knoch, T. A.**, Dümmerling, M., Rebel, W., Debus, J. & Friedrich, E. Erythropoietin Receptor in Human Tumor Cells: Expression and Aspects Regarding Functionality. *Tumori* 88(2), 150-159, 2002.
- Gil-Parado, S., Popp, O., **Knoch, T. A.**, Zahler, S., Bestvater, F., Felgenträger, M., Holoshi, A., Fernández-Montalván, A., Auerswald, E. A., Fritz, H., Fuentes-Prior, P., Machleidt, W. & Spiess, E. Subcellular localization and subunit interactions of over-expressed human μ -calpain. *J. Biol. Chem.* 278(18), 16336-15346, 2003.
- Knoch, T. A.** Towards a holistic understanding of the human genome by determination and integration of its sequential and three-dimensional organization. *High Performance Computing in Science and Engineering 2003*, editors Krause, E., Jäger, W. & Resch, M., High-Performance Computing Center (HLRS) Stuttgart, University of Stuttgart, Springer Berlin-Heidelberg-New York, ISBN 3- 540-40850-9, 421-440, 2003.
- Wachsmuth, M., Weidemann, T., Müller, G., Urs W. Hoffmann-Rohrer, **Knoch, T. A.**, Waldeck, W. & Langowski, J. Analyzing intracellular binding and diffusion with continuous fluorescence photobleaching. *Biophys. J.* 84(5), 3353-3363, 2003.
- Weidemann, T., Wachsmuth, M., **Knoch, T. A.**, Müller, G., Waldeck, W. & Langowski, J. Counting nucleosomes in living cells with a combination of fluorescence correlation spectroscopy and confocal imaging. *J. Mol. Biol.* 334(2), 229-240, 2003.
- Fejes Tóth, K., **Knoch, T. A.**, Wachsmuth, M., Frank-Stöhr, M., Stöhr, M., Bacher, C. P., Müller, G. & Rippe, K. Trichostatin A induced histone acetylation causes decondensation of interphase chromatin. *J. Cell Science* 117, 4277-4287, 2004.
- Ermiler, S., Krunić, D., **Knoch, T. A.**, Moshir, S., Mai, S., Greulich-Bode, K. M. & Boukamp, P. Cell cycle-dependent 3D distribution of telomeres and telomere repeat-binding factor 2 (TRF2) in HaCaT and HaCaT-myc cells. *Europ. J. Cell Biol.* 83(11-12), 681-690, 2004.
- Kost, C., Gama de Oliveira, E., **Knoch, T. A.** & Wirth, R. Spatio-temporal permanence and plasticity of foraging trails in young and mature leaf-cutting ant colonies (*Atta spp.*). *J. Trop. Ecol.* 21(6), 677- 688, 2005.
- Winnefeld, M., Grewenig, A., Schnölzer, M., Spring, H., **Knoch, T. A.**, Gan, E. C., Rommelaere, J. & Cziepluch, C. Human SGT interacts with BAG-6/Bat-3/Scythe and cells with reduced levels of either protein display persistence of few misaligned chromosomes and mitotic arrest. *Exp. Cell Res.* 312, 2500-2514, 2006.
- Sax, U., Weisbecker, A., Falkner, J., Viezens, F., Yassene, M., Hartung, M., Bart, J., Krefting, D., **Knoch, T. A.** & Semler, S. Grid-basierte Services für die elektronische Patientenakte der Zukunft. *E- HEALTH-COM - Magazin für Gesundheitstelematik und Telemedizin*, 4(2), 61-63, 2007.
- de Zeeuw, L. V., **Knoch, T. A.**, van den Berg, J. & Grosveld, F. G. Erasmus Computing Grid - Het bouwen van een 20 TeraFLOP virtuele supercomputer. *NIOC proceedings 2007 - het perspectief of lange termijn*. editor Frederik, H. NIOC, Amsterdam, The Netherlands, 52-59, 2007.
- Rauch, J., **Knoch, T. A.**, Solovei, I., Teller, K. Stein, S., Buiting, K., Horsthemke, B., Langowski, J., Cremer, T., Hausmann, M. & Cremer, C. Lightoptical precision measurements of the Prader- Willi/Angelman Syndrome imprinting locus in human cell nuclei indicate maximum condensation changes in the few hundred nanometer range. *Differentiation* 76(1), 66-82, 2008.
- Sax, U., Weisbecker, A., Falkner, J., Viezens, F., Mohammed, Y., Hartung, M., Bart, J., Krefting, D., **Knoch, T. A.** & Semler, S. C. Auf dem Weg zur individualisierten Medizin - Grid-basierte Services für die EPA der Zukunft. *Telemedizinführer Deutschland 2008*, editor Jäckel, A. Deutsches Medizinforum, Minerva KG, Darmstadt, ISBN 3-937948-06-6, ISBN-13 9783937948065, 47-51, 2008.

- Drägestein, K. A., van Capellen, W. A., van Haren, J. Tsibidis, G. D., Akhmanova, A., **Knoch, T. A.**, Grosveld, F. G. & Galjart, N. Dynamic behavior of GFP-CLIP-170 reveals fast protein turnover on microtubule plus ends. *J. Cell Biol.* 180(4), 729-737, 2008.
- Jhunjhunwala, S., van Zelm, M. C., Peak, M. M., Cutchin, S., Riblet, R., van Dongen, J. J. M., Grosveld, F. G., **Knoch, T. A.**⁺ & Murre, C.⁺ The 3D-structure of the Immunoglobulin Heavy Chain Locus: implications for long-range genomic interactions. *Cell* 133(2), 265-279, 2008.
- Krefting, D., Bart, J., Beronov, K., Dzhimova, O., Falkner, J., Hartung, M., Hoheisel, A., **Knoch, T. A.**, Lingner, T., Mohammed, Y., Peter, K., Rahm, E., Sax, U., Sommerfeld, D., Steinke, T., Tolxdorff, T., Vossberg, M., Viezens, F. & Weisbecker, A. MediGRID - Towards a user friendly secured grid infrastructure. *Future Generation Computer Systems* 25(3), 326-336, 2008.
- Knoch, T. A.**, Lesnussa, M., Kepper, F. N., Eussen, H. B., & Grosveld, F. G. The GLOBE 3D Genome Platform - Towards a novel system-biological paper tool to integrate the huge complexity of genome organization and function. *Stud. Health. Technol. Inform.* 147, 105-116, 2009.
- Knoch, T. A.**, Baumgärtner, V., de Zeeuw, L. V., Grosveld, F. G., & Egger, K. e-Human Grid Ecology: Understanding and approaching the Inverse Tragedy of the Commons in the e-Grid Society. *Stud. Health. Technol. Inform.* 147, 269-276, 2009.
- Dickmann, F., Kaspar, M., Löhnardt, B., **Knoch, T. A.**, & Sax, U. Perspectives of MediGRID. *Stud. Health. Technol. Inform.* 147, 173-182, 2009.
- Knoch, T. A.**, Göcker, M., Lohner, R., Abuseiris, A. & Grosveld, F. G. Fine-structured multi-scaling long-range correlations in completely sequenced genomes - features, origin and classification. *Eur. Biophys. J.* 38(6), 757-779, 2009.
- Dickmann, F., Kaspar, M., Löhnardt, B., Kepper, N., Viezens, F., Hertel, F., Lesnussa, M., Mohammed, Y., Thiel, A., Steinke, T., Bernarding, J., Krefting, D., **Knoch, T. A.** & Sax, U. Visualization in health-grid environments: a novel service and business approach. *LNCS 5745*, 150-159, 2009.
- Dickmann, F., Kaspar, M., Löhnardt, B., Kepper, N., Viezens, F., Hertel, F., Lesnussa, M., Mohammed, Y., Thiel, A., Steinke, T., Bernarding, J., Krefting, D., **Knoch, T. A.** & Sax, U. Visualization in health-grid environments: a novel service and business approach. *Grid economics and business models - GECON 2009 Proceedings, 6th international workshop, Delft, The Netherlands*. editors Altmann, J., Buyya, R. & Rana, O. F., GECON 2009, LNCS 5745, Springer-Verlag Berlin Heidelberg, ISBN 978-3-642-03863-1, 150-159, 2009.
- Estrada, K.^{*}, Abuseiris, A.^{*}, Grosveld, F. G., Uitterlinden, A. G., **Knoch, T. A.**⁺ & Rivadeneira, F.⁺ GRIMP: A web- and grid-based tool for high-speed analysis of large-scale genome-wide association using imputed data. *Bioinformatics* 25(20), 2750-2752, 2009.
- de Wit, T., Dekker, S., Maas, A., Breedveld, G., **Knoch, T. A.**, Langeveld, A., Szumska, D., Craig, R., Bhattacharya, S., Grosveld, F. G.⁺ & Drabek, D. Tagged mutagenesis of efficient minos based germ line transposition. *Mol. Cell Biol* 30(1), 66-77, 2010.
- Kepper, N., Schmitt, E., Lesnussa, M., Weiland, Y., Eussen, H. B., Grosveld, F. G., Hausmann, M. & **Knoch T. A.**, Visualization, Analysis, and Design of COMBO-FISH Probes in the Grid-Based GLOBE 3D Genome Platform. *Stud. Health Technol. Inform.* 159, 171-180, 2010.
- Kepper, N., Ettig, R., Dickmann, F., Stehr, R., Grosveld, F. G., Wedemann, G. & **Knoch, T. A.** Parallel high-performance grid computing: capabilities and opportunities of a novel demanding service and business class allowing highest resource efficiency. *Stud. Health Technol. Inform.* 159, 264-271, 2010.
- Skowny, D., Dickmann, F., Löhnardt, B., **Knoch, T. A.** & Sax, U. Development of an information platform for new grid users in the biomedical field. *Stud. Health Technol. Inform.* 159, 277-282, 2010.
- Knoch, T. A.**, Baumgärtner, V., Grosveld, F. G. & Egger, K. Approaching the internalization challenge of grid technologies into e-Society by e-Human “Grid” Ecology. *Economics of Grids, Clouds, Systems, and Services – GECON 2010 Proceedings, 7th International Workshop, Ischia, Italy*, editors Altman, J., & Rana, O. F., Lecture Notes in Computer Science (LNCS) 6296, Springer Berlin Heidelberg New York, ISSN 0302-9743, ISBN-10 3-642-15680-0, ISBN-13 978-3-642-15680-9, 116-128, 2010.
- Dickmann, F., Brodhun, M., Falkner, J., **Knoch, T. A.** & Sax, U. Technology transfer of dynamic IT outsourcing requires security measures in SLAs. *Economics of Grids, Clouds, Systems, and Services – GECON 2010 Proceedings, 7th International Workshop, Ischia, Italy*, editors Altman, J., & Rana, O. F., Lecture Notes in Computer Science (LNCS) 6296, Springer Berlin Heidelberg New York, ISSN 0302-9743, ISBN-10 3-642-15680-0, ISBN-13 978-3-642-15680-9, 1-115, 2010.

- Knoch, T. A.** Sustained Renewability: approached by systems theory and human ecology. *Renewable Energy 2*, editors M. Nayeripour & M. Keshti, Intech, ISBN 978-953-307-573-0, 21-48, 2011.
- Kolovos, P., **Knoch, T. A.**, F. G. Grosveld, P. R. Cook, & Papantonis, A. Enhancers and silencers: an integrated and simple model for their function. *Epigenetics and Chromatin 5(1)*, 1-8, 2012.
- Dickmann, F., Falkner, J., Gunia, W., Hampe, J., Hausmann, M., Herrmann, A., Kepper, N., **Knoch, T. A.**, Lauterbach, S., Lippert, J., Peter, K., Schmitt, E., Schwardmann, U., Solodenko, J., Sommerfeld, D., Steinke, T., Weisbecker, A. & Sax, U. Solutions for Biomedical Grid Computing - Case Studies from the D-Grid Project Services@MediGRID. *JOCS 3(5)*, 280-297, 2012.
- Estrada, K., Abuseiris, A., Grosveld, F. G., Uitterlinden, A. G., **Knoch, T. A.** & Rivadeneira, F. GRIMP: A web- and grid-based tool for high-speed analysis of large-scale genome-wide association using imputed data. *Dissection of the complex genetic architecture of human stature and osteoporosis*. cumulative dissertation, editor Estrada K., Erasmus Medical Center, Erasmus University Rotterdam, Rotterdam, The Netherlands, ISBN 978-94-6169-246-7, 25-30, 1st June 2012.
- van de Corput, M. P. C., de Boer, E., **Knoch, T. A.**, van Cappellen, W. A., Quintanilla, A., Ferrand, L., & Grosveld, F. G. Super-resolution imaging reveals 3D folding dynamics of the β -globin locus upon gene activation. *J. Cell Sci. 125 (Pt 19)*, 4630-4639, 2012.
- da Silva, P. S. D., Delgado Bieber, A. G., Leal, I. R., **Knoch, T. A.**, Tabarelli, M., Leal, I. R., & Wirth, R. Foraging in highly dynamic environments: leaf-cutting ants adjust foraging trail networks to pioneer plant availability. *Entomologia Experimentalis et Applicata 147*, 110-119, 2013.
- Zuin, J., Dixon, J. R., van der Reijden, M. I. J. A., Ye, Z., Kolovos, P., Brouwer, R. W. W., van de Corput, M. P. C., van de Werken, H. J. G., **Knoch, T. A.**, van IJcken, W. F. J., Grosveld, F. G., Ren, B. & Wendt, K. S. Cohesin and CTCF differentially affect chromatin architecture and gene expression in human cells. *PNAS 111(3)*, 9906-1001, 2014.
- Kolovos, P., Kepper, N., van den Werken, H. J. G., Lesnussa, M., Zuin, J., Brouwer, R. W. W., Kockx, C. E. M., van IJcken, W. F. J., Grosveld, F. G. & **Knoch, T. A.** Targeted Chromatin Capture (T2C): A novel high resolution high throughput method to detect genomic interactions and regulatory elements. *Epigenetics & Chromatin 7:10*, 1-17, 2014.
- Diermeier, S., Kolovos, P., Heizinger, L., Schwartz, U., Georgomanolis, T., Zirkel, A., Wedemann, G., Grosveld, F. G., **Knoch, T. A.**, Merkl, R., Cook, P. R., Längst, G. & Papantonis, A. TNF α signalling primes chromatin for NF-kB binding and induces rapid and widespread nucleosome repositioning. *Genome Biology 15(12)*, 536-548, 2014.
- Knoch, T. A.**, Wachsmuth, M., Kepper, N., Lesnussa, M., Abuseiris, A., A. M. Ali Imam, Kolovos, P., Zuin, J., Kockx, C. E. M., Brouwer, R. W. W., van de Werken, H. J. G., van IJcken, W. F. J., Wendt, K. S. & Grosveld, F. G. The detailed 3D multi-loop aggregate/rosette chromatin architecture and functional dynamic organization of the human and mouse genomes. *bioRxiv preprint*, 16.07.2016.
- Kolovos, P., Georgomanolis, T., Koeflerle, A., Larkin, J. D., Brant, J., Nikolić, M., Gusmao, E. G., Zirkel, A., **Knoch, T. A.**, van IJcken, W. F. J., Cook, P. R., Costa, I. G., Grosveld, F. G. & Papantonis, A. Binding of nuclear kappa-B to non-canonical consensus sites reveals its multimodal role during the early inflammatory response. *Genome Research 26(11)*, 1478-1489, 2016.
- Wachsmuth, M., **Knoch, T. A.** & Rippe, K. Dynamic properties of independent chromatin domains measured by correlation spectroscopy in living cells. *Epigenetics & Chromatin 9:57*, 1-20, 2016.
- Knoch, T. A.**, Wachsmuth, M., Kepper, N., Lesnussa, M., Abuseiris, A., A. M. Ali Imam, Kolovos, P., Zuin, J., Kockx, C. E. M., Brouwer, R. W. W., van de Werken, H. J. G., van IJcken, W. F. J., Wendt, K. S. & Grosveld, F. G. The detailed 3D multi-loop aggregate/rosette chromatin architecture and functional dynamic organization of the human and mouse genomes. *Epigenetics & Chromatin 9:58*, 1-22, 2016.